Contents Inhalt

Influence of selected parameters centipede yarns on air permeability property of woven fabrics produced with these yarns

ERHAN KENAN ÇEVEN

REZUMAT – ABSTRACT – INHALTSANGABE

Influenţa anumitor parametri ai firelor de efect asupra proprietăţii de permeabilitate la aer a ţesăturilor realizate din acestea

În lucrare sunt analizaţi factorii de influenţă asupra proprietăţii de permeabilitate la aer a ţesăturilor realizate din fire de efect. În cadrul studiului experimental, s-au folosit fire de efect produse pe o maşină de croşetat, cu diferite mărimi ale pasului de lănţişor şi cu diverse lungimi ale florului. Firele de efect au fost utilizate ca umplutură în structura ţesăturii. Testările privind permeabilitatea la aer au fost efectuate pe un aparat digital de măsurare. Conform rezultatelor analizelor statistice efectuate utilizând valorile experimentale obţinute în urma testării, s-a constatat că permeabilitatea la aer a ţesăturilor a fost influenţată de anumiţi parametri ai firelor de efect, cum ar fi mărimea pasului de lănţişor şi lungimea florului. La materialele realizate din fire de efect cu valori mai mari ale pasului de lănţişor şi ale lungimii florului, s-au constatat valori mai mici ale permeabilităţii la aer decât în cazul celor cu valori mai mici ale pasului de lănţişor şi ale lungimii florului. Permeabilitatea la aer a ţesăturilor a scăzut odată cu creşterea densităţii de lungime a firelor de efect.

Cuvinte-cheie: fire de efect, permeabilitate la aer, pas de lănţişor, lungimea florului, densitate de lungime, maşină de croşetat

Influence of selected parameters centipede yarns on air permeability property of woven fabrics produced with these yarns

This paper is focused on the selected factors that influence the air permeability property of woven fabrics produced with centipede yarns. In the experimental study, the centipede yarns were produced on a Crochet machine with varying chain numbers and band lengths. The centipede yarns were used as filling in the woven fabric construction. Air permeability measurements were performed with a digital test instrument. According to the results of the statistical analyses performed using the experimental values obtained from the tests, air permeability property of the fabrics was affected by the centipede yarns parameters like chain number and band length. Fabrics woven with the centipede yarns with higher chain number and band length had less air permeability than those with lower chain number and band length. The air permeability of the fabrics decreased with the increase in centipede yarn linear density.

Key-words: centipede yarn, air permeability, chain number, band length, chain density, crochet machine

Einwirkung der Luftpermeabilitäts- Einflussparameter bei Effektfadengewebe

Die Arbeit konzentriert sich auf die Einflussfaktoren der Luftpermeabilitätseigenschaft bei Effektfadengewebe. Im Rahmen der experimentellen Studie wurden die Effektfäden auf Strickmaschinen gefertigt, mit unterschiedlichen Kettenstichschritt und Bandlängen. Die Effektfäden wurden als Füllung in der Gewebestruktur angewendet. Die Luftpermeabilitätsteste wurden mit einem Digitalmessinstrument durchgeführt. Es wurde festgestellt, dass die Luftpermeabilität der Gewebe von unterschiedlichen Effektgarnparameter beeinflusst wurde, wie Kettenstichschritt und Bandlängen, entsprechend der experimentellen Ergebnissen statistischer Untersuchungen als Folge der Teste. Es wurden niedrigere Werte der Luftpermeabilität bei Materialien gefertigt aus Effektfäden mit hohen Werten für den Kettenstichschritt und der Bandlängen erhalten, als im Fall der niedrigen Werte der beiden Parameter. Die Luftpermeabilität der Gewebe sinkt mit dem Wachstum der Längendichte der Effektfäden.

Stichwörter: Effektfäden, Luftpermeabilität, Kettenstichschritt, Bandlängen, Längendichte, Strickmaschine

In addition to technical considerations, aesthetics is also important in the production of fashionable fabrics. Aesthetic factors provide the initial impulse of attraction and may be the only factor that influences the decision to buy. To make the fabrics more attractive to the purchasers, appearance is enhanced by various materials, structures, colors, patterns, finishes and textures [1]. The demand for yarns with structural and/or optical effects is due to the special aesthetic and high decorative effect of the woven, knitted materials and other textiles, as well. There are many different types of fancy yarns throughout the textile industry. Their uses range from upholstery to apparel and from transportation to home furnishings. Fancy yarn is regarded as a yarn that differs from normal construction of yarn due to deliberate irregularities in its construction [2].

Methods for creating a wide range of fancy yarns may be grouped into two large classes: direct and indirect. Fancy yarns produced by direct systems are obtained on the spinning frame that is modified or especially developed for this purpose. With indirect methods, the yarns are produced by modifying the conventional processing techniques both upstream of spinning (e.g., in carding) and downstream (e.g., dyeing, raising etc.). Some fancy yarns produced according to indirect methods are obtained by weaving and knitting [3].

These are made exclusively by filament yarns using adaptations of various processes, as well as tape-knit fancy yarns produced using a range of take-up rations and component yarns on a knitting machine especially designed for fancy yarn manufacture [4].

Tape yarns may be made by a variety of processes; braiding, warp knitting and weft knitting being among them. In recent years, these materials have become better known, especially in fashion knitwear and drapery. Tape yarns have different structures. One type (knitted by forming two chains and inlay connected chains) is known as ladder-knit; the other one has a ribbon type structure [5, 6]. Ladder-knit fancy yarn can be produced on a small diameter circular knitting machine with three guides feeding each knitting head [3]. Some knitted fancy yarns have effect component – short or long lengths of yarn, bunches of roving and color effects as well. Ribbon type fancy yarn is manufactured on a small diameter circular weft knitting machine from 6 to 20 needles. After knitting and finishing operations, the structure of fancy yarns has a flat, tape like effect [6].

Centipede yarn is a kind of tape yarn which is produced with warp knitting technique. Crochet machine which is a kind of flat knitting machine is used for the production of these yarns. This yarn is warp knitted by forming two
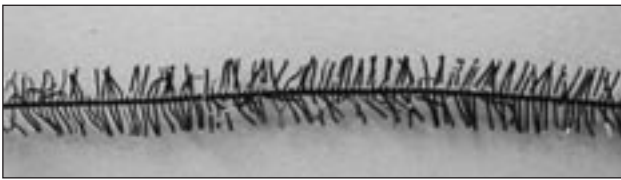
Fig. 1. Centipede yarn (Own research)

chains and inlay connecting the chains. But the inlay is cut to produce the pile and forms the centipede yarn structure. The piles project out from the core to give a hairy effect. The result is a yarn with a velvet-like surface. It must be considered that the chain number affects the number of bands (piles) per unit length of the yarn body. The picture and the basic structure of a centipede yarn are shown in figure 1 and figure 2.

In recent years, centipede yarns have become better known especially in upholstery and drapery textiles. This yarn can be an alternative to the chenille yarns for the production of drape fabrics. Chenille yarn consists of cut pile which is made of fibers helically disposed around the two axial threads that secure it. Chenille yarn has a very distinct weakness; it does not have very adequate abrasion resistance. But the abrasion resistance of centipede yarns is high enough for the weaving operations because of the chain loop structure. The piles are trapped in the loops of the chain. Therefore, studies should be performed in order to detect the characteristics of fabrics from these yarns.

The literature survey shows that there is limited research on physical properties of tape yarns like ribbon type and ladder-knit yarns. Effect of the properties of the component yarns on the final count, break tenacity, and appearance of ladder-knit fancy yarns, estimating the linear density of fancy ribbon type yarns and effects of the production conditions of ribbon typed fancy yarns on the thermo physiological properties are studied by various researchers [3, 6, 7].

However there is no research on centipede yarns. This study aims to fill this gap by contributing to the investigation of the specific influences of the centipede yarn production parameters on air permeability property of drape fabrics produced with centipede yarns. By this means, the study made possible to detect the effect of the centipede yarn structural parameters on one of the important physical property of drape fabrics from these yarns. Another expected target from this study is to trigger new studies for the determination of the effect of other structural parameters on the physical properties of fabrics produced with these yarns.

EXPERIMENTAL PART

To determine the influence of centipede yarn production parameters like chain number (chain density) and band length (pile length) on air permeability property of woven fabrics, three different levels of chain numbers and three different levels of band lengths were selected.

Characteristics of the component yarns selected for the production of centipede yarns are:

- chain yarn (the yarn for the basic chain weave) – 100% PES, 150 den (60 *Nm*) f 48, FDY type;
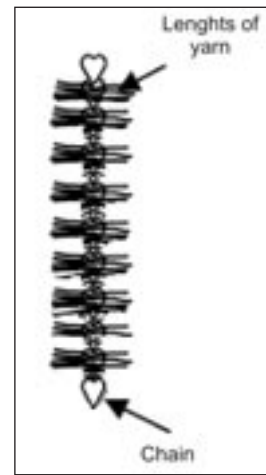
Fig. 2. Basic structure of centipede yarn [4]

- band yarn (the yarn for the pile) – 100% PES, 150 den (60 *Nm*) f 144, texturized type 100% PES chain and band yarn components were selected for the production of centipede yarns, because chain and band yarn components with PES fiber are commonly used to produce this type of fancy yarns. The yarn manufacturers prefer to use PES chain yarn especially for the convenience of the PES fiber to the process conditions.

Centipede yarns were produced with the above mentioned component yarns in the pile length of 4, 6 and 8 mm with three different chain densities of 10, 12 and 14 chains/cm on a 408/B3 model Comez Crochet machine. One band yarn is inserted in a loop of the knitted chain. The linear density values of nine different centipede yarns produced according to the experimental plan are listed in table 1.

Afterwards, nine different drape fabrics from the sample centipede yarns were woven on a PS type Dornier rapier weaving machine using the centipede yarns as filling in the fabric construction. The fabric weave type was selected as 2/2 filling rib (2/2 cords in the direction of warp). The selection process was determined according to the industrial criteria of the manufacturing plants and the commercially prevalence for the production of this type of fabrics.

The warp yarn was 100% PES, 50 den (180 *Nm*) f 24, FDY punched type. To avoid variables, the warp yarn was chosen identical to the yarn employed for the chain achievement. The warp and weft direction densities were 66 ends/cm and, respectively, 7 picks/cm.

Fabric coding

The coding of the fabrics according to structural parameters is given by:

Table 1

LINEAR DENSITY VALUES OF THE CENTIPEDE YARNS			
Band length, mm	Chain no./cm		
	10	12	14
4	1 526(5.9)	1 800(5)	2 195(4.1)
6	1 730(5.2)	2 143(4.2)	2 647(3.4)
8	1 957(4.6)	2 500(3.6)	3 000(3)

* Values in parentheses indicate the yarn linear density as *Nm* value

THE CODES OF THE WOVEN FABRICS ACCORDING TO THE CENTIPEDE YARN STRUCTURAL PARAMETERS			
Band length, mm	**Chain no./cm**		
	10	**12**	**14**
4	$f_{4,10}$	$f_{4,12}$	$f_{4,14}$
6	$f_{6,10}$	$f_{6,12}$	$f_{6,14}$
8	$f_{8,10}$	$f_{8,12}$	$f_{8,14}$

THE AIR PERMEABILITY VALUES (MEAN ± STANDARD DEVIATION) OF CENTIPEDE WOVEN FABRICS			
Band length, mm	**Chain no./cm**		
	10	**12**	**14**
4	710 ± 31 mm/s	570 ± 30 mm/s	453 ± 25 mm/s
6	650 ± 33 mm/s	510 ± 28 mm/s	360 ± 37 mm/s
8	600 ± 42 mm/s	340 ± 24 mm/s	220 ± 42 mm/s

- f_{ab}: a is chain number; b is band length;
- for a: 10 stands for 10 chains/cm, 12 stands for 12 chains/cm, 14 stands for 14 chains/cm;
- for b: 4 stands for 4 mm band length, 6 stands for 6 mm band length, 8 stands for 8 mm band length.

For example, $f_{14,4}$ means that: the rib fabric is woven with the centipede weft yarn which is having a structure of 14 chains/cm and 4 mm band length. The codes of nine different woven fabrics produced according to the experimental plan are listed in table 2.

Air permeability of a fabric is described as a measure of how well it allows the air passage through the fabric. Air permeability is measured as the rate of air flow (volume of air) passing perpendicularly through a known area of the fabric under a pre-set air pressure differential between the two surfaces of a material [8, 9].

Prior to the air permeability tests, all fabric samples were conditioned for 24 hours in standard atmospheric conditions (at a temperature of 20 ± 2°C and relative humidity of 65 ± 2%) [10].

Air permeability tests of the woven fabrics were performed according to ISO 9237 standard using a SDL Atlas Digital Air Permeability Tester Model M 021A [11].

The pressure level is of critical importance. The pre-selected test pressure was automatically maintained by the digital tester before the measurement. 100 Pa pressure drop was used in testing air permeability. The test area was 5 cm² for all samples. Pre-selected unit of measure was mm/s. Measurements were repeated ten times for each fabric type.

The air permeability (mm/s) was determined as follows [12]:

$$R = \left(\frac{\overline{q}_v}{A}\right) \cdot 167 \qquad (1)$$

where:
q_v is an arithmetical average of the debit of air flow, dm³/minute;
A – test area, cm²;
167 – coefficient of conversion from dm³/minute to cm³/second and then from cm/second to mm/second (from dm³/minute to cm³/second the coefficient is 1 000/60 and from cm/second to mm/second the coefficient is 10, total conversion coefficient is 1 000/60 x 10 = 166.6 ≈ 167).

Statistical evaluation

The SPSS 17.0 Statistical software package was used for conducting all statistical procedures. Completely randomized two-factor analysis of variance (ANOVA) as a fixed model was applied to data in order to understand the statistical importance of the centipede yarn structural parameters as chain number and band length on air permeability of the woven fabrics.

The means were compared by Student-Newman-Keuls (SNK) tests. All test results were assessed at a significance level of $\alpha \leq 0.05$. The treatment levels were marked in accordance with the mean values, and any levels marked by different letter (a, b, c) showed that they were significantly different.

RESULTS AND DISCUSSIONS

The average values of air permeability (mm/s) for centipede woven fabrics are given in table 3. Figure 3 demonstrates the effects of chain number and band length on air permeability values for fabrics woven with centipede yarns. The chart for the effect of centipede weft yarn linear density on the air permeability test results of centipede woven fabrics is shown in figure 4. According to figure 3, the minimum air permeability value was obtained as 220 mm/s from the woven
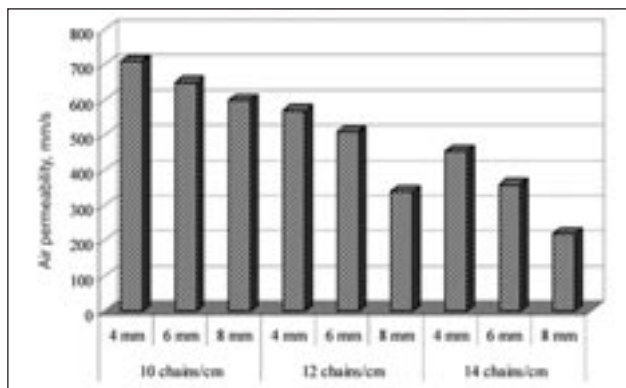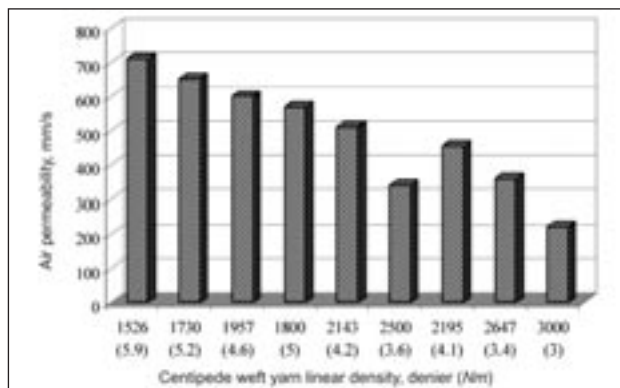

Fig. 3. Air permeability (mm/s) values for fabrics woven with centipede yarns versus chain numbers and band lengths

Fig. 4. Air permeability (mm/s) values for fabrics woven with centipede yarns versus centipede weft yarn linear density

Table 4

RESULTS OF THE VARIANCE ANALYSIS (*P* VALUES)		
Parameter		**P value**
Main effect	Chain number, *C*	0.000
	Band length, *B*	0.000
Interaction	*C x B*	0.020

Table 5

EFFECTS OF CHAIN NUMBER AND BAND LENGTH ON AIR PERMEABILITY VALUES, STUDENT-NEWMAN-KEULS TEST*		
Parameter		**Air permeability,** mm/s
Chain number, *C*	10 chains/cm	653 *a*
	12 chains/cm	473 *a*
	14 chains/cm	344 *c*
Band length, *B*	4 mm	578 *a*
	6 mm	507 *b*
	8 mm	387 *c*

* The different letters next to the counts indicate that they are significantly different from each other at a significance level of 5%

fabrics with centipede weft yarn having a chain number of 14/cm and band length of 8 mm ($f_{8,14}$ coded fabric), while the maximum air permeability value was obtained as 710 mm/s from the woven fabrics with centipede weft yarn having a chain number of 10/cm and band length of 4 mm ($f_{10,4}$ coded fabric).

When we investigate the air permeability results with respect to the centipede weft yarn linear density, it is shown in figure 4 that the minimum air permeability value was obtained as 220 mm/s from the woven fabrics with centipede weft yarn having a linear density of 3 000 denier (3 *Nm*), while the maximum air permeability value was obtained as 710 mm/s from those with centipede weft yarn having a linear density of 1 526 (5.9 *Nm*). From these findings it can be easily concluded that the air permeability of the fabrics decreased linearly with the increase in centipede weft yarn linear density. In this case it must be taken into consideration that all the fabrics were woven with constant weft density. These results can be interpreted as the centipede weft yarn linear density increases at constant weft density rendering the fabric more compact.

Fabric cover factor indicates the extent to which the area of a fabric is covered by one set of threads. In the tex system the cover factor in SI units is calculated by the expression: "number of threads per centimeter/10 x the square root of the tex". Our findings confirm that as the centipede weft yarn linear density increased, the fabric cover factor also increased. As a result of this, the gaps between the warp and weft yarns were reduced and the air flow passage through the fabric layer became difficult.

The results of the analysis of variance test (ANOVA) for air permeability values are summarized in table 4. The P values in table 4 indicated that there were statistically significant (5% significance level) differences between the air permeability values of fabrics woven with the centipede yarns having different chain numbers and band lengths. The effect of the interaction between chain number and band length on air permeability was significant.

The SNK test results for air permeability values of the fabrics woven with centipede yarns are presented in table 5.

A comparison of the woven fabrics in terms of air permeability property according to the SNK test results given in table 5 revealed that, woven fabrics with centipede weft yarns having different chain numbers and band lengths possessed different air permeability values.

When the air permeability values of the fabrics shown in figure 3 were inspected, it was observed that, the fabrics woven with centipede weft yarns of higher chain density (chain number) had less air permeability values than those of the fabrics with centipede yarns of lower chain density. Chain number increase from 10 to 14 (in one cm) led to decrease in air permeability values by 36 – 63% depending on the band length.

This situation can be interpreted as: the fabrics will have different cover factors as they are woven with centipede weft yarns of different chain densities at constant weft density. The cover factor of the woven fabric with centipede weft yarn having 14 chains/cm is more than that of the woven fabric with centipede weft yarn having 10 chains/cm. The chain density of the centipede yarn affects the linear density of the yarn under constant production conditions.

As regards another aspect, as the chain number increases, the number of the band yarns (pile yarns) in the centipede yarn body increases accordingly to the centipede yarn count (denier) and pile density will be higher. Hence the hairiness and tightness of the fabric structure will be affected. It is stated in the literature that the air permeability of the fabrics is influenced by the type of fabric structure, design of a woven, the number of warp and weft yarns and amount of twist in yarns, size of the yarns and the type of yarn structure [13]. Consequently, chain density of the centipede yarn will affect the resistance to air flow passing through the fabric woven from these yarns.

From the SNK test results given in table 5, it was observed that woven fabrics with centipede weft yarns of different band lengths possessed different air permeability values. Band length of the centipede yarn must be evaluated not only as an appearance property, but also as a very important structure parameter. Centipede yarn properties are influenced with wide range of this structure parameters.

The air permeability values of the woven fabrics with centipede weft yarns of lower band lengths were more than those of the woven fabrics with centipede weft yarns of higher band lengths. Band length increases from 4 mm to 8 mm caused a 33% average fall in the air permeability values of the fabrics. This fall is caused by the fact that, pile quantity at the surface of the sample fabrics differs from each other as the centipede yarn's band length changes.

One of the reasons of the air permeability is represented by the dimensions of gaps between warp and weft yarns in the fabric construction. These gaps are affected by the yarn dimension and surface characteristics. Therefore, centipede yarn's dimensional properties like linear density and pile length will influence the volume of air passing through the fabric. Fabrics

woven with centipede yarns having long piles had high pile quantity when the surface constructions of the fabric samples were observed. Piles covered the surface of the fabrics hence the gaps between the yarns were reduced.

CONCLUSIONS

The objective of this study was to investigate the influences of centipede yarn production parameters like chain density and band length on air permeability properties of woven fabrics from centipede yarns:

- According to the statistical tests performed on the measurements, the effect of chain number on the air permeability of woven fabrics was significant. Increments of the number of chains in the centipede yarn body led to significant decreases in the air permeability values of woven fabrics.
- This situation was caused by the fact that as the chain density increased, the linear density (denier) of the yarn increased. As the woven fabrics were produced with fixed warp and weft densities, the increase in the linear density values of the centipede weft yarns led to an increased fabric cover factor. Therefore, the woven fabric had a more tight structure. Fabric cover factor is the ratio of the area covered by the yarns to the whole area of the fabric. The void volume in the woven fabric decreased as the cover factor increased. And hence the air permeability decreased as the chain numbers were increased.
- Another cause for the difference between the air permeability results is the number of piles protruding from the centipede yarn body. One band yarn is inserted in a loop of the knitted chain. As the chain number increases, the number of the piles of the yarn body increase. The chain number increases and thus the pile number increases made the surface of the woven fabrics more hairy. It is stated in the literature that the air permeability of the fabrics is influenced by the type of fabric structure, design of a woven, the number of warp and weft yarns and amount of twist in yarns, size of the yarns and the type of yarn structure. Consequently, chain density of the centipede yarn will affect resistance to air flow passing through the fabric woven from these yarns.
- Statistically, significant differences were observed between the air permeability values of the woven fabrics produced with centipede yarns of different band lengths. Centipede yarns with higher band length led to the decrease in the air permeability values. Since higher band length increased the pile

ratio at the surface of the fabric and decreased the gaps between the weft yarns, air passage through the fabric got difficult. Air permeability behavior of a fabric is strongly affected by the yarn surface characteristics of the warp and weft yarns. And fabrics with different surface textures will have different air permeability.

- Air permeability results with respect to the centipede weft yarn linear density showed that the minimum air permeability value was obtained from the woven fabrics with centipede weft yarn having maximum linear density, while the maximum air permeability value was obtained from those with centipede weft yarn having minimum linear density at constant weft density. These results can be interpreted as the centipede weft yarn linear density increase at constant weft density made the fabric more compact and the fabric cover factor increased. As a result of this the gaps between the warp and weft yarns were reduced and the air flow passage through the fabric layer becomes difficult.
- In recent years, centipede yarns have become better known especially in upholstery and drapery textiles. This yarn can be an alternative to the chenille yarns for the production of drape fabrics.
- Finally, it could be concluded that it will be useful to make further studies on determining the effect of centipede yarn parameters on other physical properties of woven fabrics. The physical properties which should be highlighted are bending rigidity, abrasion resistance, drapability, breaking strength and bursting strength.
- It is not difficult to expect a change in the fabric physical properties by the difference in centipede yarn structural properties. Chain number of centipede yarn is a key feature for the physical properties of the woven fabrics from these yarns. The increase in the chain number is expected to improve the resistance of the fabrics to abrasion because of the increase in yarn linear density and fabric tightness. Also, the weft direction bending rigidity, drapability, breaking and bursting strengths are other properties estimated to be influenced by centipede yarn structural parameters.

BIBLIOGRAPHY

[1] Mole, K., Knox, J. S. *The properties and uses of specific hollow-spindle yarns.* In: Journal Textile Institut, 1989, vol. 80, issue 3, p. 441
[2] McIntyre, J. E., Daniels, P. N. *Textile terms and definitions.* 10th ed. The Textile Institute Terms and Definitions Committee, Biddles Ltd., U.K., 1995
[3] Nergis U. B. *Factors influencing the properties of ladder-knit fancy yarns.* In: Textile Research Journal, 2002, vol. 72, issue 8, p. 686
[4] Petrulyte, S. *Fancy yarns: Efforts to methodise, Problems and new suggestions.* In: Materials Science, 2004, vol. 10, issue 1, p. 85
[5] Gong, R. H., Wright, R. M. Fancy yarns. Their Manufacture and Application. The Textile Institute, Wood head Publishing Ltd. U.K, ISBN 1 85573 577 6, 2002, pp. 55, 81
[6] Čiukas, R., Tvarijonavičiené, B., Mikučioniené, D. *Estimating the linear density of fancy ribbon-type yarns and the structure indices of fabrics knitted from them.* In: Fibres & Textiles in Eastern Europe, 2006, vol. 14, issue 4, p. 41

[7] Turay, A., Özdil, N., Süpüren, G., Özçalik, G. *The effects of the production conditions of ribbon typed fancy yarns on the thermo-physiological properties.* In: Tekstil ve Konfeksiyon, 2009, vol. 4, p. 280
[8] Saville, B. P. *Physical testing of textiles.* Woodhead Publishing Limited, 2000
[9] Collier, B. J., Epps, H. H. *Textile testing and analysis.* Prentice Hall, New Jersey, 1999
[10] ISO 139:2005. *Textiles – Standard atmospheres for conditioning and testing*
[11] ISO 9237:1995. *Textiles – Determination of the permeability of fabrics to air*
[12] Kumpikaité, E., Ragaišiené, A., Barburski, M. *Comparable analysis of the end-use properties of woven fabrics with fancy yarns. Part I: Abrasion resistance and air permeability.* In: Fibres & Textiles in Eastern Europe, 2010, vol. 18, issue 3, p. 56
[13] Joseph, M. L. *Introductory textile science.* Fifth Edition CBS College Publishing. Prentice Hall, USA, 1986

Authors:

Dr. ERHAN KENAN ÇEVEN
Uludag University
Faculty of Engineering and Architecture
Textile Engineering Department
Gorukle, 16059, Bursa, Turkey
e-mail: rceven@uludag.edu.tr

CRONICĂ

TEXPROCESS 2011

Târgul internaţional pentru prelucrarea materialelor textile flexibile *Texprocess*, care s-a desfăşurat la Frankfurt am Main, în perioada 24–27 mai 2011, a debutat cu succes: 16 000 de vizitatori din 86 de ţări din Europa Centrală, Europa de Est, Asia şi Africa de Nord au venit pentru a vedea o gamă cuprinzătoare de exponate şi 330 de lideri în tehnologia internaţională, din 40 de ţări, au prezentat spectrul complet de soluţii inovatoare şi high-tech pentru industria textilă şi de confecţii.

Texprocess a avut loc în acelaşi timp cu *Techtextil –* Târgul internaţional pentru textile tehnice şi neţesute, care, la rândul său, a atras 24 500 de vizitatori. Techtextil este cea mai importantă platformă de marketing şi sourcing pentru clienţii şi producătorii de textile tehnice şi neţesute, cu un larg potenţial de aplicaţii în domeniul tehnic. Târgul a fost completat de o conferinţă, în care s-au prezentat punctele forte din domeniul inovării în sectoarele participante.

Prezenţa simultană în acelaşi loc a întregului lanţ de valori textile, de la aplicaţii industriale la proiecte de cercetare, s-a dovedit a fi o abordare reuşită.

Elgar Straub, director general al VDMA a afirmat: „Combinaţia Texprocess şi Techtextil este exact ceea ce era necesar acestui sector, aceasta având un mare succes atât în rândul expozanţilor, cât şi al vizitatorilor. Premiera a arătat că acest concept este calea de urmat. Sunt sigur că atmosfera pozitivă care domneşte aici se va reflecta în comenzi remarcabile".

Gama largă de produse expuse a prezentat interes nu numai pentru participanţii din sfera industriei textile şi de confecţii, ci şi pentru cei din industria automobilelor şi a mobilei.

Un mare succes a înregistrat *IT Market Place, Network@Texprocess.* Cei aproximativ 60 de expozanţi IT, prezenţi la Texprocess, au fost foarte mulţumiţi de calitatea şi numărul vizitatorilor, în special de reacţia Europei de Est şi a Federaţiei Ruse.

O reacţie excelentă a înregistrat *Texprocess Forum,* care a promovat schimbul de idei şi opinii pe plan internaţional. Cele 42 de prezentări de înalt nivel, pe teme de outsourcing, sustenabilitate şi responsabilitate socială corporativă, audiate de circa 943 de participanţi, au fost repartizate pe parcursul celor trei zile de desfăşurare a târgului. Texprocess Forum a fost organizat de asociaţia Dialog Textile Apparel, în cooperare cu asociaţia GermanFashion, Euratex şi omologul său internaţional, International Apparel Federation.

Peste 60 de companii din 19 ţări au făcut prezentări la *Texprocess Source it!* şi au fost mulţumite de calitatea şi concepţia evenimentului. Cele mai mari pavilioane internaţionale au provenit din Mauritius, Portugalia şi America de Sud.

Informaţii de presă. Messefrankfurt, mai 2011

Design Gabor filters in the frequency domain for unsupervised fabric defect detection

XINGYE ZHANG
RURU PAN
JIHONG LIU

WEIDONG GAO
WENBO XU

REZUMAT – ABSTRACT – INHALTSANGABE

Proiectarea domeniului de frecvenţă a filtrelor Gabor, pentru detectarea nesupravegheată a defectelor din ţesătură

În lucrare este prezentată o schemă de utilizare a filtrelor Gabor în detectarea nesupravegheată a defectelor din ţesătură. Spre deosebire de abordările anterioare din literatura de specialitate, în care filtrele Gabor sunt aplicate în domeniul spaţial, acestea sunt concepute într-un anumit domeniu de frecvenţă, după cunoaşterea prealabilă a parametrilor de structură a ţesăturii şi a caracteristicilor defectelor. Imaginea ţesăturilor la intrare este filtrată într-un anumit domeniu de frecvenţă de către filtrele Gabor, reglate la o frecvenţă şi orientare prestabilită, pentru a obţine o imagine de ieşire ce conţine o cantitate minimă de informaţii privitoare la structura de fond, păstrând în acelaşi timp datele necesare pentru detectarea defectelor. Se poate stabili, apoi, un prag pentru separarea defectelor din imaginea ţesăturilor. Performanţa sistemului este evaluată pe ţesături cu diferite tipuri de defecte. Rezultatele obţinute arată că, prin utilizarea acestei scheme, pot fi detectate cu mare precizie defectele din ţesătură.

Cuvinte-cheie: detectare defecte, filtre Gabor, ţesături, structură, domeniu de frecvenţă

Design Gabor filters in the frequency domain for unsupervised fabric defect detection

A Gabor filters scheme is presented for unsupervised woven fabric defect detection in this paper. Contrast to most approaches proposed in the prior literature in which Gabor filters are realized in the spatial domain, the Gabor filters are designed in the frequency domain by using the prior knowledge of woven fabric structure parameters and defect characteristics in this scheme. An input woven fabric image is filtered in the frequency domain by the Gabor filters tuned to certain frequency and orientation, which produces an output image containing the minimum amount of background texture details while preserving defect details required for defect detection. A threshold can then be performed to segment defects from the woven fabric image. The performance of the system is evaluated on woven fabrics with different types of defects. The results indicate that the scheme can detect defects with an accurate detection rate.

Key-words: defect detection, Gabor filters, woven fabric, structure, frequency domain

Entwurf von Gabor-Filtern im Frequenzbereich für unüberwachte Fehleridentifizierung der Gewebe

In dieser Arbeit wird ein Gabor-Filter Schema für die unüberwachte Fehleridentifizierung der Gewebe vorgestellt. Im Vergleich zu den meisten Angehmethoden, vorgeschlagen in der Fachliteratur, bei welchen die Gabor-Filtern in Zeit-/Raumbereich dargestellt wurden, werden hier die Gabor-Filtern im Frequenzbereich entworfen mit Anwendung der Vorkenntnisse betreff Strukturparameter und Fehlereigenschaften der Gewebe. Ein Eingangsbild des Gewebes wird im Frequenzbereich anhand Gabor-Filtern gefiltert, es wird auf eine bestimmte Frequenz und Orientierung eingestimmt, um ein Ausgangsbild mit den Basisstruktureigenschaften zu erhalten, welche die Deffekteinzelheiten der Fehlererkennung bewahrt. Ein Grenzwert kann dann gesetzt werden um die Fehler vom Gewebebild zu trennen. Die Leistung des Systems wird auf Geweben mit unterschiedlichen Fehlertypen bewertet. Die Ergebnisse zeigen, dass dieses Schema Fehler mit einer guten Genauigkeit identifizieren kann.

Stichwörter: Fehleridentifizierung, Gabor-Filter, Gewebe, Struktur, Frequenzbereich

Quality control is an important component of modern manufacturing in the textile industry. Woven fabric defect detection is usually performed by human inspectors with an accuracy of about 70% [1]. The work of inspectors is very tedious and time consuming. They have to detect small defects that can be located in a wide area that is moving through their visual field. In addition, the effectiveness of visual inspection decreases quickly with fatigue. Hence, the implementation of an automated visual inspection system for defect detection in the textile industry is of importance.

Image analysis techniques are being increasingly used to automate the detection of defects. In last 20 years, woven fabric defect detection has been studied using several approaches, and defect detection techniques have been classified into three categories: statistical, spectral and model-based [2].

Among these methods, the spectral approaches constitute the largest number of woven fabric defect detection methods proposed in the literature. Uniform woven fabric textured images are composed of repetition of some basic texture primitives with a deterministic rule of displacement. The high degree of periodicity of basic texture primitives permits the usage of spectral features for the detection of defects. The major spectral approaches used for fabric defect detection are Fourier analysis [3, 4], Gabor filters [5, 6] and Wavelet transform [7, 8].

Among these spectral approaches, Gabor filters have been well recognized as a joint spatial/spatial-frequency representation for analyzing textured images that contain highly specific frequency and orientation characteristics and are therefore well suited for woven fabric defect detection.

Since a woven fabric consists of regular repeating units, woven fabric image is a typical textural image which possesses strong periodicity. Therefore, it is possible to extract much of their structural information from the frequency transforms. Gabor filters applied in woven fabric defect detection has been studied using various approaches. Detection approaches using Gabor filters can be realized in the spatial domain and frequency domain. Most approaches proposed in the prior literature were realized in the spatial domain. Optimal filter is often used to detect defects among spatial domain methods. In optimal filters, the selection of their parameters is crucial and difficult. A set of Gabor filter parameters were determined which minimized a Fisher cost function [5]. A pixel of defected texture was classified as defective or non-defective
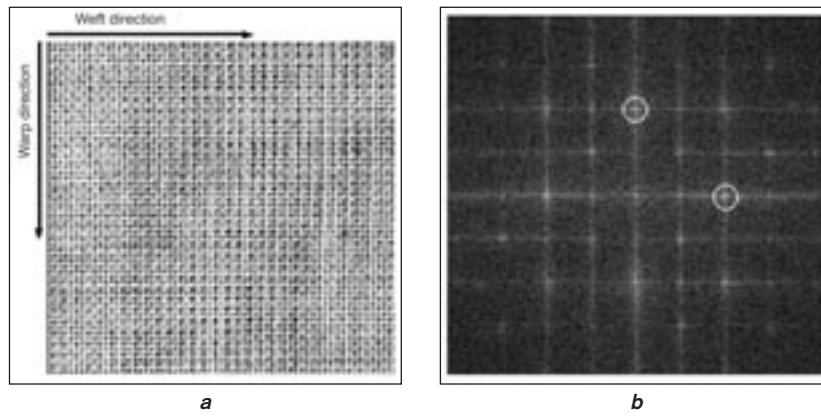
Fig. 1: **a** – woven fabric image; **b** – power spectrum

based on the Gabor filter response at that pixel. K. L. Mak and P. Peng designed Gabor filters on the basis of the texture features extracted optimally from a non-defective fabric image by using a Gabor wavelet network [6]. The defect detection scheme consisted of an odd symmetric real-valued Gabor filter, an even symmetric real-valued Gabor filter and one smoothing filter.

However, in the spatial domain, Gabor filtering methods are very computational expensive since the 2D convolution between the image and filters must be carried out in a sliding window throughout the entire image. Another problem of the above mentioned methods is that they made little use of prior knowledge about woven fabric structure parameters. In order to overcome these shortcomings, a Gabor filters scheme is proposed for automatic woven fabric defect detection in this study.

The design of Gabor filters is carried out in the frequency domain. The parameters of Gabor filters in the frequency domain are obtained by using the prior knowledge of woven fabric structure parameters and power spectrum derived from woven fabric image. The approach of Gabor filters design is proposed with a spectral characteristic analysis of woven fabric image. The results and discussion of the defect detection scheme are given and the summary for this study is presented finally.

GABOR FILTERS DESIGN
Gabor filters

A brief overview of Gabor filters is given first. In the spatial domain, the 2-D Gabor function is a Gaussian curve with aspect ratio modulated by a complex sinusoid [9]:

$$h(x,y) = g(x',y') \exp(2\pi j(Ux + Vy)) \quad (1)$$

where:

$(x',y') = (x\cos\theta + y\sin\theta, -x\sin\theta + y\cos\theta)$ are rotated coordinates;

U and V are frequencies along the x-axis and y-axis;

$g(x, y)$ is the following 2-D Gaussian:

$$g(x,y) = \frac{1}{2\pi\sigma^2} \exp\left[-\frac{(x/\lambda)^2 + y^2}{2\sigma^2}\right] \quad (2)$$

$F = \sqrt{U^2 + V^2}$ is the radial center frequency and the orientation is $\phi = \tan^{-1}(V/U)$.

In the frequency domain, the Fourier transform of the Gabor functions is:

$$H(u,v) = \exp\left\{-2\pi^2\sigma^2\left[(u'-U')^2\lambda^2 + (v'-V')^2\right]\right\} \quad (3)$$

where:

$(u',v') = (u\cos\theta + v\sin\theta, -u\sin\theta + v\cos\theta);$

$(U',V') = (U\cos\theta + V\sin\theta, -U\sin\theta + V\cos\theta).$

From equation (3), we see that the Gabor function is essentially a band pass filter centered about frequency (U, V), with bandwidth determined by σ. By varying the parameters of σ, U, V, θ, λ, Gabor filters of different frequency and orientations can be designed, which will aid in woven fabric defect detection.

Spectral characteristic analysis of woven fabric image

The design objective for the Gabor filters is to attenuate the background texture and accentuate simultaneously the defected parts. A woven fabric image often contains periodic structures, non-periodic elements, noise and background. It is difficult to separate and analyze these image components in the spatial domain since they are often embedded and entangled together. Fourier transform (FT) can be applied to monitor the frequency spectrum of a woven fabric image, in which different components will be separated by their frequencies. A periodic structure which constitutes the background texture in the image will result in a peak (a high magnitude area) in the power spectrum (fig. 1) [10]. Taking advantage of its band pass technique, the Gabor filters can be designed to restrain the frequency component of the background texture in the woven fabric image. Since peaks in the power spectrum represent periodic structure, the band-pass frequency can be constrained by excluding these peaks to attenuate the background texture.

As mentioned above, the power spectrum is derived from FT function. Since peaks in the horizontal direction correspond to warp yarn structure and peaks in the vertical direction correspond to weft yarn structure, one-dimension frequency analysis is performed in order

to explain clearly. A sequence {x(n)} can be represented by samples of its spectrum $X(\omega)$ [11].

$$X(\omega) = \sum_{n=0}^{N-1} x(n) e^{-j\omega n} \qquad (4)$$

where:

$X(\omega)$ is sampled at N equidistant frequency $\omega k = 2\pi k/N$, $k = 0, 1, ..., N - 1$.

$$X(\omega k) = X\left(\frac{2\pi k}{N}\right) \qquad (5)$$

$$X(k) = X\left(\frac{2\pi k}{N}\right) = \sum_{n=0}^{N-1} x(n) e^{-j2\pi kn/N} \qquad (6)$$

$$k = 0, \ 1, \ 2 \ ..., \ N - 1$$

For

$$\omega k = \frac{2\pi}{T} \qquad (7)$$

where:

$$\frac{2\pi}{T} = \frac{2\pi k}{N}$$

$$k = \frac{N}{T}$$

Since woven fabric is interlaced by warp yarn and weft yarn, one warp yarn (weft yarn) can be regarded as sampling once in the direction of warp yarn (weft yarn). The number of yarn is corresponding to the number of sampling.

The number of yarn:

$$m = \frac{N}{T} \qquad (8)$$

$$k = m \qquad (9)$$

As noted above, peaks in the power spectrum represent the periodic structure, the first peak which is nearest to origin in the horizontal (vertical) direction has relationship with the warp yarn (weft yarn) density of woven fabric. The distance between the first peak and the origin is equal to the numbers of yarn in woven fabric image. Then the numbers of yarn can be computed by the woven fabric density and the size of woven fabric image. For example, the warp density and weft density of the woven fabric (fig. 1a) are 70.2 ends/inch and, respectively, 70.2 picks/inch, and the size of the woven fabric image is 256 x 256 pixels. The image resolution is 0.0847 mm/pixel. By computing, the numbers of yarns in the woven fabric are 60 ends in both the warp and weft direction in the woven fabric image. Then the distances between the first peak and the origin are 60 pixels in both the horizontal and vertical direction in the power spectrum. The two white circles (fig. 1b) enclose the peaks which represent periodic yarn structure in the warp and weft direction respectively. Since the numbers of yarn can be computed easily, this relationship can be used to locate peaks and determine frequency parameters of Gabor filters.

Design for parameters of Gabor filters

The method proposed in this section obtains the proper parameters for the Gabor filters in the frequency domain according to the frequency spectral characteristic

of the woven fabric image discussed above and the characteristic of defects.

As the majority of woven fabric defects appear in the horizontal (or weft) and vertical (or warp) directions, only two values $\theta = 0$ and $\theta = \pi/2$ are considered for the orientation parameter. Parameter λ is set to 1 for most experiments get satisfactory results. F and σ are determined by the location of the peaks which can be gotten from the woven fabric density parameter. In order to attenuate the background texture, the pass-band frequency of filter should not include peaks. The central frequency F is located in the centre between the origin and the first peak and the width of pass band is smaller than the distance d between the origin and the first peak. The Gabor filters are then determined by the above parameters in the frequency domain.

The region of points, in the frequency domain, with magnitude equal 1/10 the peak magnitude can be obtained as follows:

$$\frac{1}{10} = \exp\left\{-2\pi^2\sigma^2\left[(u'-U')^2\lambda^2 + (v'-V')^2\right]\right\} \qquad (11)$$

$$-\ln 10 = -2\pi^2\sigma^2\left[(u'-U')^2 + (v'-V')^2\right] \qquad (12)$$

$$\left[(u'-U')^2 + (v'-V')^2\right] = \left(\sqrt{\frac{\ln 10}{2\pi^2\sigma^2}}\right) \qquad (13)$$

The equation (13) is a circle centered at (U', V') and the diameter d_p of the circle has length:

$$d_p = 2\sqrt{\frac{\ln 10}{2\pi^2\sigma^2}} \approx \frac{2}{3\sigma} \qquad (14)$$

$$\sigma \approx \frac{2}{3d_p} \qquad (15)$$

where:

d_p is set to $\frac{2}{3}$ d:

$$d_p = \frac{2}{3}d \qquad (16)$$

$$\sigma \approx \frac{1}{d} \qquad (17)$$

For woven fabric (fig. 2a) since the distance between the first peak and the origin is 60 pixels, the central frequency of its Gabor filters is set to 30 and σ is equal to $\frac{1}{60}$. Figure 2b shows intensity plots of Gabor filters with the above parameters.

DEFECT DETECTION SCHEME

The woven fabric defect detection scheme proposed in this paper is unsupervised and its block diagram is shown in figure 3. In the beginning of detection, the parameter of woven fabric density is required to input, which is used to locate peaks in the power spectrum. The parameters of Gabor filters in the frequency domain are determined using the approaches described in the above section of Gabor filters design. The woven fabric image is operated by fast Fourier transform (FFT)
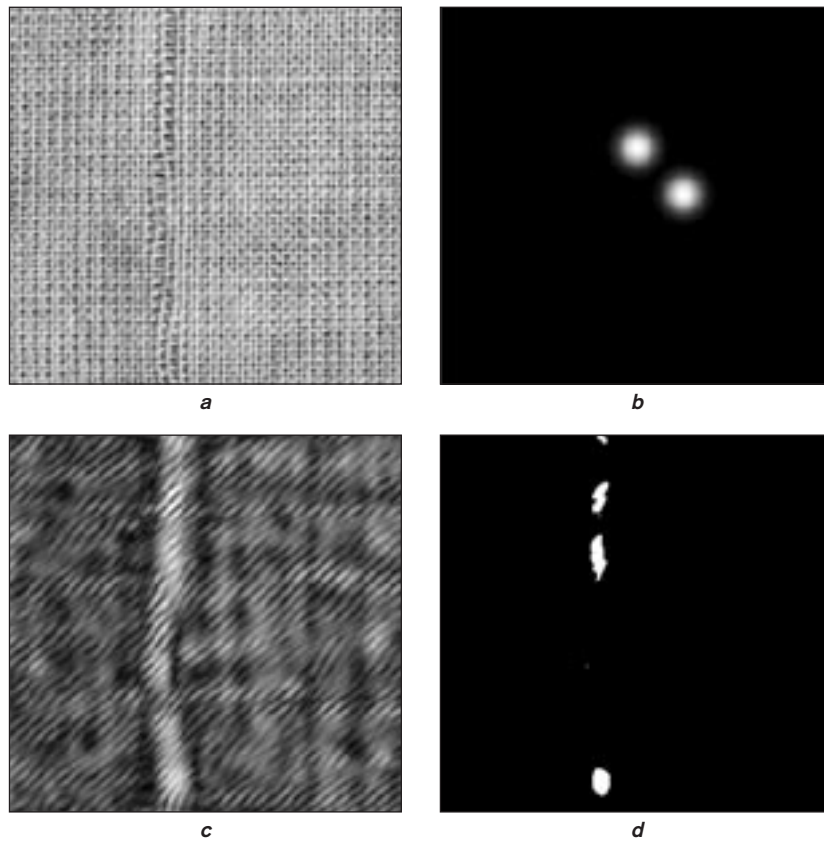
Fig. 2. Sample images:
a – defected woven fabric image; *b* – Gabor filters; *c* – filtered image; *d* – segmented defect

and then filtered by the Gabor filters designed in the frequency domain.

After the inverse Fourier transform (IFT) of the output filtered image and normalization, Gaussian filtering follows which is used to make image smooth and decrease the false detection. False detection was recognized when the defective areas of the output image do not only overlap the areas of the corresponding defects in the woven fabric image, but also appear in some other areas significantly distant from the defective areas, or when the defective areas appear in the output image even though the woven fabric image contains no defect. Since the false detections are always significantly smaller than detected defects, they could be eliminated by appropriate processing such as morphological operations or filtering operation. At last, the threshold operation is carried out. The threshold value limits λ_{max} and λ_{min} can be determined by the following equations:

$$\lambda_{max} = k_1 \cdot I_{mean} \tag{18}$$

$$\lambda_{min} = k_2 \cdot I_{mean} \tag{19}$$

where I_{mean} is the mean value of the output image. Pixel values which are higher than λ_{max} or lower than λ_{min} are considered defected pixels. k_1 and k_2 are determined by the following equations, respectively:
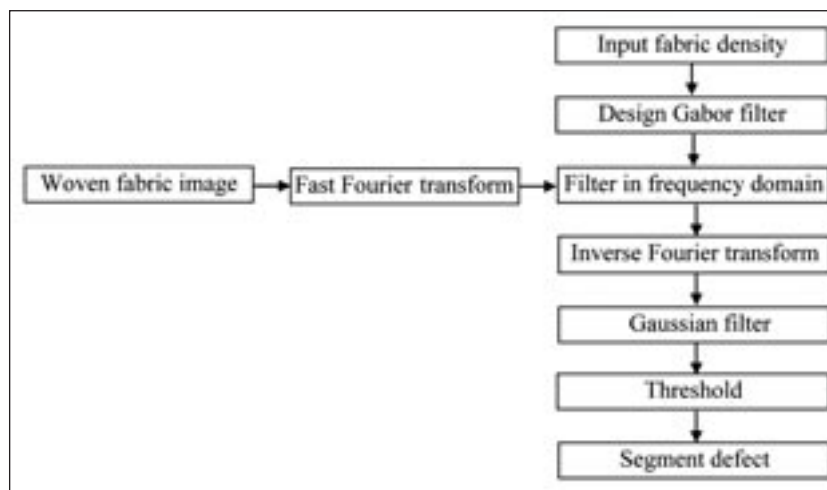
Fig. 3. Overall block diagram of the proposed algorithm
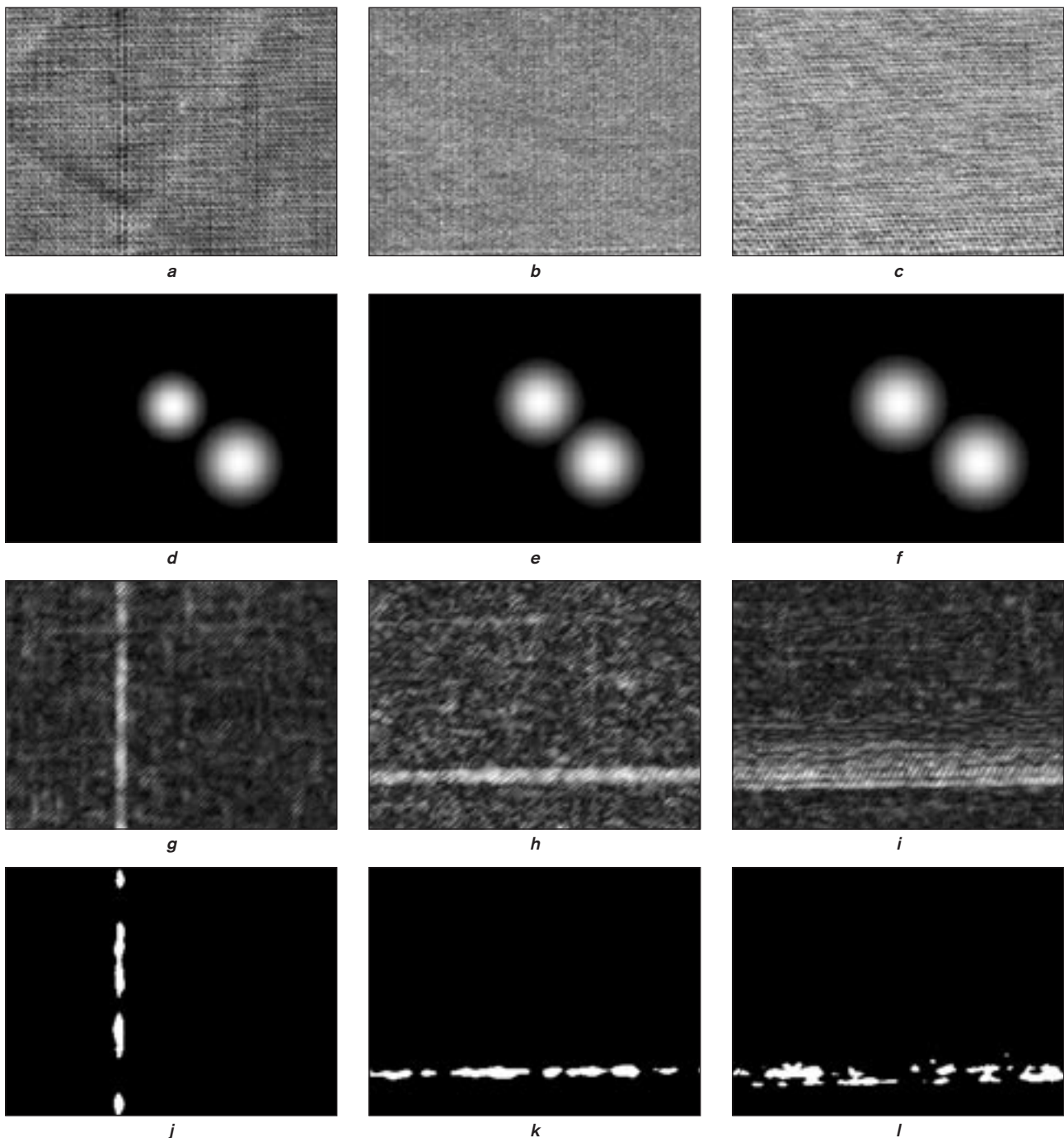
Fig. 4. Sample images and defect detection results:
a, *b*, *c* – defect woven fabric image; *d*, *e*, *f* – Gabor filters; *g*, *h*, *i* – filtered image; *j*, *k*, *l* – segmented defect

$$k_1 = \frac{I_{max}}{I_{mean}} \qquad (20)$$

$$k_2 = \frac{I_{min}}{I_{mean}} \qquad (21)$$

where:

I_{max}, I_{min} and I_{mean} are the maximum, minimum and mean value of the output image respectively, which is obtained via filtering a defect-free image. $I(x, y)$ is the output image for testing, then the output of defect segmented step is a binary image B governed by

$$B(x,y) = \begin{cases} 1, I(x,y) > \lambda_{max} \text{ or } I(x,y) < \lambda_{min} \\ \hline 0, \lambda_{min} < I(x,y) < \lambda_{max} \end{cases} \qquad (22)$$

The figure 2*c* and figure 2*d* show the output filtered image and the final detection result of the scheme. When compared with the original defected woven fabric image shown in figure 2*a*, it can be observed that defective areas are correctly detected and accurately localized.

RESULTS AND DISCUSSIONS

Performance of the proposed detection scheme was evaluated using a set of woven fabrics. A number of 30 fabric images are used in our test. In this paper, the images for detection have a size of 256 pixels x 256 pixels and an 8-bit gray level. The image resolution is 0.0847 mm/pixel. Figure 4 shows a set of typical sample images along with their corresponding Gabor filters and detect results.

The woven fabric defects tested in this study have various types. The defects which have obvious intensity changes can be easily detected via threshold techniques, while the defects which alter the textural property of woven fabric images are hard to detect using threshold techniques (fig. 4 *b,c*). Gabor filters are designed to attenuate background texture in order to increase the contrast between the defected parts and the background. Figure 4*d*, figure 4*e* and figure 4*f* show the Gabor filters designed for the corresponding woven fabric, from which it can be observed that different Gabor filter parameters are determined for different woven fabric. The Gabor filter parameters are obtained according to the approach described above. The output filtered images (fig. 4 *g, h, i*) and it can be seen that the background textures are attenuated and the defected parts are accentuated after filtering. Then the defected parts can be segmented by threshold techniques.

The detection results (fig. 4 *j, k, l*) which indicate that the defects were detected correctly and localized accurately. In our test, the true detection rate can achieve 80%.

In our study, the corresponding relationship between the woven fabric density and the peaks in the power spectrum of woven fabric image was found, which can be used to determine the parameters of Gabor filters. The input woven fabric image is filtered by the Gabor filters tuned to certain frequency and orientation, which produces an output filtered image containing the minimum amount of background texture details while preserving defect details required for defect detection. A threshold operation can then be performed to segment defects from the woven fabric image.

The advantages of our method are summarized as follows:
- make full use of prior knowledge about woven fabric structure parameters and defect characteristics;
- Gabor filters are designed using the relationship between the woven fabric density and the peaks in the power spectrum which is first presented in this paper;
- Gabor filtering is realized in the frequency domain, which can result in reducing the computation time.

CONCLUSIONS

A scheme based on Gabor filter to detect woven fabric defects has been described in this study. We make full use of prior knowledge of woven fabric structure parameters and the characteristics of defects to obtain the Gabor filter parameters. As the majority of woven fabric defects appear in the weft and warp directions, only two values $\theta = 0$ and $\theta = \pi/2$ are considered for the orientation parameter. Taking advantage of its band pass technique, Gabor filters are designed in the frequency domain to restrain the frequency component of the background texture. Since peaks in the power spectrum represent periodic structure, the radial center frequency *F* and the width of pass band frequency can be constrained by excluding these peaks to attenuate the background texture. The relationship between the peaks and woven fabric density has been discovered to locate peaks, which can be used to determine the center frequency and scaling parameters of Gabor filters. The method of Gabor filters design in the frequency domain is simple and effective.

The performance of the proposed woven fabric defect detection scheme has been evaluated by using a set of woven fabric images. The experimental results obtained have indicated that the scheme performs very well in detecting woven fabric defects. The future work is to apply the woven fabric defect detection scheme into real-time industrial environment.

BIBLIOGRAPHY

[1] Sari-Sarraf, H., Goddard, J. S. *Vision systems for on-loom fabric inspection.* In: IEEE. Trans. Ind. Appl.*,* 1999, vol. 35, issue 6, p. 1 252
[2] Kumar, A. *Computer-vision-based fabric defect detection: A survey.* In: IEEE. Trans. Ind. Electron., 2008, vol. 55, issue 1, p. 348
[3] Chan, C. H., Pang, G. K. H. *Fabric defect detection by Fourier analysis.* In: IEEE. Trans. Ind. Appl.*,* 2000, vol. 36, issue 5, p. 1 267
[4] Tsai, I. S., Hu, M. C. *Automatic inspection of fabric defects using an artificial neural network technique.* In: Textile Research Journal, 1996, vol. 66, issue 7, p. 474
[5] Bodnarova, A., Bennamoun, M., Latham, S. *Optimal Gabor filters for textile flaw detection.* In: Pattern Recognition, 2002, vol. 35, issue 12, p. 2 973
[6] Mak, K. L., Peng, P. *An automated inspection system for textile fabrics based on Gabor filters.* In: Robot. CIM - Int. Manuf., 2008, vol. 24, issue 3, p. 359
[7] Kim, S., Lee, M. H., Woo, K. B. *Wavelet analysis to defects detection in weaving processes.* In: Proc. IEEE. Int. Symp. Ind. Electron., 1999, vol. 3 , p. 1 406
[8] Tsai, D. M., Chiang, C. H. *Automatic band selection for wavelet reconstruction in the application of defect detection.* In: Image Vision Comput., 2003, vol. 21, issue 5, p. 413
[9] Daugman, J. G. *Uncertainty relations for resolution in space spatial frequency and orientation optimized by two-dimension visual cortical filters.* In: J. Opt. Soc. Am. A, 1985, vol. 2, issue 7, p. 1 160
[10] Xu, B. *Identifying fabric structures with fast Fourier transform techniques.* In: Textile Research Journal, 1996, vol. 66, issue 8, p. 496
[11] Proakis, J. G., Manolakis, D. G. *Digital Signal Processing.* In: Publishing House of Electronics Industry, Beijing, 2007
[12] Nicolaiov, P., Loghin, C., Hanganu, L. C. *Flexibility in technological process design – a key factor for developing new generations of textile equipments based on intelligent mechatronic systems.* In: Industria Textilă, 2010, vol. 61, issue 4, p. 157

Authors:

Chief of work dr. eng. XINGYE ZHANG
Conf. dr. eng. RURU PAN
Conf. dr. eng. JIHONG LIU
Conf. dr. eng. WEIDONG GAO
Conf. dr. eng. WENBO XU

Jiangnan University
LiHu Road, no. 1800
Wuxi, 214122 China
e-mail: zxy1995@163.com;
liujihongtex@hotmail.com

Pad-microwave – a novel method for manufacturing hydrophobic fabrics

AZIMEH POULADCHANG NAJAFABADI

AKBAR KHODDAMI
ZAHRA MAZROUEI-SEBDANI

REZUMAT – ABSTRACT – INHALTSANGABE

Fulardarea-fixarea cu microunde – o nouă metodă de realizare a materialelor textile hidrofobe

Tehnologia clasică de aplicare, prin fulardare-uscare-condensare la temperatură înaltă, a produselor fluorcarbon pe diferite materiale textile a fost comparată cu o nouă tehnologie de folosire prin fulardare-fixare cu microunde. Au fost evaluate proprietățile de respingere a lichidelor, de rezistență a vopsirii, precum și cele de hidrofobizare, înainte și după spălare, folosind testele 3M de respingere a apei/uleiurilor. Au fost comparate proprietățile mecanice ale materialelor textile, prin determinarea rezistenței la tracțiune. Rezultatele obținute au demonstrat eficiența procesului de fulardare-fixare cu microunde în crearea unei tensiuni de suprafață scăzute, pentru obținerea de materiale textile hidrofobe.

Cuvinte-cheie: suprafață hidrofobă, tensiune de suprafață, fulardare-uscare-condensare, fulardare-fixare cu microunde

Pad-microwave – a novel method for manufacturing hydrophobic fabrics

Traditional fluorocarbon application technology (pad-dry-cure at high temperature) on different textile fabrics was compared with a novel pad-microwave technique. Liquid repellency properties of the fabrics, before and after washing, fastness properties and decay of hydrophobicity, were evaluated using the 3M water/oil repellency tests. Fabrics mechanical properties were compared by measuring tensile strength. The results indicated the usefulness of the pad-microwave process to create low energy surface for engineering hydrophobic fabric.

Key-words: hydrophobic surface, surface energy, pad-dry-cure, pad-microwave

Das Mikrowellen-Foulardieren – eine neue Fertigungsmethode für hydrophobe Textilmaterialien

Die klassische Anwendungstechnologie (Foulardier-Trocknung-Kondensierung bei hoher Temperatur) wurde mit der neuen Mikrowellen-Foulardiertechnologie auf unterschiedlichen Textilmaterialien verglichen. Es wurden die Eigenschaften der Flüssigkeitsabstossung, des Farbwiderstands, sowie die Hydrophobisierung, vor und nach dem Waschen bewertet, mit Anwendung der 3M Teste für Wasser/ Ölabstossung. Die mechanischen Eigenschaften des Textilmaterials wurden durch Bestimmung des Zugwiderstandes verglichen. Die erzielten Ergebnisse haben die gute Leistung des Mikrowellen-Foulardierprozesses für die Erhaltung einer geringen Oberflächenspannung bei hydrophoben Textilmaterialien bewiesen.

Stichwörter: Hydrophobe Oberfläche, Oberflächenspannung, Foulardier-Trocknung-Kondensierung, Mikrowellen-Foulardieren

Finishes that repel water, oil and dry dirt are important in all parts of the textile market – for clothing, home and technical textiles [1, 2]. For the solid substrate, when the water contact angle is larger than 90°, it is called hydrophobic surface that drops of water do not spread on the surface of the textile [1]. In order to fabricate water repellent materials, the critical surface tension of the fiber's surface must be lowered by surface coating via chemicals such as fluorochemicals [3, 4]. Padders, consists of a pair of squeeze rolls, have been used to apply chemical finishes for a long time, while there are different methods to dry the wet fabric [3].

Microwaves are high frequency, electromagnetic waves composed of electrical and magnetic fields nowadays used in textile drying process because of its lowering of energy consumption, short start-up period, reliable drying, low cost, and environmentally friendly aspects [5, 6, 7]. So it is believed that trend to this technology will increase in the near future [5]. There have been attempts to fabricate water repellent and super water repellent fiber and textiles in a different methods [8, 10], but no research work has been reported applying microwave to cure repellent finished fabrics.

In this paper, the efficiency of new method of pad-microwave in producing water repellent fabrics was investigated and compared with the traditional method of pad-dry-cure. The required low surface energy layer was obtained by a fluorochemical for all samples.

EXPERIMENTAL PART
Materials used

Cotton fabric (100%, 170 g/m^2), polyester fabric (100%, 130 g/m^2), cotton-polyester fabric (40–60%, 190 g/m^2) and acrylic fabric (100%, 180 g/m^2) all with plain weave were used as the substrates. All chemicals were of analytic grade from Merck, Germany. The selected fluorocarbon was Rucostar EEE from Rudolf, Germany, and used non-ionic detergent was Sera Wet C-NR, from DyStar.

Fabric preparation

The fabrics were firstly washed to remove any possible impurities which can adversely affect the surface treatments by 1 g/l non-ionic detergent and 0.2 g/L sodium carbonate (*p*H 8-9) with L:R of 30:1 at 70-80°C for 60 minute. Then samples rinsed for 60 minute and air dried without any tension.

Fabric treatment
Fabrics' water repellent treatment by pad-dry-cure method

The scoured fabrics were impregnated in a treatment bath containing 50 g/L Rucostar EEE, and acetic acid to adjust *p*H. Subsequently, the sample was passed through a two-roll laboratory padder (Mathis, Switzerland). This treatment gave a wet pickup of 100%. After drying (1 minute, 100°C) the fabric was cured for 1 minute at 170°C in a lab dryer (Warner Mathis AG, Niederhasli/Zürich).

Table 1

WATER REPELLENCY OF FLUOROCHEMICAL TREATED COTTON FABRICS IN DIFFERENT MICROWAVE POWERS AND TIMES				
Treatment	Microwave power, W	Microwave time, minute	3M water repellency test	3M oil repellency test
Pad-dry-cure	–	–	9	7
Pad-microwave	120	15	5	3
	240	10	6	3
	360	10	7	4
	480	5	7	4–5
	600	4	8	6–7

Table 2

WATER REPELLENCY OF FLUOROCHEMICAL TREATED COTTON FABRICS IN DIFFERENT MICROWAVE PICK-UP AND TIMES				
Treatment	Wet pick-up	Microwave time, minute	3M water repellency test	3M oil repellency test
Pad-microwave	70	2	7–8	5
	70	3	7–8	5
	70	4	8–9	6
	80	2	7–8	5
	80	3	8	5–6
	80	4	8–9	6
	100	2	8	5–6
	100	3	8	6
	100	4	8–9	6

Fabrics' water repellent treatment by pad-microwave method

The scoured fabrics were impregnated in a treatment bath and passed through a two-roll laboratory padder, according to the above mentioned conditions. This treatment gave a wet pickup of 100%. Then, the samples were exposed to the microwave (Panasonic, Sanyo) at different powers of 120, 240, 360, 480 and 600 W, in variety of times by which the appropriate time of drying for the next experiments was obtained.

To find out the optimum pad-microwave conditions for the fluorocarbon finishing the samples were tested by 3 different wet pick-up, 70, 80 and 100%, and dried in 3 different times, 2, 3 and 4 minute, using the optimum power of 600 W.

According to the obtained results, the next experiments were carried out on all kind of tested fabrics by wet pick-up of 70% and 600 W microwave power for 4 minute.

Evaluation methods

The treated samples were tested for oil and water repellency according to the 3M tests [12, 13]. The samples were tested for water repellency using the water/alcohol drop test. The samples are placed flat on a smooth, horizontal surface. Beginning with the lowest numbered test liquid, 3 small droplets (approximately 5 mm in diameter) are placed onto the sample using a pipette. The droplets are observed for 10 s. If after 10 s, 2 of the 3 droplets are still visible as spherical to hemispherical, the fabric passes the test. Samples are rated as pass or fail of the appropriate test liquid, W-10. The rating given to a sample is for the highest test liquid remaining visible after 15 s. In general, water repellency rating of 2 or greater is desirable [10].

For the oil repellency, the samples are placed flat on a smooth, horizontal surface. Beginning with the lowest numbered test oil, small droplets (approximately 5 mm in diameter) are placed onto the sample using a pipette. The droplets are observed for 30 s from a 45° angle. If the droplet neither wets the fabric, nor has any sign of wicking the test is repeated using the next numbered oil. This is continued until an oil sample is found to either wet the fabric or show signs of wicking. The oil repellency rating is deemed to be the highest numbered test oil which does not wet the fabric within 30 s. Wetting of a substrate is normally seen by darkening of the substrate at the liquid-substrate interface. On dark colored samples wetting can be detected by loss of 'sparkle' within the droplet [11].

In addition, the re-orientation of fluorocarbon polymer chains after wet processing, decay of hydrophobicity, was evaluated in accordance with AATCC Test Method 61-1994 tests no. 2A by Polymat (AHIBA1000 Datacolor/Zürich) in order to assess how samples keep their performance after washing and hot-pressing (120°C for 2 minutes).

Determination of fabrics tensile properties were studied according to BS 13934-1:1999 test method on an Instron model 5564, with gauge length of 0.1 m, crosshead speed of 0.050 m/minute and 10 tests for each sample.

The effect of microwave irradiation on the samples shades, yellowness, the fabrics were measured by Data Colour reflectance spectrophotometer, Spectraflash model 600+, under D65 illumination source, with large aperture and 0% UV. Sample was measured in a triple-folded state to make it opaque at 4 points and an average value was determined.

RESULTS AND DISCUSSIONS

The first series of experiments were carried out on the cotton fabric. After passing fluorochemical saturated fabric between pad rollers, they were exposed to microwave irradiation in 5 different power levels for necessary time to dry the sample. Accordingly, the lower the applied microwave power, the longer irradiation time is required (table 1). Comparing the repellent properties of the pad-microwave treated samples with those samples finished with the conventional pad-dry-cure, PDC, method using dry heat by a lab stenter indicate that PDC method leads to maximum oil and water repellency with 3M water repellency of 9 and oil repellency of 7 while the pad-microwave, PM, best results were 3M water repellency of 8 and oil repellency of 6–7. In addition, it was revealed that the higher the microwave power, the better repellent properties could be achieved with shorter exposing time. This effect could be due to incomplete cure of fluorochemical layer in the lower powers as a consequence of lack of enough energy to polymerize the polymer.

Subsequently, the highest applied microwave power, 600 W, and maximum irradiation time of 4 minutes were selected to evaluate the other effective parameters on the repellent finishing of the substrate by PM procedure.

Table 3

		3M water repellency test			3M oil repellency test		
WATER REPELLENCY OF DIFFERENT FLUOROCHEMICAL TREATED FABRICS							
Treatment	Type of fabric	Before washing	After washing	After hot-pressing at 120°C	Before washing	After washing	After hot-pressing at 120°C
Pad-dry-cure	Cotton	9	2	9	7	0	7
	Cotton-polyester	9	2	8	7–8	0	7
	Polyester	9	1	9	7–8	0	7
	Acrylic	8	1	8	6	0	6
Pad-microwave	Cotton	8	1	8	6	0	6
	Cotton-polyester	7	1	8	6	0	6
	Polyester	6	1	9	4	0	7
	Acrylic	7	1	9	5	0	7

The effect of fabric impregnation by the fluorochemical on the cotton sample performance was studied using 70, 80 and 100 percent wet pick-up (table 2). The results indicate that 70% wet pick-up is fair enough for the fluoropolymer to form a film on the top most layers of hydrophilic cotton fibres. Thus, there is no necessity to use higher add-on which is more acceptable for economical aspects, lower chemicals cost and lower energy to cure the polymer. Furthermore, it is evident that the increase in exposing time from 2 minutes to 4 minutes does not have significant effect on the obtained repellent properties. However, 4 minute microwave irradiation was used, in order to assure complete drying and curing, for the rest of experiments with applied power of 600 W and 70% wet pick-up.

After confirmation of the validity of new finishing method, it was crucial to examine the usefulness of the procedure for the other textile substrates. Therefore, in addition to cotton, cotton-polyester, one of the most common blend fabrics, polyester, and acrylic fabrics were finished using the fluorochemical by PM and conventional PDC methods.

The results showed in table 3 indicate that although the level of the obtained repellency depends on the fibres type, the high repellent fabric can be manufactured by the new PM method. However, the 3M water and oil repellency of the PDC method are more or less higher than the comparable PM finished samples. The difference between achieved repellency by two methods initiate from the nature of the treatments. It seems that drying at 100°C and curing at 170°C transfers more energy to the textile substrates than the microwave irradiation under tested conditions because after washing and hot-pressing, the synthetic fibre fabrics and their blend showed better oil and water repellency. In other words, after heating the PM fluorocarbon finished samples enhances the fabric performance with better air ward orientation of the fluorocarbon chain.

The results of table 3 also reveal that the applied fluorocarbon, Rucostar EEE, is a hybrid fluorochemical. Applying a block copolymer, Rucostar EEE, containing both highly fluorinated and highly hydrophilic polymer segments within a single chain molecule, the required surface energy in air or in an aqueous environment can be obtained. Thus the hybrid fluorochemical functions effectively as a stain repellent in air and also as an effective oily soil release finish in washing. Accordingly,

fluorocarbon finished samples using PDC method with no after treatment show high repellent properties (table 3). Furthermore, studying repellency properties after washing revealed that the samples lost their repellency due to the surface movement of the fluorocarbon segments which can be resulted from the effects of polarity and surface tension of the environments on polymer chains [12, 13]. This decay of the hydrophobicity, not retrieving original configuration, is a drawback of this finishing. As tables 3 indicate, the re-orientation of Rucostar EEE during air drying is incomplete. Therefore, they need to be hot pressed to retrieve their original repellency performances. However, these results indicate that the treated sample by the PDC method has no fastness problems, therefore after activation the fluorocarbons molecules by high temperature. They show high level of water and oil repellency, 3M water repellency of 8–9.

Samples treated with PM method showed the same trends as the samples treated with PDC method and almost similar deficiency of molecular re-orientation after washing. Once again, for the PM finished samples the decay of the repellency after wet treatment is not on account of removing of the hydrophobic moieties, because they retrieve their original repellency performance after hot pressing at 120°C. So migrations of hydrophobic moieties caused by the water are at least partially reversible. The buried fluorine-containing moieties migrate toward the surface on heat treatment [16]. In spite of the decay of hydrophobicity after washing, all treated samples show minimum 3M water repellency of 1–2 which is fair enough for water repelling.

Moreover, the results indicate the acceptable durability and wash fastness of the samples finished with both PM and PDC methods.

Tensile strength of fluorocarbon finished samples as can be seen in table 4 does not show statistically significant difference. This effect could be due to the nature of fluorocarbon finishing that is of surface treatment in which the bulk of substrates would not be affected. In this finishing a thin surface layer covered the topmost surface layer. Accordingly the bulk properties like tensile strength more or less remained intact. In addition, comparison of the differences in the samples tensile strength finished by both methods show no clear pattern so that it can be said that the finishing by the PM method has no adverse effect with

TENACITY CHANGE IN HYDROPHOBIC FINISHED SAMPLES		
Treatment	Fabric	Change of tenacity*
Pad-dry-cure	Cotton	−7.6
	Cotton-polyester	−1.6
	Polyester	−2.0
	Acrylic	3.1
Pad-microwave	Cotton	−4.9
	Cotton-polyester	−2.5
	Polyester	−3.5
	Acrylic	4.6

* Minus shows the tenacity loss compared with control sample

Table 5

YELLOWNESS INDEX OF HYDROPHOBIC FINISHED SAMPLES		
Treatment	Fabric	Yellow index*
Pad-dry-cure	Cotton	−8.7
	Cotton-polyester	−24.5
	Polyester	21.4
	Acrylic	34.1
Pad-microwave	Cotton	−11.6
	Cotton-polyester	−31.3
	Polyester	13.2
	Acrylic	9.1

* Minus shows the tenacity loss compared with control sample

less than 10% reduction in the samples tenacity which is so important for industrial applications.

From the results it appeared that the fabric's yellowness were affected by the finishing method and the type of fibre in which having cotton fibres as a hydrophilic substrate reduced the samples yellowness of the PM treated samples while using polyester and acrylic fibres with hydrophobic nature, in fluorocarbon finishing by PM method adversely influenced the yellowness. However, comparison the PDC and PM methods indicate that application of dry heating method with high temperature in PDC procedure enhanced the yellowness more than PM method. In other words, coating these samples with a fluorocarbon film, via PM finishing method, decreased the samples yellowness.

CONCLUSIONS

In this work, a new method was established to manufacture hydrophobic surface via pad-microwave method compared to the conventional pad-dry-cure method.

The results indicated that proper hydrophobicity would be created on different fabrics with pad-microwave method, at power of 600 W for short treatment time as 2–4 minutes. This novel method not only can be down in one short step, compared to pad-dry-cure method that is done in two steps, dry and cure, but also does not show any adverse effect on the samples tensile strength as well as yellowness index. In addition, it was clarified that, the decay of hydrophobicity in this process is not at that level to diminish the samples water repellency. Over all, using the pad-microwave, as novel method for textile finishing and particularly fluorocarbon finishing, it could be possible to decrease the energy consumption with short start-up period, as well as reliable drying and finishing, low cost, and having environmentally friendly process.

BIBLIOGRAPHY

[1] Schindler, W. D., Hauser, P. J. *Chemical finishing of textiles.* Wood head Publishing Limited, Cambridge England, 2004, p. 74
[2] Carr, M. C. *Chemistry of the textile industry.* Department of textile, UMIST, Blackie Academic & Professional, 1995, p. 210 (Chapter 7)
[3] Tomasino, C. *Chemistry & technology of fabric preparation & finishing.* North Carolina State University, 1992, p. 154 (Chapter 9)
[4] Holme, I. *Innovative technologies for high performance textiles.* In: Coloration Technology, 2007, vol. 123, p. 59
[5] Mallakpour, S. H., Rafiee, Z. *Application of microwave assisted reactions in step growth polymerization.* In: Iranian polymer journal, 2008, vol. 17, nr. 12, p. 907
[6] Neral, B., Turk, S. S., Schneider, R. *Microwave fixation of ink-jet printed textiles.* 4th International Textile, Clothing and Design Conference-Magic World of Textiles, 2008
[7] Fang, C. Y., Hai, Y., Zhiwei, L. *An investigation on microwave dying of cotton fabrics.* In: Journal of China Textile University, 1993, vol. 10, nr. 1, p. 25
[8] Nishino, N., Meguro, M., Nakamae, K., Matsushita, M., Ueda, Y. *The lowest surface free energy based on -CF3 alignment.* In: Langmuir, 1999, vol. 15, p. 4 321
[9] Morra, M., Occhiello, E., Grabassi, F. *Contact angle hysteresis in oxygen plasma treated poly (tetrafluoroethylene.* In: Langmuir, 1989, vol. 5, p. 872
[10] *3M Technical Data. Test Method.* Water Repellency Test II- Water/Alcohol Drop Test, 1996
[11] *3M Technical Data. Test Method.* Oil Repellency Test I, 1996
[12] Khoddami, A., Avinc, O., Mallakpour, S. *A novel durable hydrophobic surface coating of poly (lactic acid) fabric by pulsed plasma polymerization.* In: Progress in Organic Coatings, 2010, vol. 67, p. 311
[13] Inagaki, N., Tasaka, S., Mori, K. *Hydrophobic polymer films plasma-polymerized from CF3/hydrocarbon and hexafluroacetone/hydrocarbon mixtures.* In: Journal of Applied Polymer Science, 1991, vol. 43, p. 581
[14] Yasuda, T., Okuno, T., Yoshida, K. *A study of surface dynamics of polymers. P. II. Investigation by plasma surface implantation of fluorine-containing moieties.* In: Journal of Polymer Science: Part B, Polymer Physics, 2003, vol. 26, p. 1 781

Authors:
AZIMEH POULADCHANG NAJAFABADI
AKBAR KHODDAMI
ZAHRA MAZROUEI-SEBDANI
Isfahan University of Technology
Department of Textile Engineering
Isfahan 84156-8311, Iran
e-mail: a.pouladchangnajafabadi@tx.iut.ac.ir
khoddami@cc.iut.ac.ir
z.mazrouei@tx.iut.ac.ir

Analysis of thermal degradation kinetics of high performance fibers at air, by thermogravimetry

GUANGMING CAI   WEIDONG YU

REZUMAT – ABSTRACT – INHALTSANGABE

Analiza cineticii degradării termice la aer a fibrelor de înaltă performanţă, prin termogravimetrie

Fibrele de înaltă performanţă, cum ar fi cele polimerice, au aplicaţii extinse în industria aerospaţială şi în mediile cu temperaturi ridicate. Atunci când aceste fibre sunt utilizate la temperatură înaltă, acestea sunt supuse degradării. Tehnica de analiză termogravimetrică a fost utilizată pentru a evalua degradarea termică şi parametrii cinetici ai fibrelor de înaltă performanţă, la 50–800°C în aer. Procentul de descompunere a fibrelor şi temperaturile caracteristice au fost obţinute din curbele TG şi DTG. Cinetica degradării termice a fost analizată conform metodei Freeman-Carroll şi au fost estimate energiile de activare a fibrelor. Astfel, s-au obţinut date privind energia de activare şi reacţia de degradare a patru tipuri de fibre de înaltă performanţă. S-a constatat că, în condiţiile celei mai ridicate temperaturi iniţiale de degradare a PBO, energia sa de activare în aer nu este cea mai ridicată. Dacă temperatura de degradare iniţială a fibrei Nomex are valoarea cea mai scăzută, temperatura de descompunere finală a fibrei Nomex are valoarea cea mai ridicată.

Cuvinte-cheie: fibre de înaltă performanţă, parametri cinetici, degradare termică, metoda Freeman-Carroll, fibre polimerice

Analysis of air thermal degradation kinetics of high performance fibers at air, by thermogravimetry

High performance fibers, such as polymer material, have extensive applications in aerospace and high temperature environment. When these fibers were used in such high temperature, these would be subjected to degradation. Thermogravimetry analysis technique has been performed for evaluating the thermal degradation and the kinetics parameters of high performance fibers from 50 to 800°C under air atmosphere. The decomposition rate and the characteristic temperatures of fibers are achieved from both the TG and DTG curves. The kinetics of the thermal degradation has also been analyzed according to the Freeman-Carroll method and the activation energies of the fibers were estimated. The respective activation energy and reaction order of the degradation of four kinds of high performance fibers are achieved. It indicated that the initial degradation temperature of the PBO is the highest but its activation energy is not the highest in air. The initial degradation temperature of Nomex fiber is the lowest, but the end decomposition temperature of Nomex is highest.

Key-words: fibers, high performance, kinetics parameters, thermal degradation, Freeman-Carroll method, polymer material

Thermogravimetrie-Analyse der thermischen Abbaukynematik der Hochleistungsfaser in Luftgegenwart

Die Hochleistungsfaser, wie die Polymerischen Faser, haben breite Anwendungen in der Luftfahrt und bei Hochtemperaturen. Diese Faser sind bei Hochtemperaturen einem Abbau ausgesetzt. Es wurde die Thermogravimetrische-Analysetechnik angewendet um den thermischen Abbau und die kynetischen Parameter der Hochleistungsfaser zu bewerten, bei 50–800°C in der Luft. Das Abbauprozent und die charakteristischen Fasertemperaturen werden sowohl von TG als auch von DTG Kurven erhalten. Die Kynematik des thermischen Abbaus wurde gemäss der Freeman-Caroll Methode analysiert und es wurde die Faser-Aktivierungsenergie eingeschätzt. Es wurde die entsprechende Aktivierungsenergie und Reaktionsreihenfolge des Abbaus von vier Hochleistungsfasertypen erzielt. Man kann schlussfolgern, dass die ursprüngliche Abbautemperatur der PBO den höchsten Wert hat, jedoch seine Aktivierungsenergie nicht den höchsten Wert in der Luft hat. Die ursprüngliche Abbautemperatur der Nomex-Faser hat den niedrigsten Wert, jedoch die Endzersetzungstemperatur der Nomex-Faser hat den höchsten Wert.

Stichwörter: Hochleistungsfaser, kynematische Parameter, thermischer Abbau, Freeman-Caroll Methode, polymerische Faser

Polymers have found applications in each branch of our daily life. Some of these applications require a deep knowledge about the durability and a predictability of the properties under different environmental conditions and over long periods to cover the whole lifetime of the object. In the last few decades, the demand of advanced industries, particularly the aerospace, has been the driving force for the development and applications of high performance fibers in many fields, such as structural, composite, and reinforced materials. To know and evaluate the thermal degradation behavior of materials under the thermal environment, effective characterization and research methods must be adopted. Thermogravimetry (*TG*) is an important technique to characterize the thermal degradation of polymer under different atmospheres. Many previous studies have focus on the thermal aging of high-performance fibers by *TG*. Many studies have discussed on the thermal degradation behavior of Kevlar and Nomex fiber and obtained decomposition rate and the characteristic temperatures [1–6]. Some studies also reported the effects of temperature on the tensile properties of aramid fiber and fabric [7–9]. PBO shows a heat resistance about 100°C higher than poly(p-phenylene

terephthalamide (PPTA) and there have been some reports about thermal analysis of PBO fibers [10–11]. Although the considerable efforts have been devoted to study the high performance fibers structure, thermal properties, and their relationship, and thermal stability and thermal degradation of aramid fibers, but there are few publications on the comparison in their thermal stability and analysis of thermal degradation process by *TG*. Besides these results, there are less detailed reports about the kinetics of these fibers. Therefore, the characteristic behavior and the kinetics of the thermal degradation for these high performance fibers are discussed in this paper.
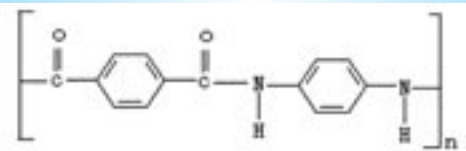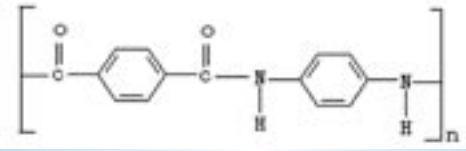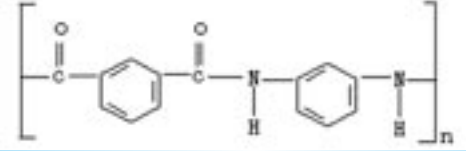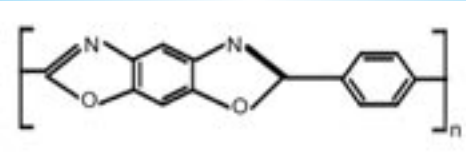
EXPERIMENTAL PART
Materials used

Four types of high performance fibers were collected, including Kevlar 49, Kevlar 129, Nomex and PBO. The specifications are listed in table 1.

Methods used

Thermal degradations of high performance fibers were performed in a TG 209 F1 Iris device. The thermal scanning mode ranges from 50°C to 800°C at a

THE SPECIFICATIONS OF SAMPLES		
Name	Chemical structure	Manufacturer
Kevlăr 49		DuPont/USA
Kevlar 129		DuPont/USA
Nomex		DuPont/USA
PBO(AS)		TORY/Japan

programming heating rate of $20^{\circ}C$ min^{-1} in air atmosphere with a gas flow of 20 mL min^{-1}. Each of the samples was controlled within 5–6 mg in primary mass and held in an alumina crucible, and then the loss of the sample mass was measured under a temperature program. The *TG* curves were recorded and displayed simultaneously during the measurement. Regarding the temperature parameters, they are the initial temperature of decomposition (T_0), the temperature of half decomposition ($T_{1/2}$), the temperature at the maximum rate of weight loss (T_c), and the end decomposition temperature (T_l), respectively.

RESULTS AND DISCUSSIONS
Thermal degradation of high performance fibers
The thermal decomposition properties of four kinds of high performance fibers under air atmosphere were studied by *TG*. Figure 1 shows *TG* and *DTG* curves of fibers at a heating rate of 20 K min^{-1}. The measured curves of Kevlar 49 and Kevlar 129 fibers have the same shape. It indicates that the thermal degradation mechanism of Kevlar fibers is similar in air. However, the degradation behavior of the Nomex fiber is different from the Kevlar fibers, which has two extremum points at *DTG* curves. The *TG* curve exhibits a weight loss,
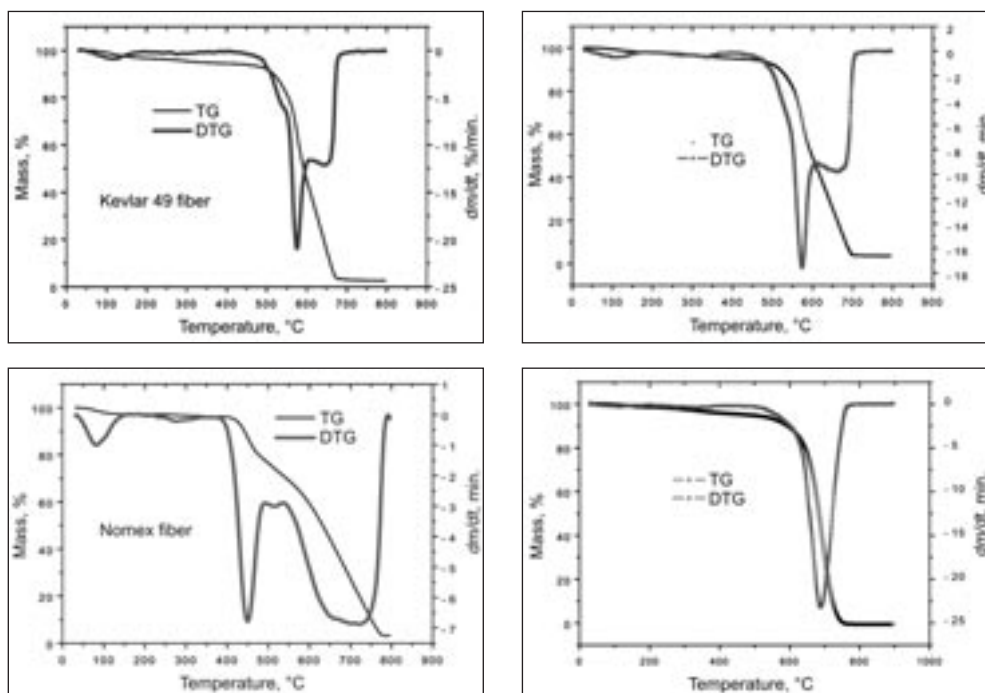

Fig. 1. TG & DTG curves during thermal degradation of high performance fibers by TG in air

THE CHARACTERISTIC TEMPERATURE OF HIGH PERFORMANCE FIBERS IN AIR				
T, °C	Kevlar 49	Kevlar 129	Nomex	PBO
T_o	548.1	542.4	423.7	648.0
$T_{1/2}$	592.7	598.6	632.24	683.9
T_c	575.6	574.0	449.8/721.2	688.4
T_t	643.7	660.4	784.2	726.5
$T_{1/2}\sim T_o$	44.6	56.2	208.54	35.9
$T_c\sim T_o$	27.5	31.6	26.1/297.5	40.4
$T_t\sim T_o$	95.6	118	360.5	78.5

Table 2

THE KINETIC PARAMETERS OF FIBERS IN AIR					
Fibers	Temperature, °C	Mass, %	Energy, E, $E/KJ/mol$	Reaction order, n	Correlation coefficient, r
Kevlar 49	498.6–548.1	92.16–82.09	93	0.51	0.94
	548.1–575.6	82.09–64.79	205	0.43	0.97
Kevlar 129	492.4–542.4	92.9–83.83	84	0.46	0.98
	542.4–574	83.83–66.08	196	0.42	0.99
Nomex	383.7–499.7	96.2–76.55	105	0.59	0.98
	499.7–721.2	76.55–19.9	36	0.37	0.96
PBO	598–648.5	89.4–78.77	14	8.32	0.88
	648.5–688.4	78.77–44.35	174	0.44	0.97

Table 3

which is ascribable to the release of adsorbed moisture that extends from room temperature to 105°C, which coincides with the *DTG* curve. Table 2 shows the characteristic temperatures of thermal decomposition of high performance fibers. It indicated that the initial degradation temperature of the PBO is the highest. The initial degradation temperature in air, T_o, is in the range of 423.7 – 648°C and in the order of PBO > Kevlar 49 > Kevlar 129 > Nomex. It can be concluded that the PBO fiber is the best in thermal stability, the following are the two Kevlar fibers, and then Nomex fiber. PBO fiber shows the most stable thermal property of the tested samples, which is associated with its production procedure where no isomer occurs. The temperature of half decomposition in air, $T_{1/2}$ is in order of PBO > Nomex > Kevlar 129 > Kevlar 49. The T_o of Nomex fiber is the lowest, but the T_t of Nomex is the highest. It indicated that the decomposition rate of Nomex fiber is the lowest. The *TG* curve of Nomex indicates that it decomposes in two stages and the second decomposition step occurs slowly.

Thermal degradation kinetics of high performance fibers

It is well known that the kinetic procedure and parameters of degradation are important as they affect the degradation rate. The initial degradation temperature and activation energy value are the most important factors, which effect the thermal degradation of polymer. In order to understand the thermal degradation of fiber, the activation energy E of fiber should be obtained. The apparent activation energy value, E, of thermo degradation was determined by the Freeman-Carroll method based on the following equation 1.

$$\frac{d\alpha}{dt} = Ae^{-\frac{E}{RT}}(1-\alpha)^n \qquad (1)$$

where:

$\alpha = \dfrac{w_o - w_t}{w_o}$ is the transformation rate;

w_0 – the initial mass;
w_t – the mass of t time;
n – the apparent reaction order;
R – the universal gas constant;
T – the degradation temperature;
A – the preexponential factor.

According to equation (1), we can obtain the equation (2):

$$\ln\frac{d\alpha}{dt} = \ln A + -\frac{E}{RT} + n\ln(1-\alpha) \qquad (2)$$

We can obtain equation (3) by equation (2):

$$\frac{d\ln\frac{d\alpha}{dt}}{d\ln(1-\alpha)} = -\frac{E}{R}\frac{d\frac{1}{T}}{d\ln(1-\alpha)} + n \qquad (3)$$

Obviously, equation (3) is a linear equation of $y = \alpha x + b$; where y is $\dfrac{d\ln\frac{d\alpha}{dt}}{d\ln(1-\alpha)}$, x is $\dfrac{d\frac{1}{T}}{d\ln(1-\alpha)}$, a is the slope of the line of $y = ax + b$; b is the intercept and equals to n. So the E values can be easily found from the $y - x$ regression line of equation (3). It is mentioned that E and n are here calculated within the range of $T_o - 50°C \sim T_o$ and $T_o \sim T_c$.

By using equation (3) and *TG* curves, the kinetics parameters, E, n and the corresponding correlation coefficient r can be obtained for each high performance fiber, and the calculated results are shown in table 3. At the same time, the calculation results of high performance fibers under air are illustrated in figure 2 according to the Freeman-Carroll method. From the slope of the curves, the activation energy E value of fibers can be found, and from the intercept of the straight line, the reaction order n can also be obtained. It can be found that the slope of the curves is variation, which indicates that the energy E is not constant.

From table 3, it can be found that the Kevlar fibers have similar reaction order n and activation energy E in the second phase and the results are in accordance with the shape of *TG* and DTG curve (fig. 1). It implies that the thermal degradation mechanism of Kevlar fibers is similar in air. Kevlar 49 and Kevlar 129 fibers have higher activation energy in the second phase, indicating that they are relatively great thermal stability. Although the degradation temperature of PBO fiber is the highest, its activation energy is not the highest: only 14 KJ/mol in the initial phase. The activation energy of Nomex fiber is higher in the first phase, indicating that the thermal decomposition of fiber is more difficult in the initial phase. In addition to Nomex fibers, the other fibers have higher activation energy in the second phase, indicating that in the heating process, thermal properties of fibers changed greatly, the higher the temperature the higher the activation energy of fibers.
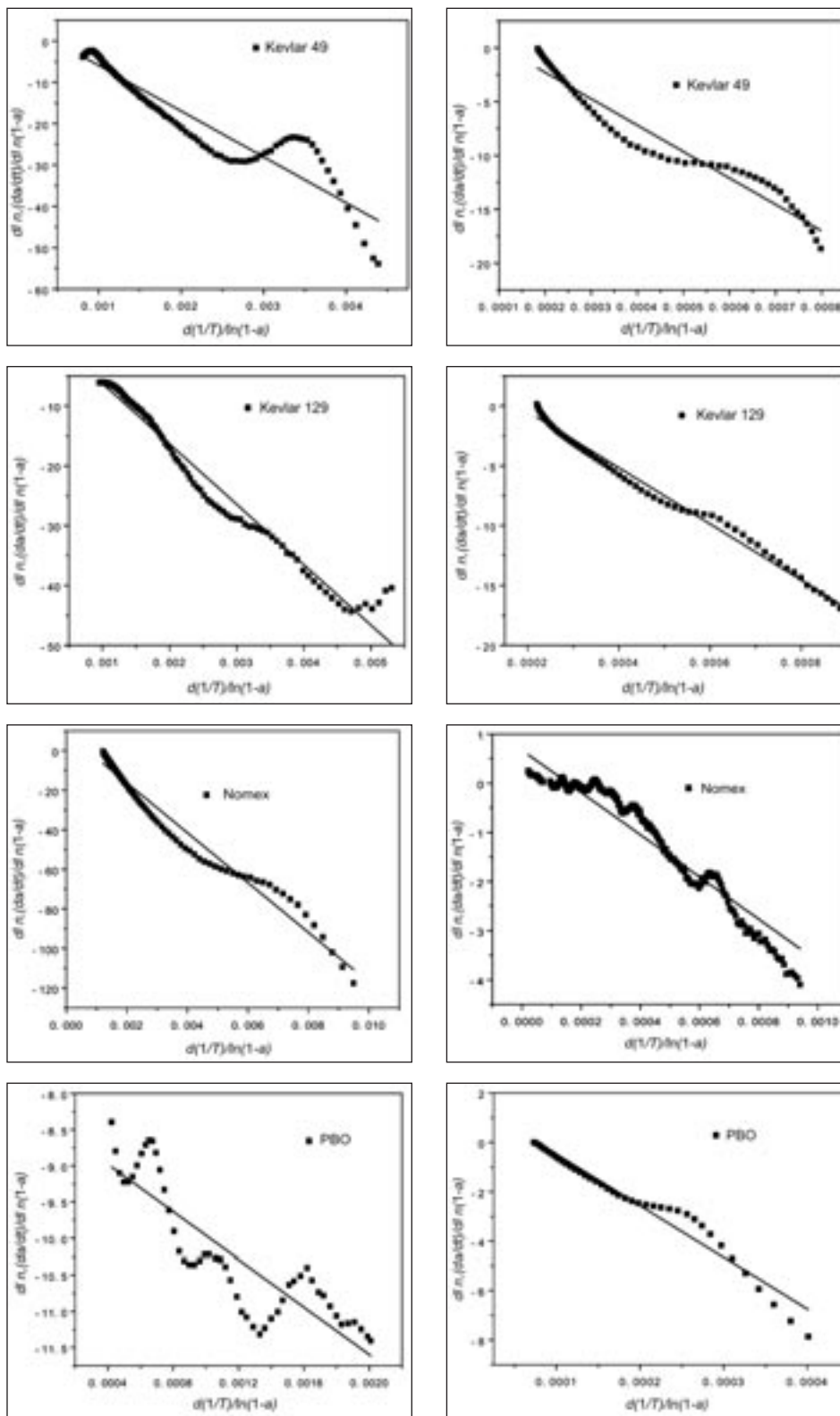
Fig. 2. The calculated results by Freeman-Carroll

CONCLUSIONS

The *TG* and *DTG* results indicate that the thermal stability of the high performance fibers can be characterized with the typical degradation temperatures (T_i, $T_{1/2}$, T_c and T_t). The thermal degradations of the high performance fibers Kevlar 49, Kevlar 129, Nomex, PBO in the air were characterized by *TG*. The characteristic temperatures of the kinds of fibers in air were obtained. The heat resistance of PBO fiber was best and initial decomposition temperatures of PBO fiber was the highest. Despite the beginning decomposition temperatures of the Nomex fibers were the lowest and less than 450°C, the termination decomposition temperature was close to 800°C.

From the thermal degradation kinetics of these fibers, it can be found that the four kinds of para-aramids, Kevlar 49, Kevlar 129 have similar reaction order *n* and activation energy *E* in air atmosphere. Although the degradation temperature of PBO fiber is the highest, its activation energy is not the highest. The activation energy of initial degradation *E* is closely related with the initial temperature.

BIBLIOGRAPHY

[1] Brown, J. R., Ennis, B. C. *Thermal analysis of Nomex and Kevlar fibers.* In: Textile Research Journal, 1977, vol. 47, issue 1, p. 62

[2] Brown, J. R., Hodgeman, D. K. C. *An ESR study of the thermal degradation of Kevlar 49 aramid.* In: Polymer, 1982, vol. 23, p. 365

[3] Brown, J. R., Power, A J. *Thermal degradation of aramids.* Part I. *Pyrolysis/Gas chromatography/Mass spectrometry of poly(1,3-phenyleneisophthalamide) and poly(1,4-phenylene terephthalamide).* In: Polymer, Degradation and Stability, 1982, issue 4, p. 379

[4] Brown, J. R., Power, A. J. *Thermal degradation of aramids.* Part II. *Pyrolysis/Gas chromatography/Mass spectrometry of some model compounds of poly (1,3-phenyleneisophthalamide) and poly(1,4-phenylene terephthalamide).* In: Polymer, Degradation and Stability, 1982, issue 4, p. 479

[5] Villar-Rodil, S., Martinez-Alonso, A. *Studies on pyrolysis of Nomex polyaramid fibers.* In: Journal of Analytical and Applied Pyrolysis, 2001, vol. 58, issue 2, p. 105

[6] Villar-Rodil, S,, Martinez-Alonso, A., Tascon, J. M. D. *Nanoporous carbon fibres by pyrolysis of nomex polyaramid fibres – TG and DTA studies.* In: Journal of Thermal Analysis and Calorimetry, 2005, vol. 79, issue 3, p. 529

[7] Siminiceanu, I., Marchitan, N., Duca, Gh., Mereuţă, A. *Mathematical models based on thermodynamic equilibrium and kinetics of an ion exchange process.* In: Revista de chimie, iulie 2010, vol. 61, nr. 7, p. 623

[8] Yue, C. Y., Sui, G. X., Looi, H. C. *Effects of heat treatment on the mechanical properties of Kevlar 29 fiber.* In: Composites Science and Technology, 2000, vol. 60, issue 3, p. 421

[9] Cai, G. M., Yang, H. H., Yu, W. D. *Evaluation of light and thermal aging performance of aramid fabric.* Textile Bioengineering and Informatics Symposium Hong Kong, 2008, p. 313

[10] Cai, G. M., Yu, W. D. *Investigation on the fabrication and properties of high performance aramid fabrics.* In: Industria Textilă, 2010, vol. 61, nr. 3, p. 106

[11] Tamargo-Martinez, K., Villar-Rodil, S. *Thermal decomposition of poly(p-phenylene-benzobisoxazole) fibres: monitoring the chemical and nanostructural changes by Raman spectroscopy and scanning probe microscopy.* In: Polymer Degradation and Stability, 2004, vol. 86, p. 263

[12] Serge, B., Xavier, F., Franck, P. *Study of the thermal degradation of high performance fibres application to polybenzazole and p-aramid fibres.* In: Polymer Degradation and Stability, 2001, vol. 74, p. 283

Authors:

GUANGMING CAI
Wuhan Textile University
College of textile
430073 Hubei
People's Republic of China
e-mail: guangmingcai2006@163.com

WEIDONG YU
Donghua University
Textile Materials and Technology Laboratory
201620 Shanghai
People's Republic of China

DOCUMENTARE

Noi tehnologii

MATERIALE TEXTILE DE PROTECŢIE ÎMPOTRIVA RADIAŢIILOR INFRAROŞII

Cercetătorii de la **Institutul Hohenstein** – Bönnigheim şi **ITCF Denkendorf** au elaborat un nou tip de material textil pentru absorbţia radiaţiilor infraroşii.

În prezent, în realizarea uniformelor militare şi a sistemelor de camuflaj militar al obiectelor şi clădirilor sunt utilizate imprimeuri de camuflaj, care să se confunde cu mediul înconjurător. Există şi materiale speciale care oferă o ecranare a radiaţiilor infraroşii. Până acum, pentru absorbţia IR, se foloseau coloranţii de cadă în realizarea imprimeurilor de camuflaj, asigurând purtătorilor o „invizibilitate" semnificativă în prezenţa senzorilor CCD din sistemele de nocturnă.

Cercetătorii germani au descoperit că, prin peliculizarea fibrelor chimice cu nanoparticule de oxid de indiu şi staniu, radiaţia termică poate fi absorbită mult mai eficient, putându-se realiza un efect de ecranare mai bun decât în cazul imprimeurilor de camuflare convenţionale. Dificultatea pe care cercetătorii au trebuit să

o rezolve a fost cea legată de modul în care nanoparticulele pot să adere la textile, astfel încât să nu afecteze alte proprietăţi ale acestora, cum ar fi confortul fiziologic. Totodată, tratamentul aplicat textilelor trebuie să confere acestora rezistenţă la spălare, la abraziune şi la intemperii.

Pentru a evalua efectul de ecranare al tratamentului textil, au fost măsurate absobţia, transmisia şi reflexia în gama lungimilor de undă de 0,25–2,5 µm, ale radiaţiei ultraviolete (UV), luminii vizibile şi infraroşu apropiat (IRA). Efectul de ecranare IRA, important pentru sistemele de nocturnă, a fost mult mai bun, comparativ cu mostrele de textile netratate.

Pe baza recentelor rezultate obţinute, vor fi optimizate performanţele textilelor destinate absorbţiei radiaţiilor infraroşii, în special a celor legate de managementul căldurii şi al transpiraţiei. Scopul îl constituie prevenirea formării radiaţiei infraroşii apropiate şi medii, sub forma căldurii degajate de corp, ceea ce ar face ca detecţia să fie şi mai mult îngreunată. Menţinând procesele fiziologice din corpul uman în limite normale, aceste textile ajută personalul militar să obţină performanţe pe măsura abilităţilor lor, în condiţii climatice extreme sau de stres fizic major.

Smarttextiles and nanotechnologies, iunie 2011, p. 1

Construction of pilling grade evaluation system based on image processing

WEIDONG GAO   RURU PAN
JIHONG LIU   SHANYUAN WANG

REZUMAT – ABSTRACT – INHALTSANGABE

Construcţia sistemului de evaluare a efectului piling, pe baza procesării imaginilor

În lucrare este prezentat un sistem de evaluare a efectului piling pe baza procesării imaginilor digitale. Imaginea materialului textil cu efect piling, iluminată de o sursă LCD, este preluată de o cameră matriceală Basler. Imaginile nopeurilor de pe suprafaţa plană a materialului textil sunt filtrate, mărite şi extrase cu ajutorul filtrului Gabor. Raportul nopeuri/suprafaţă este introdus într-un software specializat. Prin comparaţie cu imaginile standard ale nopeurilor de pe o suprafaţă plană, poate fi evaluat în mod automat efectul piling al materialului textil analizat. Testările efectuate pe mostre de materiale textile plane au scos în evidenţă eficienţa sistemului de evaluare propus.

Cuvinte-cheie: nopeuri, material textil, procesare a imaginilor, evaluare, efect piling, sistem, construcţie, filtru Gabor

Construction of pilling grade evaluation system based on image processing

A system for pilling grade evaluation is constructed based on digital image processing in this paper. The pilled fabric image is first captured by an Basler industrial area-array camera, under the illumination of a LCD light source. The pills in the fabric surface are then filtered, enhanced and extracted with the theory of Gabor filter. The area ratio of the pills is computed in the software. With the differences of area ratio among standard pilling images, the pilling grade of actual pilled fabric can be assessed automatically. Experiment on some actual fabrics has proved the efficiency of the proposed system.

Key-words: pills, fabric, image processing, evaluation, pilling grade, system, construction, Gabor filter

Aufbau des Pilleffekt-Bewertungssystems aufgrund der Bildbearbeitung

In der Arbeit wird ein Bewertungssystem des Pilleffektes aufgrund der digitalen Bildbearbeitung vorgestellt. Das Textilmaterialbild mit Pilleffekt, welches von einer LCD Lichtquelle beleuchtet wird, wird von einer Basler Matrix-Kamera aufgenommen. Die Bilder der Noppen auf der ebenen Oberfläche des Textilmaterials, werden filtriert, vergrössert und ausgeschnitten anhand der Gabor-Filter-Theorie. Das Verhältniss Noppen/Oberfläche wird in der Software eingetragen. Durch Vergleich mit den Standardbildern der Noppen auf einer ebenen Oberfläche, kann das Pilleffekt des analysierten Textilmaterials automatisch bewertet werden. Die Teste durchgeführt auf ebenen Textilmaterialmuster haben die gute Leistung des vorgeschlagenen Bewertungssystems hervorgehoben.

Stichwörter: Noppen, Textilmaterial, Bildbearbeitung, Bewertung, Pilleffekt, System, Aufbau, Gabor-Filter

In the process of wearing and washing, pills will appear in the fabric surface because of friction. Pills cause an unsightly appearance and premature wear. Resistance to pilling is one of the most important criteria for evaluating the quality of fabric and it is normally tested in the laboratory by simulating accelerated wear, followed by a manual assessment of the degree of pilling by an expert based on a visual comparison the fabric sample to a set of standard pilling images. According to the pilling degree, the pilled fabrics can be assigned into 1–5 grades. Although the method is easy to carry out, a frequent complaint about this manual evaluation method is the inconsistency and inaccuracy of the grade results. In order to obtain more objectivity results in the pilling grading process, a number of automated systems based on image analysis have been developed and described in the literature since 1990s [1–10]. But there are some problems that need to be solved out before constructing an entire system for evaluating the fabric pilling grades.

- *The equipment of acquitting the fabric image.* Most of these existing methods employ expensive or complicated equipment, such as laser triangulation imaging [1], projection imaging [3, 4], to capture the pilled fabric images. They are hard to be operated and extended into the practical applications.
- *Image processing algorithm.* Most of the systems proposed in the literature employed complex image processing algorithms involving multiple stages [2–7]. These algorithms are only applied in the theory research and the effects of these algorithms for evaluating actual fabric pilling grade need to be further validated, and it also limits the extension of the existed systems.

To solve these problems, the standard pilling images have been analyzed in references [11] and the area ratio was proposed as differential parameter for grading the pilled fabric. In references [12], Gabor filter was selected as the tool to enhance the pilled fabric image and locate the pills. In this paper a complete system for grading the pilled fabrics is constructed based on image processing. The hardware and software of system are explained first, and then Gabor filter is selected to process the pilled fabric image captured by an industrial camera. The pills are located and the area ratio of pills is computed. At last, the pilling grade of the fabric is evaluated by comparing the area ratio of the actual pilled fabric to that of the standard pilling images.

HARDWARE AND SOFTWARE

As explained in the previous section, the equipment for capturing the pills is very important. To construct a system which can be extended into practical applications, the equipment should not be too expensive or too complicated. In our system, an industrial area-array camera Basler SCA 1600 is selected to capture the pilled fabric image. The structure of the image acquisition system including the camera is shown in figure 1.
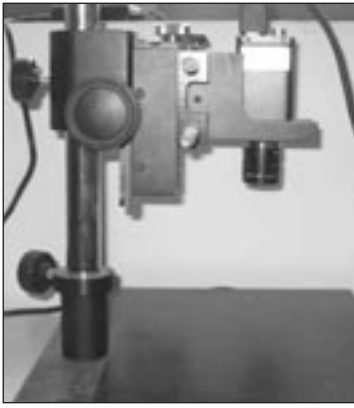
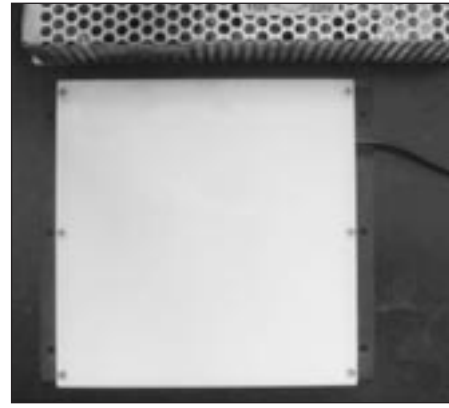Fig. 1. Structure of the image acquisition system

Fig. 2. LCD light source

To exclude the influence of environment light condition, an area-array LCD light source (24V, DC) shown in figure 2, is chosen to illuminate the fabric during the image acquitting process.

Visual Basic 6.0 is chosen as the software to construct the image capture and analysis system. The interface of the final software is shown in figure 3. In the software system, the pilled fabric is captured and then converted into gray scale. The Gabor filter can be adjusted manually by selecting the parameters. The gray fabric image is filtered by the Gabor filter and the pills can be segmented in the filter image with threshold method. The pilling grade can be finally assessed based on the area ratio of the pills in the fabric.

THEORETICAL METHODS

Gabor filters is one of the most important time-frequency domain analysis methods, which was firstly proposed by Gabor in 1946 [13]. Gabor filter can be applied in time domain and frequency domain. Frequency Gabor filter is actually a special Window-Fourier transform and the window selected is a kind of Gaussian function. By selecting the parameters of Gaussian function, the most needed information in the time-domain of the image can be chosen to obtain the required information in frequency-domain. Woven fabric is a typical periodic texture which formed by warp and weft yarns [14]. There are some significant peaks in the Fourier transform results of fabric image. Thus, 2-D frequency-domain Gabor filter is selected to eliminate the fabric texture and enhanced the pilling information in the paper. In the enhanced image, threshold processing can be used to segment and locate the fabric pills.

In the time domain, 2-D Gabor filter can be seen as a Gaussian function tuned sinusoidal function. The expression of 2-D Gabor filter in time domain is as follows:

$$h(x,y) = g(x',y') \cdot \exp(2\pi j(Ux + Vy)) \quad (1)$$

where:

$\begin{cases} x' = x\cos\theta + y\sin\theta \\ y' = -x\sin\theta + y\cos\theta \end{cases}$ is the corresponding coordinate of (x, y) after clockwise rotation angle θ;

U, V is the frequency along the x axis and y axis;

$F = \sqrt{U^2 + V^2}$ is the center frequency of Gabor filter;

$g(x,y) = \dfrac{1}{2\pi\lambda\sigma^2} \exp\left[-\dfrac{(x/\lambda)^2 + y^2}{2\sigma^2}\right]$ is the Gaussian function.

The Gabor filtering result $f(x, y)$ of given fabric image $I(x, y)$ in time domain can be obtained as follows:

$$f(x,y) = I(x,y) * h(x,y) \quad (2)$$

where:
"*" represents the convolution operation.

Fourier transform of Gabor function in equation (1) is still a kind of 2-D Gaussian function which can be expressed as follows:

$$H(u,v) = \exp\left\{-2\pi^2\sigma^2\left[(u'-U)^2\lambda^2 + (v'-V)^2\right]\right\} \quad (3)$$

where:

$\begin{cases} u' = u\cos\theta + v\sin\theta \\ v' = -u\sin\theta + v\cos\theta \end{cases}$ is the corresponding coordinate of (μ, v) after clockwise rotating angle θ, and $\theta = \tan^{-1}(V/U)$.

The Gabor filtering result $f(x, y)$ of given fabric image $I(x, y)$ in frequency domain can be obtained as follows:

$$f(x,y) = I(x,y) \cdot H(x,y) \quad (4)$$

where:
"." represents the point multiplication operation.

As the Gabor filter in the frequency domain is kind of Gaussian function window, it can be seen as band-pass filter in essence. In our system, Gabor filter in the frequency domain is selected to enhance the pilling information and remove the fabric texture. To obtain satisfactory filtering results, the parameters of Gabor filter should be properly selected. The parameters of Gabor filter include:
– center frequency, F;
– rotating angle, θ;
– radial frequency bandwidth parameter, B;
– filter directional ratio scale, λ

where:

$$B = \log_2\left[(\lambda\pi F\sigma + \alpha)/(\lambda\pi F\sigma - \alpha)\right]$$
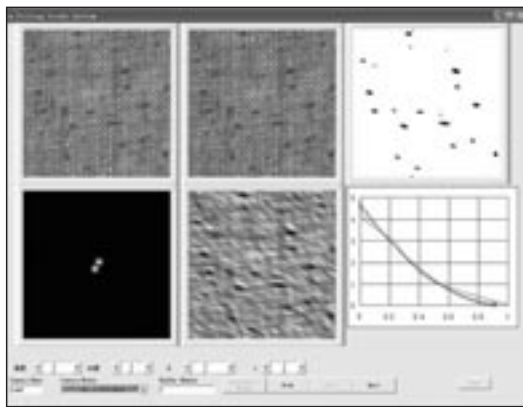
$$\alpha = (\ln 2 / 2)^{0.5}$$

Fig. 3. Interface of software system

EXPERIMENTAL PART
Image acquisition

In the experiment, a Digital Martindale abrasion and pilling tester (YG401) is used to simulate the accelerated wear to generate pills. According to the standards in GB/T 4802.1-1997, the pressure is set as 780 cN and the pilling rotational number is 600. As mentioned in references [11], when people grade the pilled fabric, only part of the fabric image and some parameters of pills determine the pilling grade. Before constructing the whole system, we have tested for many times with the help of some experts and found that the pills in the center of pilled fabric determine the pilling grade of fabric actually. Figure 4 *a* shows the whole reflective pilled fabric image with the size of 9 cm x 9 cm. In the experiment, the center of the image is

cropped with the actual size of 2.1 cm x 2.1 cm and the image size is 600 pixels x 600 pixels. As described in references [3–10], the pills such as circled in figure 4 *b* can be detected with certain image processing algorithms. From figure 4 *b*, it can be seen that pills has only a little contrast with adjacent pixels, so it is hard to segment the pills from fabric background. The complicated algorithms imported in extracting the pills are to enhance the contrast between the pills and fabric background formed by warp and weft yarns.

One of the important works we have done before constructing the system is to obtain satisfactory image in which the pills can be easily detected. In the experiment, we tried to put the light source in different angles and different places to make the pills be easily extracted. Finally, we found that the pills in the transmitted fabric image have satisfactory contrast with the adjacent pixels. As shown in figure 5 *a*, the pills are expressed as local dark pixels. In the system, the gray image shown in figure 5 *b* is used for segmenting the pills. Compared to the pills in the reflective images adopted in most references, the pills in the transmitted fabric image are more distinct and they may be easily located with certain image processing algorithms.

Pill location

To grade the pilled fabric, the pills should be segmented from the fabric background. The accurate location of fabric pills is the foundation of extracting the pilling parameters and it is the critical stage for constructing the whole system. In the transmitted fabric
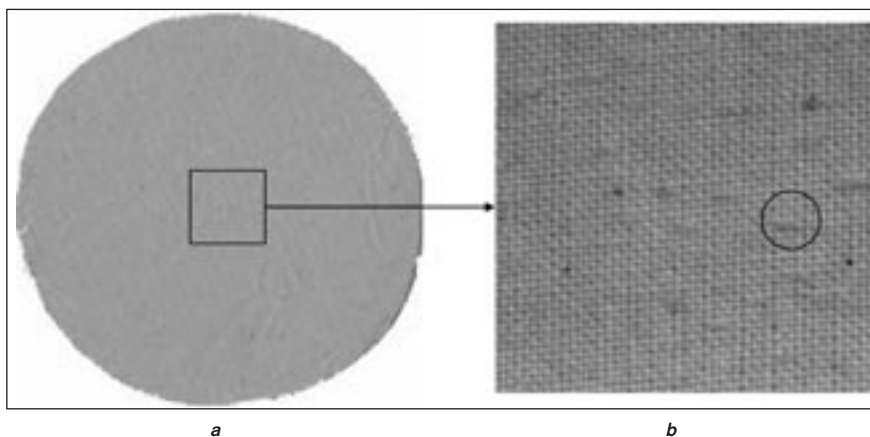

a *b*

Fig. 4: *a* – the whole reflective pilled fabric image; *b* – the cropped fabric image
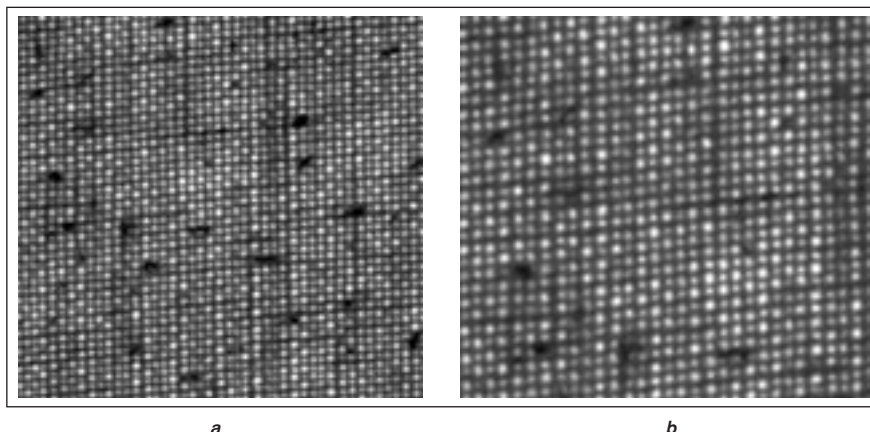

a *b*

Fig. 5: *a* – color transmitted pilled fabric image; *b* – gray scale of the pilled fabric image
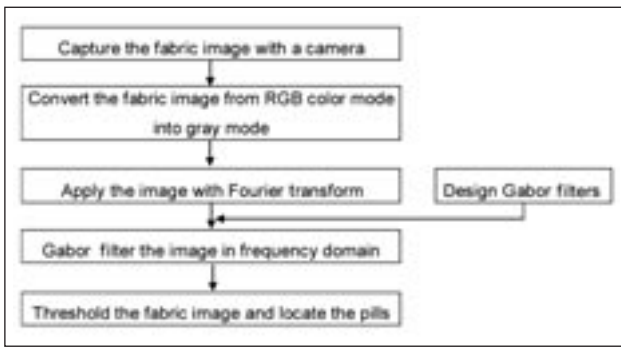
Fig. 6. Procedure chart of locating the fabric pills

image, the pills have the satisfied contrast with the adjacent pixels. The pills are still hard to locate in the time-domain using threshold method for the yarns in the image are also expressed as dark pixels. The frequency-domain Gabor filter is adopted to filter and enhance the pilled fabric image. In the enhanced fabric image, the fabric texture formed by warp and weft yarns can be eliminated and the pills are enhanced. Thus, the pills can be extracted with some threshold method. The procedure chart of locating the fabric pills in the experiment is shown in figure 6.

RESULTS AND DISCUSSIONS
Selection of Gabor filter parameters

The selection of Gabor filters parameters is the most important procedure in this system. The proper parameters can result in good filtered image, where fabric texture is clearly removed and pilling information is well enhanced. The pills can be easily segmented and located in the resulted image. The manual selection of the parameters is carried out in the software system with amount of pilled fabric image and the satisfactory parameters are saved automatically.

- *Rotating angle* θ. Woven fabric is consisted by two sets of perpendicular yarns, and the Fourier transform of the fabric image shows significantly directional property. Thus, the selection for rotating angle of Gabor filter is important. In the experiment, we found that when the Gabor filter is selected to avoid from the peaks corresponding to the fabric texture, the good filtering result will be obtained. The rotating angle should be changed when the fabric is put in different angles. In the experiment, the fabric is laid to keep the wefts in the horizontal direction and the rotating angle is set θ = 60 degrees.
- *Radial frequency bandwidth parameter B*. The parameter determines the covering region of Gabor filter in the frequency domain. As the essence of Gabor filter is band-pass filter in the frequency domain, when the value of B is too small, the covering region of Gabor filter in the frequency domain is too small to represent the information of pills in the fabric image. When the value of B is too large, the covering region is too large to remove the texture in the fabric image. In the experiment, we found that when B = 2.3, the texture was eliminated clearly and the pilling information is well enhanced. With selected B value, σ in equation (3) can be computed as follows:

$$\sigma = \frac{\alpha\left(2^B + 1\right)}{\lambda \pi F\left(2^B - 1\right)} \qquad (5)$$
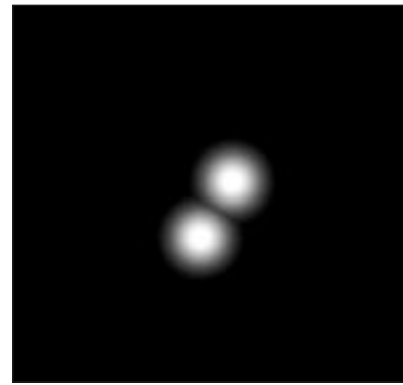

Fig. 7. Gabor filter with selected parameters

- Filter directional ratio scale λ. This parameter determines the shape of Gabor filter. When λ = 1, the Gabor filter is a symmetric filter and it is suitable for symmetric texture. When the texture is not arranged in a square lattice, asymmetric Gabor filter is more useful. It means λ ≠ 1 and its value is determined by the horizontal and vertical texture scale ratio. In the experiment λ is set into arrange of [0.5, 2]. The value is determined by the actual fabric structure parameters, such as warp and weft count and density. In our system, its original value is set as 1 and it can be adjusted automatically by the location of the peaks corresponding to warp and weft texture.
- *Center frequency F*. This parameter determines the location of Gabor filter. It selects some region in the frequency domain to represent the pills in the fabric image. The selection of this parameter is determined by the fabric structure parameter and the distance between the fabric and the camera lens. It means the enlargement ratio of fabric image determine the value of center frequency. In the research, $F = 2^{k+1}$, $k = 3$, 4, 5, 6, 7 and in our experiment $k = 4$.

The Gabor filter with the selected parameters is shown in figure 7 and its borders are cropped to make the readers understand the filter easily.

The fabric image shown in figure 5 *b* is filtered according to equation (4). The values in the filtered results are stretched into 0 ~ 255 and the result is expressed as a gray image in figure 8. From the image, it can be seen that texture formed by yarns is successfully removed and the pills are darker than their adjacent pixels and they can be located with simple threshold method.

Threshold method

After Gabor filtering, the fabric texture is eliminated. The pilling information is enhanced and the contrast between the pills and the fabric background satisfies the need for segmenting the pills. Threshold processing is adopted to segment and locate pills. The intensity of fabric background is related with the illumination condition, so it is not suitable to use fixed threshold value to locate the pills. The threshold value T is selected as follows:

$$T = \mu \pm n \cdot \alpha \qquad (6)$$

where:
μ is the mean value of the filtered fabric image;
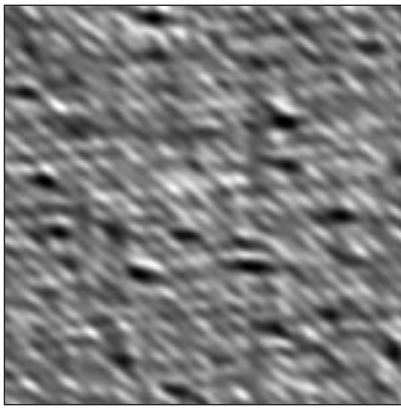α – the standard deviation value of the filtered fabric image;

Fig. 8. Enhance of fabric pills image

Fig. 9. Detection results of fabric pills

n – the constant value and in the experiment it is set as 3.

When the intensity of the pixel falls into the arrange $[\mu - n \cdot a, \mu + n \cdot \alpha]$, it is considered as background pixel and it is set as a black pixel. Otherwise, it is considered as pilling pixel and it is set as white pixel in the result. Figure 9 shows the detection results of the pills, where the white pixels represent pills and black pixels represent fabric background.

Pilling grade

As described in references [11], to evaluate the pilling grade of the fabric, the parameters of the pills should be inspected. In our system, the area ratio of the pills is used as the criterion to grade the fabrics. To get the area ratio of the pills, the white pixel number in figure 9 should be counted and the ratio of the pixels can be detected as follows:

$$Ratio = \frac{N_{pills}}{N_{total}} \cdot 100\% \qquad (7)$$

where:
$Ratio$ is the area ratio of the pills;
N_{pills} – the pixel number of the pills;
$N_{pills} = H \times W$ – total pixel number of the image,
               where:
                 H is the image height;
                 W is the image width.

As described in references [11], by comparing the area ratio of pills in actual fabric to those in standard pilling fabric images, the pilling grade can be evaluated automatically. The area ratio of the pills in the fabric sample shown in figure 9 is 1.07% with N_{pills} = 3 863 and N_{total} = 600 x 600 = 360 000. With the distinctive criteria proposed in references [11], the pilling grade of this sample is level one.

CONCLUSIONS

To evaluate the fabric pilling grade, a whole system based on image processing is described in this paper. The hardware and software are introduced first. To obtain satisfied pilled fabric image, a LCD light source is put under the fabric to get transmitted image. A Gabor filter with selected parameters is used to remove the yarn texture and enhance the pill information. In the enhanced fabric image, the pills are located with threshold method. The pilling grade can finally be determined by the area ratio of pills. The experiment on actual fabric samples proves the system can evaluate the fabric pilling grade automatically.

BIBLIOGRAPHY

[1] His, H. C., Bress, R. R., Annis, P. A. *Characterizing fabric pilling using image-analysis techniques. Part I: Pill detection and description.* In: Journal of the Textile Institute, 1998, vol. 89, issue 1, p. 80
[2] His, H. C., Bress, R. R., Annis, P. A. *Characterizing fabric pilling using image-analysis techniques. Part II: Comparison with visual pilling rating.* In: Journal of the Textile Institute, 1998, vol. 89, issue 1, p. 96
[3] Chen, X., Huang, X. *Evaluating fabric pilling with light-projected image analysis.* In: Textile Research Journal, 2004, vol. 74, issue 11, p. 977
[4] Chen, X., Xu, Z. *Detecting pills in fabric images based on multi-scale matched filtering.* In: Textile Research Journal, 2009, vol. 79, issue 15, p. 1 389
[5] Xu, B. *Instrumental evaluation of fabric pilling.* In: Journal of Textile Institute, 1997, vol. 88, p. 488
[6] Xin, B. J., Hu, J. L., Yan, H. J. *Objective evaluation of fabric pilling using image analysis techniques.* In: Textile Research Journal, 2002, vol. 72, p. 1 057
[7] Abril, H. C., Millan, M. S., Torres, Y. *Automatic method based on image analysis for pilling in fabric.* Optical Engineer, 1998, vol. 37, issue 6, p. 1 477
[8] Ramgulan, R. B., Amirbayat, J. *The objective assessment of fabric pilling. Part I: Methodology.* In: Journal of the Textile Institute, 1993, vol. 84, issue 2, p. 221
[9] Kim, S., Park, C. K. *Evaluation of fabric pilling using hybrid imaging methods.* Fibers and Polymers, 2006, vol. 7, issue 1, p. 57
[10] Zhang, J., Wang, X., Palmer, S. *Objective grading of fabric pilling with wavelet texture analysis.* In: Textile Research Journal, 2007, vol. 77, issue 11, p. 871

[11] Zhou, Y., Pan, R., Gao, W., Liu, J. *Evaluation of fabric pilling based on standard images and image analysis.* In: Journal of Textile Research, 2010, vol. 31, issue 10, p. 29

[12] Gao, W., Wang, S., Pan, R., Liu, J. *Automatic location of pills in woven fabric based on Gabor filter.* In: CJCM'2010, Paper ID: C017.

[13] Gabor, D. *Theory of communication.* Journal of the Institute of Electrical, Engineers, 1946, vol. 93, p. 429

[14] Xu, B. *Identifying fabric structures with fast Fourier transform techniques.* In: Textile Research Journal, 1966, vol. 66, issue 8, p. 496

Authors:

Chief of work dr. eng. WEIDONG GAO
Conf. dr. eng. JIHONG LIU
Conf. dr. eng. RURU PAN
Conf. dr. eng. SHANYUAN WANG
Donghua University
1882 West Yan'an Rd
Changning District Shanghai
200051 China
Jiangnan University
1800 LiHu Road
Wuxi, 214122 China

NOTE ECONOMICE

2010 – UN AN DE REDRESARE PENTRU PRODUCĂTORII DE MAȘINI TEXTILE DIN ITALIA

Conform datelor statistice întocmite de Asociația producătorilor de mașini textile din Italia – ACIMIT, în anul 2010 a avut loc o redresare decisivă a sectorului de utilaje textile italiene, comparativ cu anul 2009, care a fost marcat de o scădere vizibilă a producției.

În ceea ce privește valoarea producției de mașini textile din Italia, s-a înregistrat o creștere cu 18% față de 2009, de la 1,9 la 2,3 miliarde de euro.

Exporturile au atras o creștere favorabilă similară, de 19%, atingând o valoare de până la 1,8 miliarde de euro.

Tabelul 1

EVOLUȚIA SECTORULUI DE MAȘINI TEXTILE DIN ITALIA, în milioane de euro			
	2009	**2010***	**Variația**
Producția	1931	2279	+18%
Exporturile	1506	1796	+19%
Importurile	359	516	+44%
Cererea internă	784	999	+27%

* Date preliminare

De asemenea, mai ales în prima parte a anului 2010, s-a înregistrat o creștere continuă a cererii de utilaje tex-

tile în multe zone geografice și în special pe piețele importante ale lumii, cum ar fi China, India și Turcia.

În ansamblu, exporturile italiene au obținut performanțe pozitive pe principalele piețe de textile, Asia și America de Sud reprezentând forțele motrice ale creșterii cererii globale.

Și pe piața internă s-a înregistrat o tendință mult mai dinamică de creștere, comparativ cu cea din anii 2008–2009.
Cererea internă a crescut cu 27% față de anul precedent, înregistrându-se o cifră de afaceri de aproape un miliard de euro.
Evoluția acestui sector în anii 2009–2010 este prezentată în tabelul 1.

„Aceste date preliminare sunt, fără îndoială, încurajatoare, însă rămâne un profund sentiment de incertitudine în ceea ce privește scenariul la nivel mondial" – a afirmat Sandro Salmoiraghi – președintele ACIMIT.

Un studiu efectuat de către ACIMIT în primul trimestru al anului 2011 arată o tendință staționară, în comparație cu primul trimestru al anului 2010, atât pe piața internă, cât și pe cea externă.

Informații de presă. ACIMIT, februarie 2011

Design of fashioning lines in 3D knitted fabrics

LUMINIȚA CIOBANU

DORIN SAVIN IONESI
ANA RAMONA CIOBANU

REZUMAT – ABSTRACT – INHALTSANGABE

Proiectarea liniilor de conturare a tricoturilor cu geometrie 3D

Tricoturile cu geometrie 3D prezintă un potențial deosebit pentru aplicațiile tehnice, în principal datorită posibilităților lor de a dezvolta, prin tricotare, structuri cu forme complexe, fără a necesita modificări majore la nivelul utilajului. Tricoturile conturate spațial, obținute prin tehnica tricotării pe rânduri incomplete, sunt caracterizate prin dispunere 3D, putând atinge un grad extrem de ridicat de complexitate. Proiectarea unor astfel de tricoturi trebuie să se facă atât din punct de vedere al formei finale – proiectarea trebuind să pornească de la corpul 3D, a cărui desfășurată coincide cu desfășurata tricotului, cât și din punct de vedere al tricotului, proiectarea trebuind să ia în considerare liniile de conturare care generează geometria spațială. Modelarea matematică a acestor linii, în funcție de parametrii săi – increment și dimensiunile ochiurilor, permite, în final, corelarea cu dimensiunile corpului 3D. Lucrarea prezintă proiectarea liniilor de conturare din tricot, având în vedere cele două cazuri posibile: linii de conturare drepte, cu increment constant și linii curbe, cu increment variabil.

Cuvinte-cheie: tricoturi conturate spațial, linii de conturare, increment, modelare matematică

Design of fashioninf lines in 3D knitted fabrics

Knitted fabrics with 3D geometry have a good potential for technical applications, especially due to the possibility of developing complex shapes through the knitting process, without major modification of the equipment. The spatial fashioned knitted fabrics obtained by the technique of incomplete rows knitting are characterized by 3D geometries with the highest complexity degree. The designing of such fabrics must take into consideration the two sides of the problem. From the point of wiev of the final 3D shape of the fabrics, the designing has to start from the 3D body of which lateral area gives the fabric geometry. From the knitted fabric point of wiev, the designing has to take into consideration the fashioning lines that generate the spatial geometry. The mathematical modelling of these lines according to their parameters – line increment and stitch dimensions – allows the correlation between the fabric and the 3D body sizes. The paper presents the designing of the fashioning lines of the knitted fabric, considering the two possible cases: straight fashioning lines with constant increment and curved line with variable increment.

Key-words: knitted fabrics with spatial geometry, fashioning lines, increment, mathematical modelling

Konturlinienentwurf bei Abstandsgewirke

Abstandsgewirke haben ein besonderes Potential für technische Anwendungen, insbesondere dank der Möglichkeit komplexe Strukturen durch Wirken zu entwickeln, ohne wesentliche Ausrüstungsänderungen vorzunehmen. Die Abstandsgewirke, gefertigt durch die Gewirktechnik der unvollständigen Reihen, werden durch eine 3D Form mit hohem Komplexitätsgrad charakterisiert. Der Entwurf solcher Gewirke kann sowohl von der Endform beginnen – die Entfaltung des 3D-Körpers stimmt überein mit der Gewirkentfaltung, als auch vom Gewirke – die Konturlinien generieren die Raumgeometrie. Die mathematische Modellierung dieser Linien, in Abhängigkeit der Parameter – Inkrement und Maschengrösse, erlaubt am Ende die Korrelierung mit den 3D Körperdimensionen. Die Arbeit präsentiert der Entwurf der Konturlinie eines Gewirkes, wenn die zwei möglichen Fälle in Betracht gezogen werden: gerade Konturlinien mit konstantem Inkrement und runde Linien, mit variablen Inkrement.

Stichwörter: Abstandsgewirke, Konturlinien, Inkrement, mathematische Modellierung

Knitted fabrics with three-dimensional geometry have known a significant development, mainly due to their use in technical applications, especially as preforms for advanced composite materials.

There are 3 groups of knitted fabrics with 3D architecture: multiaxial (warp) knitted fabrics, spacer/sandwich fabrics and shell knitted fabrics (with spatial fashioning).

The last group of fabrics represents an extremely interesting domain with regard to the shapes that can be produced and their complexity. Practically, these fabrics are characterised by a spatial geometry of their surface, according to the lateral area of a 3D body. This way they are also known as shell structures [1]. The main applications of the shell fabrics are: preforms for composite materials, medical textiles (grafts and scaffolds in tissue engineering), and clothing for persons with special needs.

The shell fabrics are produced using the spatial fashioning technique [2, 3], that involves areas in the knitted fabric where the stitches are produced on a variable number of needles so that a supplementary amount of stitches is generated. These stitches will be forced out of the fabric plan and will have a spatial geometry.

The design of spatial fashioned fabrics requires their correlation with the 3D shape (geometric forms/bodies) of which lateral area represents the final fabric geometry. These bodies can have a regular or irregular geometry. The regular 3D geometric forms include solids of revolution (cylinder, cone, frustum of a cone, hemisphere and sphere, ellipsoid, hyperboloid, toroid) and polyhedrons (pyramid, frustum of a pyramid, parallelepiped, cube etc.). The evolutes of these 3D forms are known; some of these evolutes cannot be knitted, due to technological limitations. The 3D bodies with irregular geometry present some problems with regard to the definition of their lateral area and evolutes, best approach to this problem being through spline curves.

A special mention must be made with regard to the knitting techniques able to produce such fabrics. In the case of some solids of revolution the spatial fashioning technique is not the only one that can be used. It is the case of cylinders, ellipsoids, hyperboloids and their derivatives, when the specific shape can be obtained using 2D fashioning technique (narrowings and widenings), combined with tubular knitting. The use of one or the other technique is motivated by the shape specifics, the knitting direction and the machine limitations.
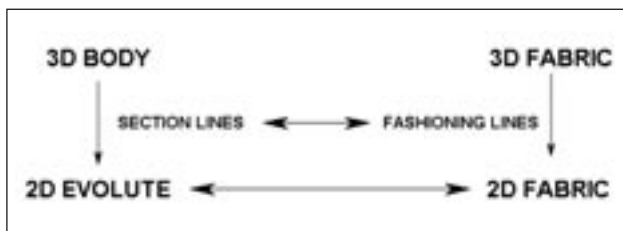
Fig. 1. Correlation betweenthe 3D body and the 3D knitted fabric

Figure 1 illustrates the correlation between the 3D geometrical body and the 3D knitted fabric that is evident at evolute's level. The body's evolute defines the 2D fabric dimensionally, while the section lines are converted into fashioning lines in the fabric. In reverse, a knitted fabric with fashioning lines will acquire in the end a spatial geometry, according to the lateral area of the 3D body.

The mathematical modelling of the body's evolute allows the modelling of the fabric plan by defining its fashioning lines and their dimensions expressed through the line increment and the stitch dimensions.

The paper approaches a certain part of the design of 3D knitted fabrics with spatial geometry, namely the design of the fabric fashioning lines.

DEFINITION OF FASHIONING LINES

A fashioning line is defined as a zone in the knitted fabric where the knitting process takes place on a variable number of needles, first decreasing and then increasing and that in the end will have a spatial geometry [4].

The fashioning has two components: one corresponding to a gradual decrease in the number of working needles and another corresponding to their reintroduction in work, as illustrated in figure 2. In the knitted fabric, these components are united, creating the real fashioning line.

The final 3D geometry is given by a sequence of fashioning lines placed on the fabric area. The fashioning lines can be characterised by a set of parameters. From the point of view of the knitting programming, the fashioning lines are defined by its increment – the number of needles Δa that are stop/start working at one moment and the number of rows Δr after which the number of needles varies. The repeats of the line increment give its dimensions (the total number of needles and rows in the fashioning area). Geometrically, a fashioning line can be expressed using its dimensions (height h and width l) and slope angle (the angle α between the line and the row direction, see figure 3).

DESIGN OF THE FASHIONING LINES

The design of the fashioning lines is related to the evolute of the 3D body. Geometrically, the section lines of a 3D body can be straight or curved and thus the fashioning lines in the knitted fabric can be defined accordingly:
- straight section line that determines a straight fashioning line, with a constant increment, the straight fashioning lines can be considered in its integrity.
- curved section line that determines a curved fashioning line that has a variable increment. A curved
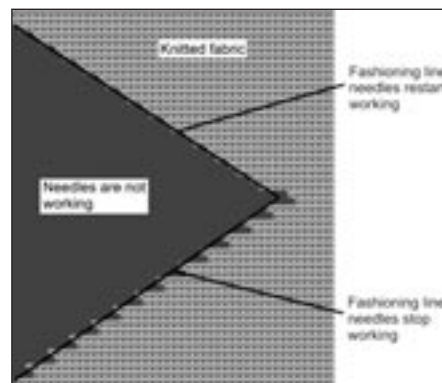

Fig. 2. Aspect of fashioning line – knitting programme

line is considered in its entire length or divided in zones. It can be approximated with arcs of ellipse or straight segments. Such a line is specific to spherical or irregular bodies.

Because the fashioning lines are not continuous, as it is the case with the section lines, they are quantified using the line increment Δr and Δa. The basic element is the knitted stitch and its dimensions – the stitch pitch and height. The fashioning line can be therefore considered as a polygonal line that follows the stitches in the knitted fabric.

Case I – straight fashioning line (constant increment)

Due to the fact that a polygonal line can be considered as a compound of straight segments with 0 or ∞ slope, its equation is given by the segment parity. For uneven segments, the line equation is:

$$\begin{cases} x_i = x_{i-1} \\ y_i = y_{i-1} + \Delta r \end{cases}, \quad i = 2k+1 \qquad (1)$$

where:
Δr is vertical increment of the fashioning line;
i – number of steps (repeats) in the fashioning line.
In the case of even segments, the equation becomes:

$$\begin{cases} x_i = x_{i-1} + \Delta a \\ y_i = y_{i-1} \end{cases}, \quad i = 2k+1 \qquad (2)$$

where:
Δa = horizontal increment of the fashioning line.
Equations (1) and (2) are general and they can be particularised according to the starting point of the fashioning line and its vertical and horizontal increment, as follows:

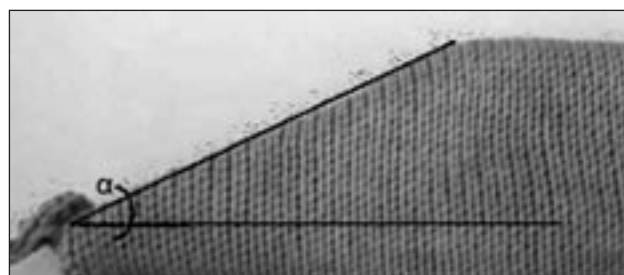$$x_i = x_o + \left[\frac{i}{2}\right]\Delta r \qquad (3)$$
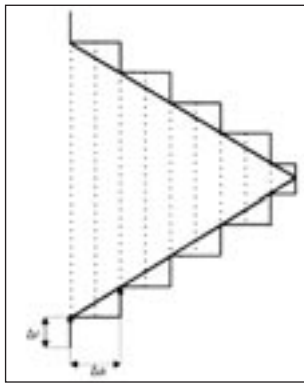

Fig. 3. The slope angle of a fashioning line

Fig. 4. Geometry of the straight fashioning line, with constant increment

Fig. 5. Curved fashioning line, with variable increment

$$y_i = y_o + \left[\frac{i+1}{2}\right]\Delta a \qquad (4)$$

The expression of the segments based on the line increment allows correlating the line dimensions with the stitch dimensions, as follows:

$$y = mx + b \qquad (5)$$

where:
m   represented the slope of the fashioning line;
b – y   –   intercept of the line.
The slope of the fashioning line is:

$$m = c * ctg\frac{\Delta r}{\Delta a} \qquad (6)$$

So, the line equation defining the fashioning line with constant increment becomes:

$$y = c * ctg\frac{\Delta r}{\Delta a} * x + \Delta a \qquad (7)$$

The parity of the connecting points must be considered when defining the equation of the resulting fashioning line (fig. 4). The dotted lines in figure 4 represent the connection through knitting of the two components of fashioning line. The line dimensions can be adjusted through the line increment and the fabric density.

Case II – curved fashioning line (variable increment)

In the case of fashioning line with variable increment, the section line of the 3D body is a variable broken line, ascending or descending according to case. The fashioning line will be formed by arcs of ellipse or circle and line segments. The shape of the arcs is given by the contour points of the fashioning line, as presented in figure 5.

The equation of the resulting curved lines is given by the sum of the constituent segments. The calculus of the line segments was presented above in case I, for straight fashioning lines with constant increment. The only difference is that in this case it refers to a part of the fashioning line.

The curved segments of the fashioning line are calculated using the relations defining the ellipse:

• ellipse general equation

$$\frac{x^2}{a^2} + \frac{y^2}{b^2} = 1 \Rightarrow \frac{x^2}{\Delta a_i^2} + \frac{y^2}{\Delta r_i^2} = 1 \qquad (8)$$

where:
Δr_i and Δa_i are line increment for segment i;
a and b   –   ellipse axis;
• ellipse eccentricity e

$$e = \sqrt{1 - \frac{\Delta r_i^2}{\Delta_i^a}} \qquad (9)$$

If e = 1, the arc of ellipse becomes a circle arc.
The length of the ellipse arc is calculated using elliptic integrals. Because the primitives of these functions are not elementary functions, the calculus can not be carried out using the Leibniz-Newton formula. These elliptic integrals are solved using approximation methods with tabled values [5]. The general equation for the length of an ellipse arc is:

$$L_{arc} = 2\pi a\left[1 - \left(\frac{1}{2}\right)^2 e^2 - \left(\frac{1*3}{2*4}\right)^2 \frac{e^4}{3} - \right.$$
$$\left. - \left(\frac{1*3*5*}{2*4*6*}\right)^2 \frac{e^6}{5} - ...\right] \qquad (10)$$

The ellipse eccentricity can be expressed using the vertical and horizontal increments of the fashioning line for segment i, resulting:

$$L_{arc} = 2\pi\Delta a_i\left[1 - \left(\frac{1}{2}\right)^2 \sqrt{1 - \frac{\Delta r_i^2}{\Delta a_i^2}}^2 - \left(\frac{1\cdot3}{2\cdot4}\right)^2 \right.$$
$$\left. \frac{\sqrt{1 - \frac{\Delta r_i^2}{\Delta a_i^2}}^4}{3} - \left(\frac{1\cdot3\cdot5}{2\cdot4\cdot6}\right)^2 \frac{\sqrt{1 - \frac{\Delta r_i^2}{\Delta a_i^2}}^6}{5} - ...\right] \qquad (11)$$

When the ellipse arc can be considered a circle arc ($a = b \Rightarrow \Delta a = \Delta r$, figure 6), its length is:

$$L_{arc} = \frac{\pi * r * a_i}{180} \qquad (12)$$

where:
L_{arc} is   length of the circle arc;
r   –   circle radius = $\Delta a_i = \Delta r_i$;
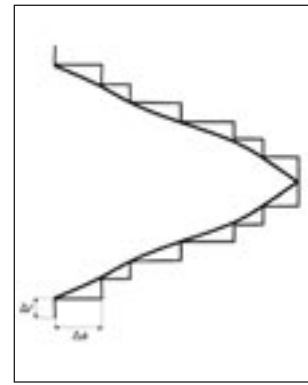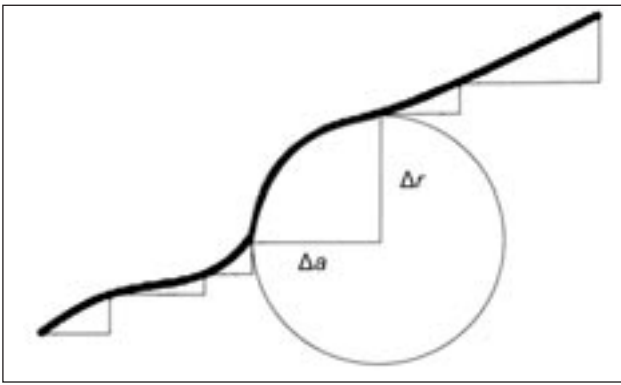a_i –   slope angle of the fashioning line (fig. 7)

Fig. 6. Curved fashioning line, with variable increment, with a zone where $\Delta a = \Delta r$
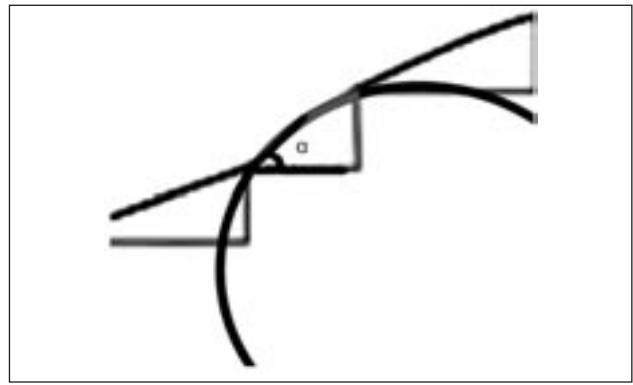

Fig. 7. Zone in the fashioning line with a circular geometry

$$tga_i = \frac{\Delta r_i}{\Delta a_i} \cdot C = C \qquad (13)$$

where:

C = density coefficient = B/A.

Same as in the case of straight fashioning lines, the parity of the points defining the line (the edge point for each increment) must be taken into consideration when calculating the geometry of the final fashioning line. Its amplitude can be controlled through the value of the vertical and horizontal line increment for each segment and stitch dimensions.

CONCLUSIONS

The 3D knitted fabrics obtained using the spatial fashioning technique presents a good potential with respect to the complexity of the shapes that can be produced. The design of such fabrics starts with its final 3D shape that gives the evolute and subsequently the fabric 2D plan and the position, type and dimensions of the fashioning lines.

The mathematical modelling of the fashioning lines used to create the 3D geometry of the fabric allows for the correlation between the 3D shape/body and the knitted fabric, expressed at stitch and line increment level. The paper considers both types of fashioning lines – straight line, with constant increment and curved line, with variable increment. In the last case, the line calculus is carried out according the geometry of each line component segment (line or arc of ellipse/circle).

The next step in the design of 3D spatial fashioned fabrics refers to the mathematical modelling of the 3D body which lateral area represents the final shape of the fabric and the correlation between the section lines giving the body evolute and the fashioning lines (the optimum increment) in the fabric.

BIBLIOGRAPHY

[1] D i a s , T., Fernando, A., Choy, P. K., Xie, P. *Knitting seamless three-dimensional shell structures on modern electronic flat bed knitting machines.* Bolton College, 1999, p. 36
[2] P o w e r , J. *Knitting shells in the third dimension.* In: JTATM, 2004, vol. 4, no. 4, p. 1
[3] S o n g , G., Wu, J., Wei, Y. C*omputer aided-design of three dimensional knitwear.* In: JOTI, 2006, vol. 97, no. 6, p. 549
[4] C i o b a n u , L., Dumitraş, C., Filipescu, F. *Systemic approach to the design of 3d knitted fabrics.* Part I. In: Industria Textilă, 2010, vol. 61, no. 3, p. 129
[5] C r a i n i c , N. *Elemente de analiză matematică pe spaţiul R.* Editura Institutului European, ISBN 978-973-611-627-8, 2009

Authors:

Şef de lucrări dr. ing. LUMINIŢA CIOBANU
Cerc. şt. DORIN SAVIN IONESI
Cerc. şt. ANA RAMONA CIOBANU
Universitatea Tehnică Gheorghe Asachi
Facultatea de Textile, Pielărie şi Management Industrial
Bd. D. Mangeron nr. 53, 700050 Iaşi
e-mail: lciobanu@tex.tuiasi.ro.
dorin1985ro@yahoo.com

The strength of the composite textiles at sewing

FLORENTINA HARNAGEA

MARTA-CĂTĂLINA HARNAGEA
MARIANA PĂȘTINĂ-COSTEA

REZUMAT – ABSTRACT – INHALTSANGABE

Rezistența la coasere a materialelor textile compozite

Lucrarea prezintă cercetări experimentale privind rezistența la coasere a unor materiale textile compozite, folosite la producerea încălțămintei de protecție. Rezistența și alungirea la rupere au fost analizate cu ajutorul aparatului de testare a rezistenței la tracțiune SATRA, dotat cu software digital și 466F. Au fost înregistrate valorile maxime ale forței de rupere a ochiului, ale rezistenței la rupere, ale alungirii la rupere și ale modulului lui Young. Software-ul asigură vizualizarea graficii pe măsura efectuării testelor. Rezistența la coasere a materialelor textile compozite depinde de: tipul și grosimea materialelor asamblate, tipul cusăturii, lungimea pasului, diametrul acului, numărul de rânduri, finețea acului și finețea aței de cusut.

Cuvinte-cheie: coasere, rezistență, alungire, ac, ață de cusut

The strength of the composite textiles at sewing

The paper presents experimental researches on the stitching strength of some composite textile materials used at manufacturing protection footwear. The breaking strength and elongation at break has been observed at the SATRA tensile testing machine with 466F attachment and digital software control. The maximum force at break of the stitch, the tensile strength at break, the breaking strength, the elongation at break, Young's modulus are registered and the ready-to-load software provides a visualization of the graphics as tests are undertaken. The stitching strength of composite textile materials is dependent on: type and thickness of the assembled materials, the manner of sewing, the stitch density, the needle's diameter, number of stitching rows, needle and thread fineness.

Key-words: stitching, strength, elongation, needle, thread

Nahtwiderstand bei Textilverbundwerkstoffen

Die Arbeit präsentiert experimentelle Untersuchungen für den Nahtwiderstand bei Textilverbundwerkstoffen, gefertigt für Protektionschuhware. Der Reisswiderstand und die Reissdehnung wurden wurden mit Hilfe des SATRA Zugwiderstandstestapparates analysiert, mit 466F und Digitalsoftware. Es wurden Maximalwerte der Maschenreisskraft, des Reisswiderstandes, der Reissdehnung und des Young-Moduls aufgeschrieben. Die Software sichert die Grafikvisualisierung während der Testdurchführung. Der Nahtwiderstand der Textilverbundwerkstoffe ist abhängig von: Art und Dicke der Verbundmaterialien, Nahtart, Stichlänge, Nadeldurchmesser, Reihennummer, Nadelfeinheit und Fadenfeinheit.

Stichwörter: Nähen, Widerstand, Dehnung, Nadel, Nähfaden

The composite textiles are being used more and more for manufacturing footwear products and leather goods, along with leather and leather substitutes [1]. Thus, for manufacturing uppers for protection footwear there is used a diversified range of composite textile materials, respectively materials made of synthetic threads, laminated with plain-weave or twill woven fabrics.

At sewing the component parts of the footwear uppers there must be assured the assembly's strength through choosing an adequate sewing needle and thread in correlation to material's thickness [2, 3].

The breaking strength of the stitch is given by the material's strength after punching for sewing and the thread strength [2]. The material's strength after stitching is dependent on the initial characteristics of the material and how it weakens during sewing, on the stitch density, the needle's diameter and the number of seams [4].

For sewing flexible patterns, the needles present different forms of point's section. The needle's point section is chosen considering the type and thickness of material. The needle's point can be sharp (for sewing textile materials and leather substitutes on textile layer or blunt-pointed (for sewing leather). The blunt needles can have the profile lensshaped, rhombic, triangular, with four edges or special [2, 5].

The lens-shaped needle point perforates the material at an angle to the seam: 0º, 45º, 90º and 135 [5]. The needle's point section must be a little more bigger (with 0,04–0,05 mm) or at most equal to the blade's diameter in order to avoid the fact that the needle deforms under warming effect at cutting the material [6]. The thread strength is dependent on the initial characteristics of the thread and on how the thread is weakened at stitching due to abrasion [7].

The paper presents results on the stitching strength of some textile composite materials used for manufacturing uppers for the protection footwear.

METHODS USED

The materials used for the tests have been provided by SAFETY, manufacturer of shoe uppers.

The physical and mechanical characteristics [8] of the tested materials are shown in table 1, and those of the thread's characteristics in table 2.

In order to assemble the samples there have been used the 301 stitch, needles of different diameters – *Nm* 100 and 120, synthetic threads Coats *Nm* 40/3; 30/3 and 20/3.

The samples have been sewed at different stitches, for textile materials being used the open seam (fig. 1) and for textiles sewed with leather was used the lapped seam (superposed patterns) (fig. 2).

After the samples are sewed and the thread is knotted, tests are being undertaken at the tensile testing machine SATRA (STM 466) with 466 F attachment and SATRA software, providing quick and simple to understand results (fig. 3 *a, b*).

Table 1

PHYSICAL-MECHANICAL PROPERTIES OF THE TESTED MATERIALS							
Materials	MT_1		MT_2		MT_3		Leather
Property	Value						
Components	Fabric face side	Fabric reverse side	Fabric face side	Fabric reverse	Fabric face side	Fabric reverse side	–
	polyester	cotton	cotton	cotton	polyester 3	cotton	–
The density of yarns in the fabric, yarns/10 cm	U 560 B 440	U 340 B 180	U 520 B 300	U 200 B 100	U 330 B 300	U 200 B 100	– –
The linear density of yarns based on mass per unit length, tex	U 19.7 B 20.3	36 43.2	U 30.7 B 40	28.6 81.6	U 17.3 B_1 184.2 B_2 10	36.7 100	– –
Type of woven fabrics	Basket weave 2/2	Twill 3/1	Basket weave 2/2	Plain-weave	Canvas	Plain-weave	–
Thickness, mm	0.9		1.0		1.1		1.1
Weight, g/m²	54		60		66		–
Tensile stress, at break, N/mm²	22.665 ± 0.15		24.63 ± 0.69		46.07 ± 0.33		30.014 ± 1.98
Breaking strength, N/mm	22.395 ± 0.135		24.63 ± 0.69		50.68 ± 0.36		27.385 ± 0.64
Elongation at break, %	39.262 ± 1.08		17.125 ± 0.675		55.68 ± 2.38		57.737 ± 1.032
Young's modulus, N/mm²	290.376 ± 1.6		223.494 ± 1.458		154.476 ± 2.914		64.264 ± 0.976

Table 2

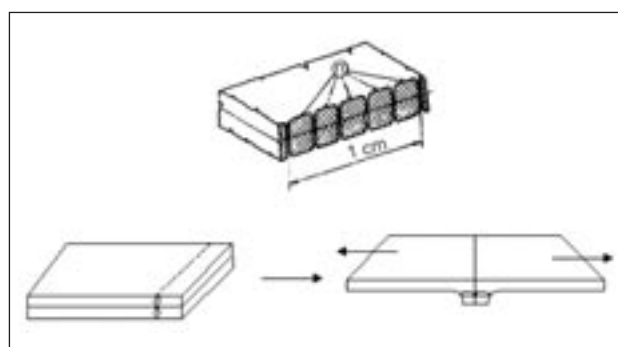| THREAD CHARACTERISTICS			
Property \ **Sample**	Coats Gral 40 TKT	Coats Gral 30 TKT	Coats Gral 20 TKT
		Value	
Composition	PES 100%	PES 100%	PES 100%
Metric number	40/3	30/3	20/3
Strength, N	42.65 ± 1.15	49.70 ± 0.5	74.85 ± 0.85
Elongation at break, %	25.812 ± 1.412	33.25 ± 0.85	35.75 ± 1.0

Fig. 1. Open seam

The testing has been done at a loading speed of 100 ± ± 5 mm/minutes, in conformity with the norm SR EN 13 522/2003. The maximum force at break of the stitch (N), the tensile strength at break (N/mm²), the breaking strength (N/mm), the elongation at break (%), Young's modulus (N/mm²) and as well the load-distance graphs (fig. 4) are registered and the medium values and the coefficients of variation are calculated. The software allows real-time graphics as the tensile strength tests are undertaken.

The breaking strength of the material, respectively the stitching strength at break are compared with the values from the norm STAS 9689/3-1984.

As for the norm concerning the textile materials, respectively leathers, the minimum strength is 40 N/cm (4 N/mm) for 1 seam and 60 N/cm (6 N/mm) for 2 seams.

RESULTS AND DISCUSSIONS

After testing the composite textile materials at break, the software of the tensile machine SATRA STM 466 has registered for each experimental type the load-distance graphics as well as maximum force at break of
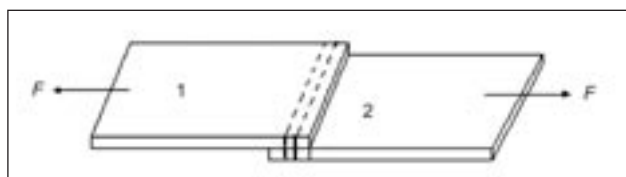
the stitch (N), the tensile strength at break (N/mm²), the breaking strength (N/mm), the elongation at break (%), Young's modulus (N/mm²).

Figures 5–11 show the load-distance graphs for the materials tested with tensile strength apparatus SATRA-STM 466, both for simple samples as for the sewed ones. The loaddistance graphics are presented for the stitched samples for a medium stitch density (n = 5 stitches/cm), thread Nm 40/3 and needle NM 100 (diameter of the needle blade = 1 mm), respectively for 2 stitches when assembling leather with textiles.

As in figure 5, the breaking of MT_1 material of 0.9 mm thickness (textile material made of synthetic yarns

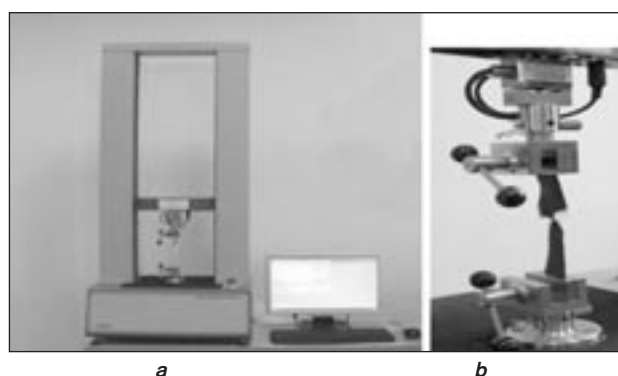Fig. 2. Lapped seam: 1 – leather; 2 – fabric

Fig. 3: a – the tensile testing machine SATRA STM 466; b – the 466F attachment
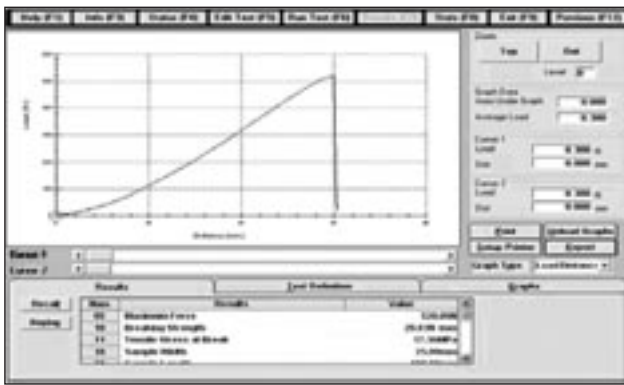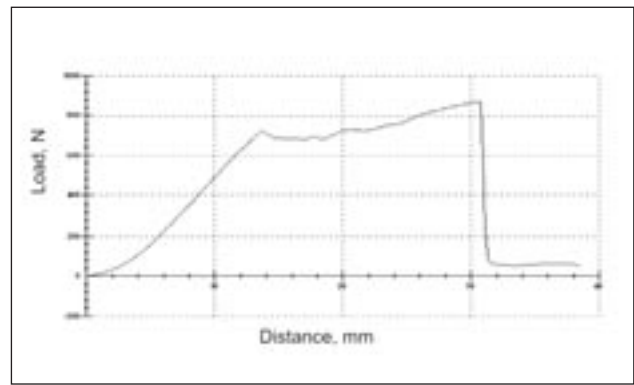
Fig. 4. The load distance graph
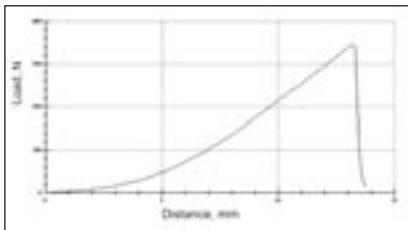

Fig. 5. Load-distance graph for MT₁

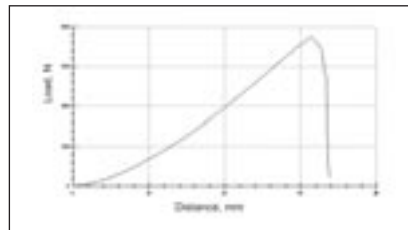Fig. 6. Load distance graph for MT₁ –
open seam

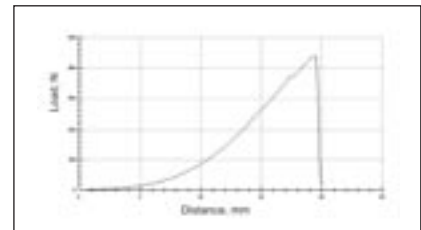Fig. 7. Load distance graph for MT₁ –
lapped seam

Fig. 8. Load distance graph for MT₂ –
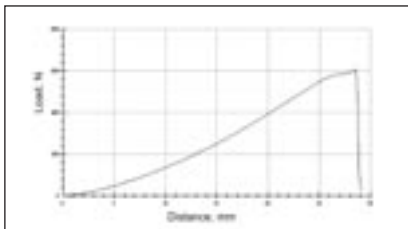open seam

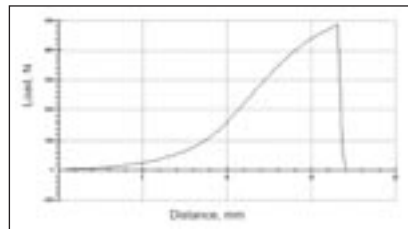Fig. 9. Load distance graph for MT₂ –
lapped seam

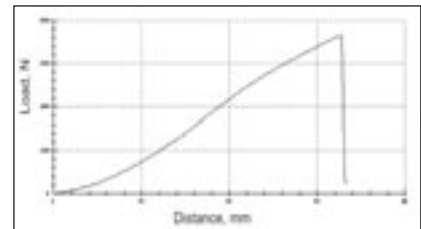Fig. 10. Load distance graph for MT₃ –
open seam

Fig. 11. Load distance graph for MT₃ –
lapped seam

laminated with cotton fabric), before stitching, a maximum elongation of 38.18% produced, corresponding to a maximum force at break of 869.4 N. The assembly is broken firstly at the second layer and the registered value is at 720 N, corresponding to an elongation of 14%. The value of elongation for a tensile stress of 10 N/mm² is inferior to an elongation of 14%, so the deformation in the lasting process is very small for this material.

For the open seam, the elongation at break (fig. 6) is about 13.225%, corresponding to a maximum force of 346.6 N. The elongation at break of 13.86 N/mm corresponds to the moment when the thread breaks in the holes. The graphic allows to establish the elongation and the force in the case of an imposed tensile stress of 10 N/mm² (F = 250 N, ε = 10%). It results that footwear uppers resist during the process of lasting.

When superposing textile material with leather, the elongation at break is much higher, 33.225% corresponding to a maximum force of 746.4 N (fig. 7). The assembly starts breaking at a force of 560.9 N. The breaking strength of 22.436 N/mm corresponds to the break of the textile material.

Before stitching the MT₂ composite material, 1.0 mm thickness, presents an elongation at break of 16.45%, corresponding to a breaking force of 591 N. When using an open seam for MT₂, an elongation of 19.55%

is registered, that corresponds to a breaking force of 439.6 N (fig. 8). The breaking strength of 17.58 N/mm is achieved when the thread breaks at the holes.

For the lapped seam the maximum force is equal to the force at break of 605.5 N (fig. 9) and the elongation at break is of 28.6%. In this case there is registered the break of the textile material at punching holes (the second row of stitch), the breaking strength is 24.22 N/mm.

The MT₃ material (1,1 mm thickness) breaks before stitching at an elongation of 67.55%, corresponding to a maximum force of 1061.5 N. For this material the first break is registered at the second layer for a value much smaller, respectively of 422.5 N. As in graphic from figure 10, the elongation at break is 16.525%, and the breaking force is 489 N. The same, the breaking of the assembly corresponds to a break of the thread in the punching holes, the breaking strength is 19.56 N/mm.

The elongation at break is 32.75%, in conformity to the load-distance graphs (fig. 11) and it corresponds to a breaking force of 792.2 N. In this case the leather breaks at the second row of stitching; the breaking strength is equal to 29.168 N/mm.

For an adequate illustration of the characteristics registered at the tensile testing machine STM 466 there have been used the medium values corresponding to each experimental type.
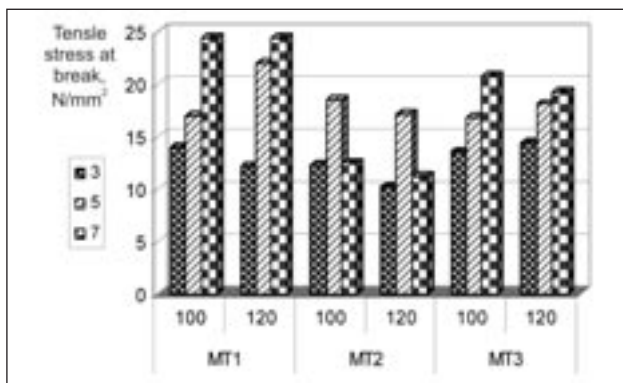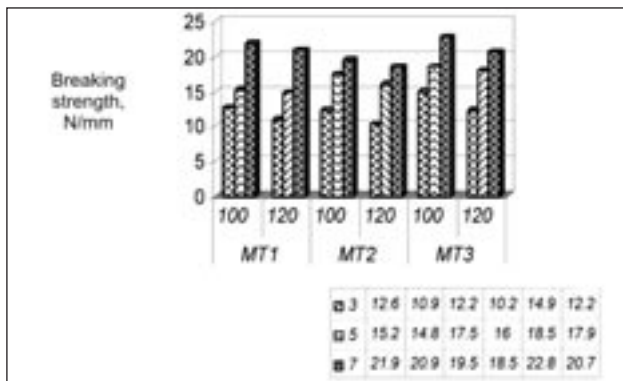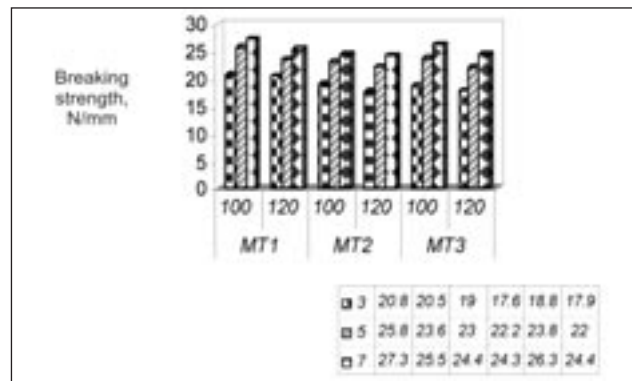
a
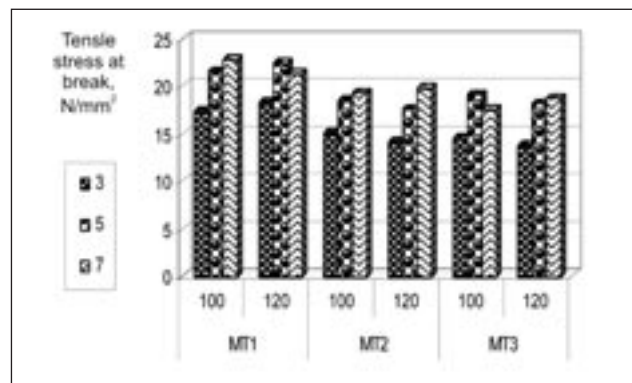
b

Fig. 12. The variation of the tensile strength at break as function of the needle's diameter, the stitch density and the type of materials: **a** – open seam; **b** – lapped seam

	3	12.6	10.9	12.2	10.2	14.9	12.2
	5	15.2	14.8	17.5	16	18.5	17.9
	7	21.9	20.9	19.5	18.5	22.8	20.7

a

	3	20.8	20.5	19	17.6	18.8	17.9
	5	25.8	23.6	23	22.2	23.8	22
	7	27.3	25.5	24.4	24.3	26.3	24.4

b

Fig. 13. The variation of the breaking strength at break as function of the needle's diameter, the stitch density and the type of materials: **a** – open seam; **b** – lapped seam
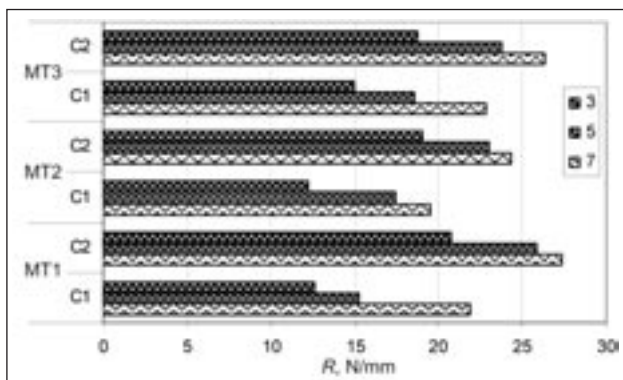

Fig. 14. The breaking strength of the two types of seam: C_1 – open seam; C_2 – lapped seam with two rows of stitching
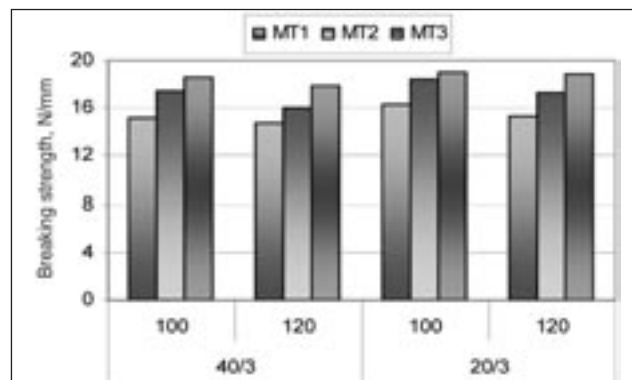

Fig. 15. The variation of the breaking strength as function of the needle's fineness (*Nm* 100 and 120) and of the sewing thread (*Nm*) 40/3 and Nm 20/3) – open seam

The variation of the tensile strength at break, in N/mm², is calculated automatically as a ratio between the breaking force, corresponding to the moment the reverse of fabric breaks, and the area of the sample's section (b x δ) is illustrated in figure 12 *a*, for the open seam and in figure 12 *b*, for the lapped seam.

The variation of the stitch breaking strength in N/mm, defined as a ratio between the registered force at break of the sewed assembly in N and the stitch length, in mm for the tested materials as in figure 13 *a* for the open seam and in figure13 *b* for the lapped seam. In conformity to the norm SR EN 13522/2003, the breaking strength is given by the ratio between the force at break and the sample's width, the width being equal to the stitch length.

In order to compare the breaking strength (in N/mm) of the two types of seams a variation of the strength is illustrated in figure 14 for needle NM 100.

As the graphic shows the breaking strength for MT₃ – polyester textile material, lace weave, laminated with woven fabrics with plain-weave presents the biggest values of the open seam, stitched with needle NM 100 and thread *Nm* 40/3. In the case of the lapped seam, the textile material MT₁ stitched with leather has the biggest values of the breaking strength. For all the other experimental types, the breaking strength of the lapped seam with 2 rows of stitching is higher.

In figure 15 it is resented the breaking strength of the open seam, when thread 40/3 and thread *Nm* 20/3 are used. From figure 15 it results that when using 20/3
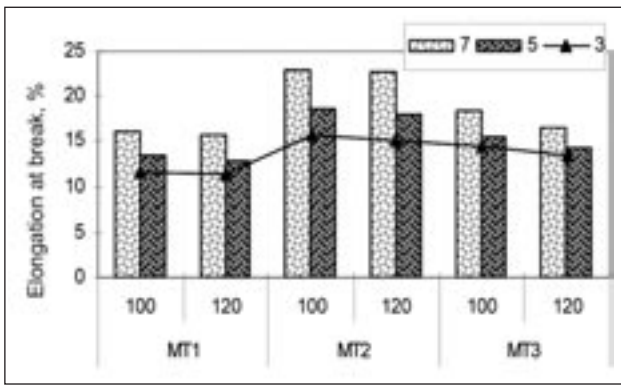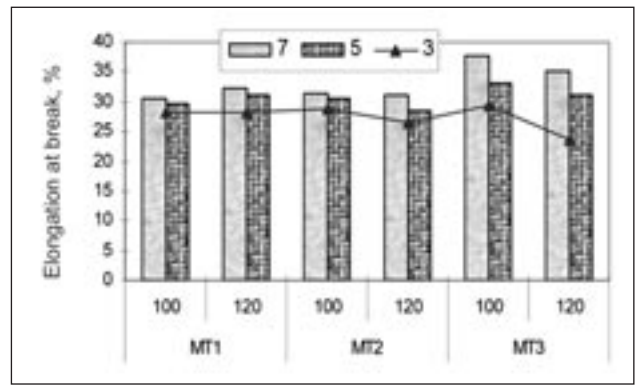
Fig. 16. The variation of the elongation at break as function of the needle's diameter and the type of tested materials:
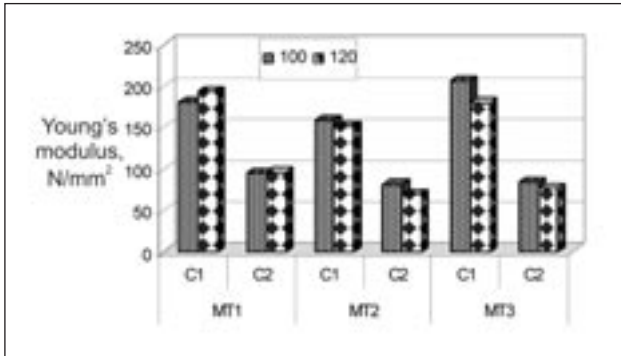*a* – open seam; *b* – lapped seam

Fig. 17. The variation of Young's modulus, N/mm²

thread, higher values are obtained for the breaking strength, as compared to the case of sewing with 40/3 thread.

The variation of the elongation at break, in %, for textile materials is illustrated in figure 16 *a* for the open seam and in figure 16 *b* for the lapped seam with 2 rows of stitching. As in figure 16, the elongation at break is dependent on the material's type, needle's diameter (NM 100 and 120), the stitch density and its type. The values of the elongation at break increase for a bigger stitch density for the same value of the needle's diameter, being higher in the case of lapped seam. The textile material MT_3 sewed with leather with two rows of stitching presents the biggest value of elongation. This value is mostly given by the leather's elongation. In the case of MT_2 material, for the open seam, the values

of the elongation at break are comprised between 12–23%, and for the lapped seam between 26–38%. The variation of the Young's modulus for a stitch density of 5 stitches/cm, thread 40/3, is presented in figure 17.

As in figure 19, the highest values of the Young's modulus are obtained for the open seam (C_1), in the case of MT_3 material, followed by MT_1 and MT_2, in comparison to the lapped seam (C_2).

As the graphics show, for an open seam the thread breaks at holes, and for the lapped seam with 2 rows of stitching either the leather or the textile material breaks at holes. The values of the breaking strength are superior to the minimum value marked by the norm STAS 9689/3-1984.

The stitch strength is dependent on the stitch density. Figure 18 *a,b* illustrates the variation of strength as function of the stitch density for MT_2.

As shown in figure 18 the unifactorial regression models, resulted after editing the experimental data are linear models, with the following general equation:

$$Rc = an + b \qquad (1)$$

where:
Rc represented stitching strength, N/mm;
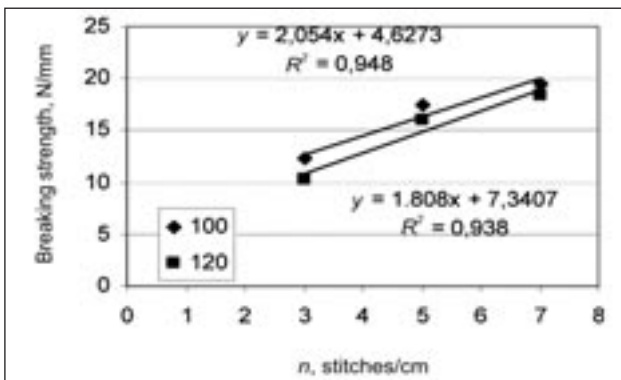n –   stitch density, stitches/cm;
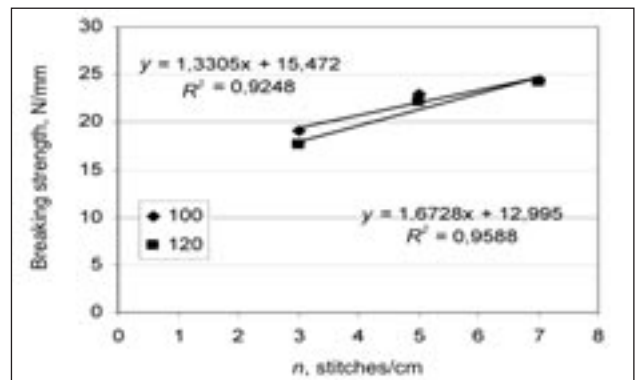a –   regression coefficient;
b –   the constant of regression equation.

The influence of the stitch density upon the elongation for the same material is illustrated in figure 19 *a,b*.
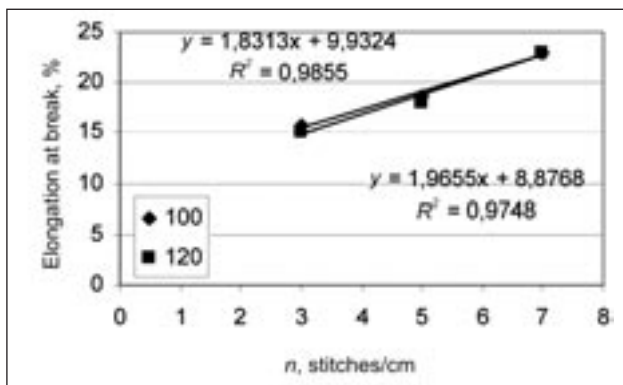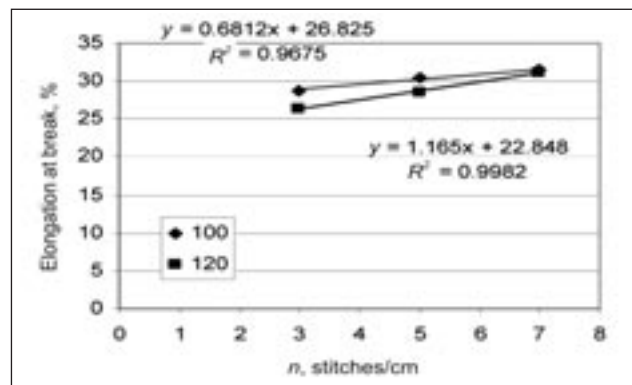

Fig. 18. Variation of the breaking strength of the MT_2 material:
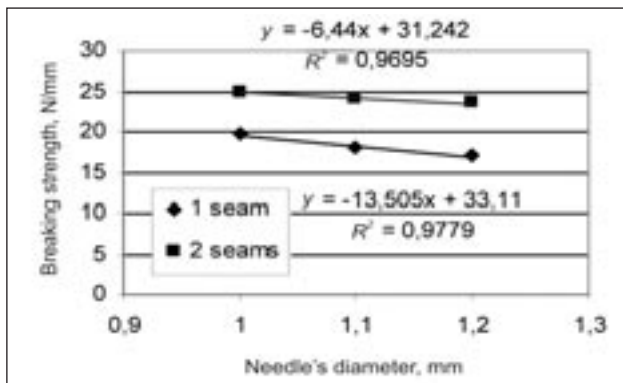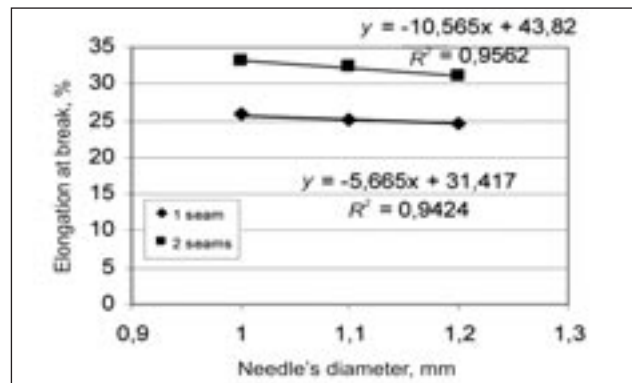*a* – open seam; *b* – lapped seam

Fig. 19. The variation of the elongation ar break of the MT$_2$ material:
a – open seam; *b* – lapped seam

Fig. 20. The influence of the needle's diameter on the breaking strength and elongation at break:
a – open seam; *b* – lapped seam

Table 3

Coefficient	MT$_1$ Nm 40/3				Coefficient	MT$_1$ + leather Nm 40/3 2 stitches			
	Rc, N/mm		Elongation, %			Rc, N/mm		Elongation, %	
	Metric number (*Nm*) needle					Metric number (*Nm*) needle			
	100	120	100	120		100	120	100	120
a	2.497	2.327	1.078	1.023	c	1.6383	1.2413	0.5708	0.9605
b	3.0577	4.938	7.937	8.1857	d	16.446	16.995	26.54	26.67
R^2	0.9835	0.9415	0.9581	0.988	R^1	0.9087	0.9811	0.9418	0.9313
Coefficient	MT$_2$				Coefficient	MT$_2$ + leather			
a	2.054	1.808	1.8313	1.9655	c	1.3305	1.6728	0.6812	1.165
b	4.6273	7.3407	9.9324	8.8768	d	15.42	12.995	26.825	22.848
R^2	0.948	0.938	0.9855	0.9748	R^2	0.9248	0.9588	0.9675	0.9982
Coefficient	MT$_3$				Coefficient	MT$_3$ + leather			
a	1.9705	2.1033	0.9803	0.7700	c	1.879	1.6168	2.0438	1.9012
b	8.8962	6.4208	11.23	10.873	d	13.566	13.341	23.165	21.709
R^2	0.9978	0.9608	0.9169	0.9338	R^2	0.964	0.9768	0.997	0.9981

The influence of the elongation upon the stitch density is described by an equation of linear type, as it follows:

$$\varepsilon = cn + d \qquad (2)$$

where:
ε represented elongation at break, %;
n –   stitch density;
c –   regression coefficient;
d –   the constant of regression equation.
The values of the regression coefficients are dependent upon the nature of assembled materials, upon the stitch type, stitch density, thread fineness and the needle (table 3).

The strength of the stitched assembly leather and textile material with 1 stitch and with 2 stitches is dependent on the diameter of the needle. For MT$_3$ (fig. 20 *a,b*) there is presented the dependence of the tensile strength and elongation at break, for the cases when it is being used 1 row of stitch and 2 rows of stitches, at a stitch density of 5 stitches/cm.
It is highlighted the decrease of the breaking strength and elongation at break as the needle's diameter grows (fig. 20). Obviously, the stitching strength increases as the number of rows of stitching becomes higher.

The influence of the needle's diameter upon the breaking strength and elongation at break is described by an equation of linear type, as it follows:

$$y = -ex + f \qquad (3)$$

where:

y represented breaking strength in N/mm, respectively the elongation at break in %;

x   –   needle's diameter;

e   –   regression coefficient;

f   –   the constant of regression equation.

The negative sign of the regression coefficient illustrates the inverse variation of the strength, respectively of the elongation as function of the stitch density. The values of the regression coefficients are dependent on the material's type, the stitching way and the needle's fineness.

CONCLUSIONS

- The breaking strength of the stitched composite materials is dependent on the stitch density, the needle's diameter, the thread fineness and the sewing needle.
- The strength of the open seams is smaller than the lapped seam's strength; for two rows of stitching the strength of the stitched materials grows as compared to one row of stitching.
- The values obtained for the breaking strength of the composite materials in the process of stitching are superior to the minimum value of 4 and 6 N/mm.
- The elongation at break of the stitched composite materials is dependent on the stitch type, needle's diameter and the thread's fineness, with values between 13 and 35%. In comparison to the elongation at break of the natural leathers (20–30%), for the MT_1 and MT_2 values of elongation at break are under 25% and over 30% for MT_3.
- The dependence of the breaking strength and elongation at break on the stitch density, for different values of the needle's diameter, is highlighted by regression models, of linear type, whose estimation functions are given by the next general expressions:

$$Rc = na + b \qquad [N/mm]$$
$$\varepsilon = cn + d \qquad [\%]$$

the positive sign of the regression coefficient illustrates the direct variation of the strength, respectively of the elongation as function of the stitch density.

- The dependence of the breaking strength and the elongation at break as function of the needle's diameter is described by a regression equation, linear type, such as $y = -ex + f$, the negative sign of the regression coefficient illustrates the inverse variation of the strength, respectively of the elongation as function of the stitch density.
- The load-distance graphics registered at the tensile testing machine SATRA, respectively graphics of dependence of the force on the elongation, offer very useful information for describing the way the composite materials break. For the tested materials it can be established the fact that the elongation at break of the first layer is the same as the elongation at break of the second layer, but there have been experiments where the break of the second layer was produced at a value inferior to the maximum force.
- Load-distance graphs registered at the testing tensile machine SATRA (STM 466) permit to establish the value of the elongation at a tensile stress of 10 N/mm^2 in order to highlight the deformation capacity of the tested materials in the lasting process (where the tensile stresses are of 7–8 N/ mm^2).
- The representations, using the bar-charts, show that for all the experimental variants, the obtained values, for the breaking strength of the stitched composite materials, correspondent to a 5 stitches/cm density, are superior to the values accepted by the standards. In practical conditions, for this case, is recommended that the textile material assembly to be done with needles NM 100 and thread *Nm* 40/3.

BIBLIOGRAPHY

[1] Enrico D'Amato. *Nonlinearities in mechanical behavior of textile composites.* In: Composite structures, 2005, vol. 71, p. 61
[2] Cociu, V., M Iureanu, G. *Bazele tehnologiei produselor din piele și înlocuitori.* Rotaprint, I. P. Iași, 1993
[3] Harnagea, F., Mihai, A., Mălureanu G. *Aspects regarding the stitching strength of the fabrics used for footwear uppers.* International Scientific Conference Unitech '05 Gabrovo. Proceedings vol. II, Technologies in textile production. ISBN 954-683-325-8, Gabrovo/ Bulgaria, 24-25 November 2005, p. 370
[4] Won Young Jeong, Seung Kook An. *Seam characteristics of breathable waterproof fabrics with various finishing methods.* In: Fibers and Polymers, 2003, vol. 4, no. 2, p. 71
[5] Harnagea, F. *Quality assurance for the glove manufacturing.* Proceedings of the 13th International Conference, Iași-Chișinău. ModTech 2009, 21–23 mai 2009, Romania, p. 303, ISSN 2006-3919
[6] Böllinghaus, T., Byrne, G., Cherpakov, B. I., Chlebus, E., Cross, C. E., Denkena, B., Dilthey, U., Hatsuzawa, T., Herfurth. K., Herold, H. et al. *Manufacturing Engineering.* Springer Handbook Of Mechanical Engineering 2009. Part B, p. 523, doi: 10.1007/978-3-540-30738-9_7
[7] Bedenko, V. E., Ivanov, N., Rudin, E. *Evaluating the properties of sewing thread for items for industrial and special applications in standardizing them.* In: Fibre Chemistry, 2009, vol. 41, no. 6
[8] Olaru, S., Săliștean, A., Niculescu, C. ș.a. *Optimization models of parachute manufacture process.* În: Industria Textilă, 2010, vol. 61, nr. 3, p. 124

Authors:

Conf. dr. ing. FLORENTINA HARNAGEA
Drd. ing. MARTA-CĂTĂLINA HARNAGEA
Drd. ing. MARIANA PĂȘTINĂ-COSTEA
Universitatea Tehnică Gheorghe Asachi
Facultatea de Textile, Pielărie și Management Industrial
Bd. D. Mangeron nr. 29, 700050 Iași
e-mail: florentinaharnagea@yahoo.com

The optimization of sealing parameters of assembling intended for products made of composite materials

IONUŢ DULGHERIU
CRISTIAN-CONSTANTIN MATENCIUC

DORIN IONESI
JUDITH MORICZ

REZUMAT – ABSTRACT – INHALTSANGABE

Optimizarea parametrilor de etanşeizare a asamblărilor, la produsele realizate din materiale compozite

Lucrarea prezintă aspecte referitoare la tehnologia de realizare în două etape a asamblărilor materialelor compozite, într-o primă fază cu ajutorul cusăturii 304, asamblări din clasa 304-FSn-1, urmate de etanşeizarea cu bandă adecvată, utilizând metoda cu instalaţii exoterme, ce funcţionează pe bază de convecţie cu aer cald, de joasă presiune. S-a urmărit ca, prin etanşeizare, să se stabilească un grup de parametri, format din temperatură, presiune şi viteză, pentru care se menţin, şi în zona de tratare, limitele indicatorilor de calitate specifici materialului de bază, netratat. Bazele de date experimentale, prezentate tabelar, au permis prelucrări în sistemele 2D şi 3D, care introduc de asemenea, elemente importante de optimizare, evidenţiate de modele matematice verificabile.

Cuvinte-cheie: convecţie, asamblare, etanşeizare, parametri de tratare, optimizare, sisteme

The optimization of sealing parameters of assembling intended for products made of composite materials

This paper tackles aspects concerning the two-phase technology of assembling composite materials in the first phase by means of the stitch type 304, assemblies of the 304-FSb-1 class, followed by sealing with an adequate tape, using the method of exothermic installations which operates on low pressure hot air convection. The aim of the sealing was to establish the group of parameters consisting in temperature, pressure and speed for which the limits of the quality indicators specific to the basic, untreated material are also maintained in the treatment area. The experimental databases, presented in the tables, allowed the 2D and 3D system processing which also introduces important optimization elements, highlighted by verifiable mathematical models.

Key-words: convection, assembling, sealing, treatment parameters, optimization, 2D and 3D systems

Optimierung der Dichtungsparameter bei Zusammenstellung von Verbundwerkstoffprodukte

Die Arbeit umfasst Aspekte betreff der Fertigungstechnologie der Zusammenstellung von Verbundwerkstoffen in zwei Phasen. In der ersten Phase benutzt man den 304 Stich, mit der 304-FSb-1 Einnaht-Klasse, dann die Dichtung mit einem entsprechendem Band, indem die Methode der exothermischen Instalationen angewendet wird, welche mit Konvektions-Warmluft bei niedrigem Druck arbeiten. Anhand der Dichtung wurde eine Parametergruppe bestimmt, gebildet aus Temperatur, Druck und Geschwindigkeit, für welche die Grenzwerte der Qualitätsindizies spezifisch dem unbehandelten Basismaterial sich auch in der Behandlungszone erhalten. Die experimentelle Datenbasis in Tabellenform, erlaubte die Bearbeitung in 2D- und 3D-Systemen und somit die Einführung von wichtigen Optimierungselemente, durch Anwendung von verifizierbaren mathematischen Modellen.

Stichwörter: Konvektion, Einnaht, Dichtung, Behandlungsparameter, Optimierung, 2D- und 3D-Systeme

The research represents a novelty in the field required both at the national and international level as a result of the development of new raw materials as well as of the various performance equipment. As a result of the theoretical and experimental research which was conducted, an experimental database was created, being very useful as far the optimization of these technologies is concerned.

Firstly, to this purpose was suggested a documentary synthesis concerning the new types of weld able materials, the applications to the product, the specific technologies, the equipment and installations existing at the national and international level [1–4].

Aspects relating to the new types of materials, the possibilities of assembling and using them in products having different purposes are presented in the first phase. Problems regarding the possibilities of using unconventional assemblies and their role in the improvement of the use value of clothing articles have been specially treated.

In the case of products having a special purpose, after seaming, it is very important to recur to sealing joints by means of secondary materials (sealing band) which is in fact a process of joining by convection in the case of which the heating agent is a current of hot gas, in most of the cases compressed air at low pressure [5–7].

At the basis of this technology lies the thermal adhesive welding process which, as it is well known, lies between thermal adhesion and welding. The sealed joints are obtained in two phases and namely:
– assembling by seaming the marks of the product;
– applying the sealing band to the assembling line in its length.

The schematic diagram of the working area in the case of a hot jet welding machine is represented in figure 1 [1].

The hot air jet is oriented towards the surface of the sealing band *5* by means of the nozzle *1*. The sealing band *5* and the semi-manufactured product *4* are fed in parallel between the conveyer idler *3* and the top roll *2* with a rotating motion, the result being the sealing subsystem *6*. The pressing force exerted by the roll
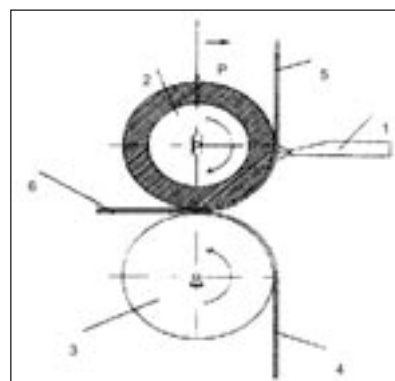

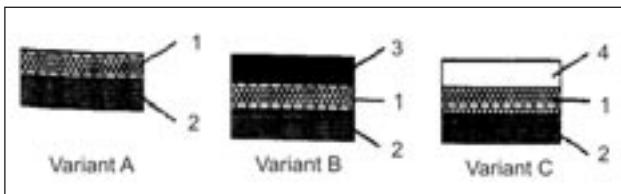Fig. 1. The process of hot air welding

Fig. 2. Types of sealing bands:
1 – coverage polymer; *2* – thermoadhesive type "hot-melt";
3 – warp-knit fabric; *4* – paper support Variant *A* – for lamination 2L; variant *B* – for lamination 3L; variant *C* – with silicone coated paper support

Fig. 3. Technological variants of the sealing sub-assemblies:
1 – textile support; *2* – coverage polymer; *3* – thermal adhesive; *4* – support polymer; *5* – lining; *6* – textile surface (knit or unwoven material) used as support for the intermediate layer; *a* – main laminated material 2L; *b* – main laminated material 3L; *c* – intermediate main layer 2L processed at the same time with the lining layer; *d* – laminated lining 2L; *e* – intermediate main layer 2L

2 generates the pressure necessary for the welding process.

The technology is specific to the manufacturing of waterproof clothing products or of those intended for thermal protection, products made of materials, with two or three layers. The sealing band has a morphological and a chemical structure adapted to each type of material (fig. 2) [1].

Consequently, the chemical structure of layer *1* is similar to or compatible with the coverage polymer used in order to obtain the composite material which is processed, this thing being a condition for the completion of the welded joint. The thermal adhesive *2* is placed in a thin layer on the surface of polymer *1* and has a low softening temperature.

In some cases, in order to avoid deformations which may appear while processing or transportation, we resort to attaching an additional paper band acting as a support which is withdrawn after welding. The succession of the process phases is: heating, pressing, cooling.

As it also results from the tables with experimental data, the technological parameters of the process are: the temperature of jet air at the outlet of the heating system, (T, $^{\circ}$C), the pressing force (P, N/m^2) and the welding speed (v, m/s) which is equivalent to the tangential speed of the conveyer idlers.

The technological variants of sealing sub-assemblies which are established according to the structure of materials results from figure 3 [1].

The experimental research was extended to assemblies similar to variant *c*, but another type of stitch being considered, adequate details are provided in figure 4 where we can notice the observance of the two phases for the achievement of the sealing joints.

The main material is made of the layers *1, 2* and *3* as it also results from the diagram in figure 4.

From the content of the paper we can notice the connection between the treatment parameters, the characteristics of materials and those of the assembly completed by thermal welding such as: the charge and the breaking extension, the permeability and the resistance to the of the vapour, air permeability, the in-
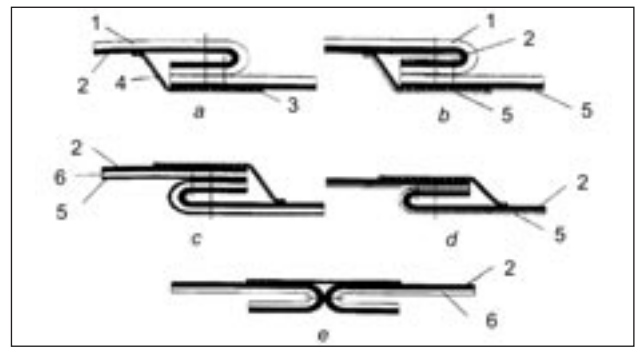
dicator for the passage of air, the conductivity and thermal resistance.

The experimental research can be also associated with the manufacturing technology of the products presented in the content of the paper and for which we can notice an extended demand both on the internal and the international market.

Following the content of the paper, we can notice the results regarding the optimization of comfort indicators connected with the parameters specific to the unconventional technology of assembling. This fact required the presentation: of general aspects concerning the welding mechanism, the relationship between the indicators influencing comfort and the specific treatment parameters.

The variants of research concerning the parameters influencing comfort have been extended as it was noticed for an area specific to the assembling class represented in figure 4 and in this respect, adequate details are presented below. All the indicators relating to the behaviour in a wet environment, thermal insulation and air permeability are shown in tables and diagrams for each variant and the relationship between these parameters and the treatment parameters of installations: pressure, temperature, speed are objectified by means of mathematical models registered in figures wherefrom the correlation coefficients also result. Besides the processing in the 2D system, the research was also extended to the 3D system, centralizing the main comfort indicators: the vaporization indicator, the air permeability indicator and the thermal conductivity. Their correlation can be noticed in the 3D processing which reinforces the conclusions presented in the 2D system. The above-mentioned indicators influencing comfort, indicators specific to the treatment area were established by means of well-known methods and the processing in the 2D and 3D systems was completed in Excel,
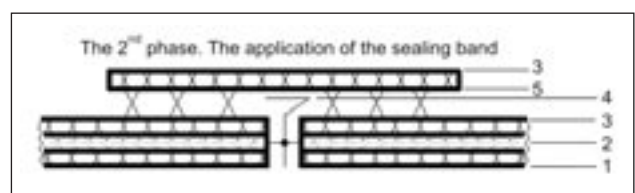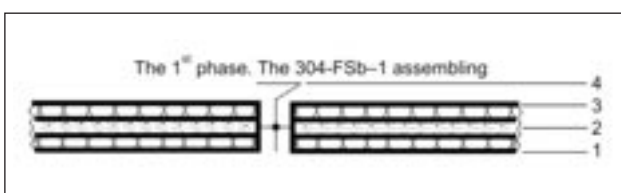

Fig. 4: *1* – main material; *2* – unwoven material; *3* – polymer layer; *4* – stitch type 304; *5* – thermal adhesive film

| | | | | | Table 1 |

CENTRALIZING DATA CONCERNING THE VAPOUR PERMEABILITY COEFFICIENT					
Sample	Temperature, °C	Pressure, Pa	Speed, m/s	P_v, kg	M, (kg/m²s) 10^{-6}
1	248	0.00004	0.01328	0.000291	1.709
2	299	0.00004	0.01328	0.000268	1.576
3	300	0.00004	0.01328	0.000268	1.578
4	325	0.00004	0.01328	0.000254	1.495
5	336	0.00004	0.01328	0.000252	1.481
6	341	0.00004	0.01326	0.000244	1.44
7	396	0.00004	0.01328	0.000223	1.315
8	396	0.00004	0.01328	0.000223	1.315
9	433	0.00004	0.01328	0.000202	1.185
10	436	0.00004	0.01328	0.000204	1.204
11	Standard sample-E				2.193

| | | | | | | Table 2 |

CENTRALIZING DATA CONCERNING THE AIR PERMEABILITY INDICATOR						
Sample	Temperature, °C	Pressure, Pa	Speed, m/s	Q, l/s	P_v, l/s · m²	i, kg/m²s
1	248	0.00004	0.01328	0.011	5.553333	0.0066
2	299	0.00004	0.01328	0.0121	6.108667	0.0073
3	300	0.00004	0.01328	0.0127	6.386333	0.0076
4	325	0.00004	0.01328	0.0132	6.664	0.0079
5	336	0.00004	0.01328	0.0135	6.802833	0.0081
6	341	0.00004	0.01328	0.0141	7.0805	0.0084
7	396	0.00004	0.01328	0.0157	7.9135	0.0094
8	396	0.00004	0.01328	0.0157	7.9135	0.0094
9	433	0.00004	0.01328	0.0166	8.33	0.0099
10	436	0.00004	0.01328	0.0171	8.607667	0.0103
11	Standard sample-E					0.0104

| | | | | Table 3 |

CENTRALIZING DATA CONCERNING THE THERMAL CONDUCTIVITY COEFFICIENT				
Sample	Temperature, °C	Pressure, Pa	Speed, m/s	λ, W/m°C
1	248	0.00004	0.01328	0.055
2	299	0.00004	0.01328	0.0613
3	300	0.00004	0.01328	0.0614
4	325	0.00004	0.01328	0.062
5	336	0.00004	0.01328	0.0626
6	341	0.00004	0.01328	0.0684
7	396	0.00004	0.01328	0.0684
8	396	0.00004	0.01328	0.0684
9	433	0.00004	0.01328	0.0719
10	436	0.00004	0.01328	0.073
11	Standard sample-E			0.0669

| | | Table 4 |

CENTRALIZING DATA WITH A VIEW TO THE ANALYSIS IN THE 3D SYSTEM		
M, (kg/m²s) 10^{-6}	i, kg/m²s	λ, W/m°C
1.709	0.0066	0.055
1.576	0.0073	0.0613
1.578	0.0076	0.0614
1.495	0.0079	0.062
1.481	0.0081	0.0626
1.44	0.0084	0.0684
1.315	0.0094	0.0684
1.315	0.0094	0.0684
1.185	0.0099	0.0719
1.204	0.0103	0.073
2.193	0.0104	0.0669

respectively by using the program of the company Jandel Table Curve 3D v2 [8].

EXPERIMENTAL RESEARCH, RESULTS AND INTERPRETATIONS

The data obtained after the experimental research, are registered in the tables 1, 2 and 3 in order to analyzed in the 2D system and in table 4 for being analyzed in the 3D system.

As it also results from the diagrams, each histogram, created in relation to the treatment parameter, is also accompanied by the processing and the analysis in the 2D system, to the diagram being added the corresponding mathematical model and the related correlation coefficient.
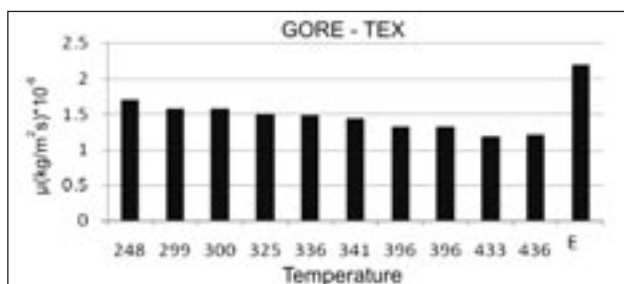

Fig. 5. The histogram of the vapour permeability indicator

The research concerning the comfort parameters was carried out in the context of the optimization of treatment parameters, namely, in these conditions are ensured the functions of durability and of presentation value in the treatment area, functions which are not modified in comparison with those of the main materials.

As a result of the experiments conducted on the main material, the following values, considered as comparison or standard values were established:

- the coefficient of vaporization equal to $2,19 \cdot 10^{-6}$ kg/m²s;
- the coefficient of thermal conductivity equal to 0,0669 W/m°C;
- the coefficient for the passage of air equal to 0,0104 kg/m²s.

The data registered in the tables 1, 2, 3, lay at the basis of drawing up the diagrams in figures 5, 6, 7, 8, 9 and 10, specific to the processing in the 2D system.

Although experimental research can be also extended to some functions specific to indicators of durability and presentation value, at the beginning, an analysis was performed from the theoretical and experimental point of view on the way in which the variation of the temperature of hot air jet at low pressure can lead to the modification of the vaporization coefficient, of the indicator for the passage of air and of the thermal conductivity
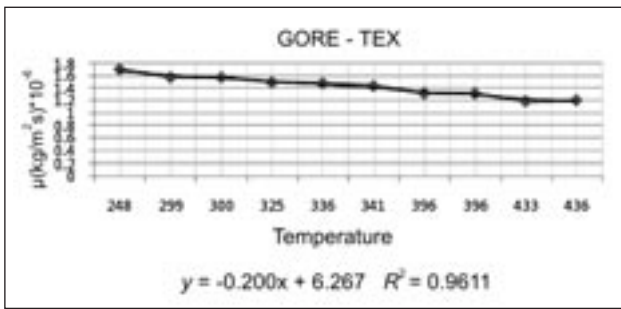
Fig. 6. The relationship between the vapour permeability indicator and temperature
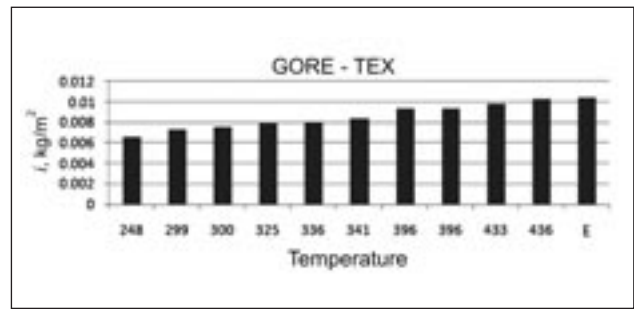

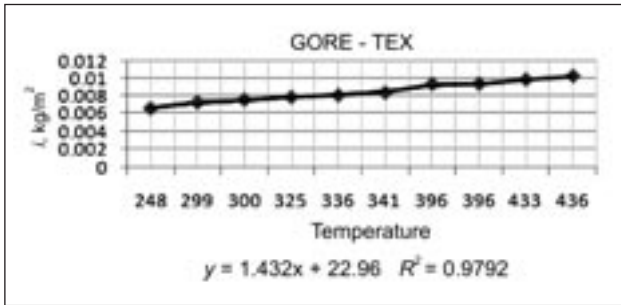Fig. 7. The histogram of air permeability indicator

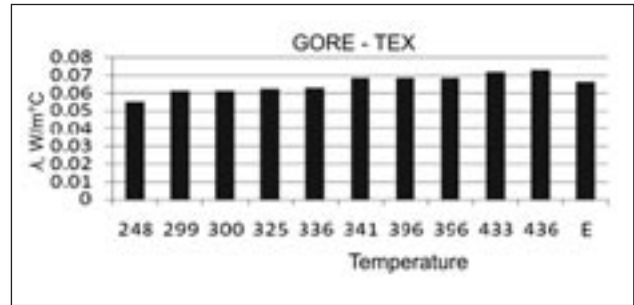Fig. 8. The relationship between the air permeability indicator and temperature

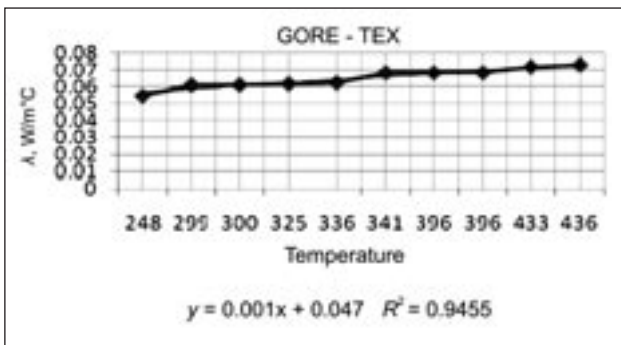Fig. 9. The histogram of thermal conductivity

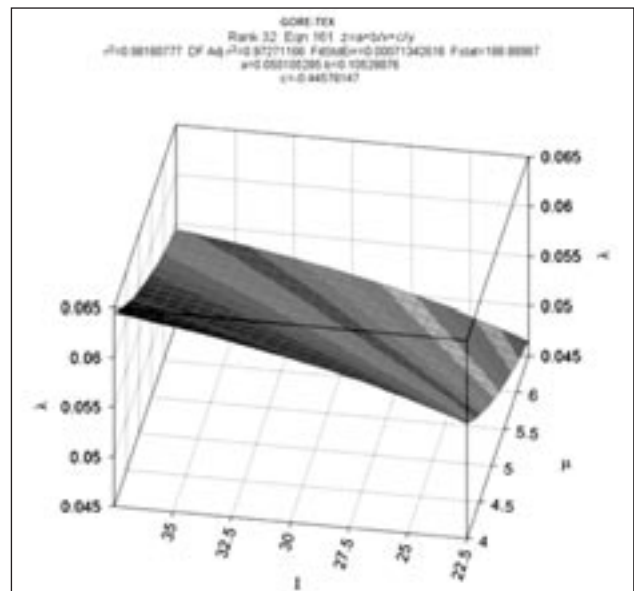Fig. 10. The relationship between thermal conductivity and temperature

Fig. 11. The relationship between the thermal conductivity, the vaporization coefficient and the coefficient for the passage of air

coefficient. Having regard to the wide range of temperature variation, within the limits 248–436°C, in the assembling area were carried out 10 experimental tests and a test for the main material considered as standard test. From the tables 1, 2 and 3 results the fact that experimental research was carried out in the conditions of temperature modification, by keeping the pressure and the movement speed of the semi-manufactured product constant.

The analysis carried out in the 3D system led to achieving some very complex mathematical models also registered in the diagram in figure 11, created in the triorthogonal system wherefrom the correlation coefficient also results. It is mentioned that out of the multitude of mathematical models displayed was selected the model which expresses more clearly and in the best possible way the interdependence between the three parameters: the thermal conductivity coefficient, the vaporization coefficient and the indicator for the passage of air.

We can notice a slight decrease in the thermal conductivity, within limits which are very close in relation to the increase in air permeability but the increase in vapour permeability has a more visible effect on its de-

crease. This fact is also in conformity with the specific physical processes which appear in the relationship body-clothing environment. When the human body becomes warm due to perspiration, it has to eliminate more heat and at the same time there should also exist the possibility of aerating it. The diagram in figure 11 justifies this fact and the mathematical model and the correlation coefficient are in conformity with the statements mentioned above. The complex mathematical models and the correlation coefficients above 0.95 attest the trustworthiness of experimental results and at the same time support the proposed optimization elements. This is the point wherefrom results the correlation between the treatment parameters specific to the technology analyzed and the parameters influencing comfort.

Table 5

CENTRALIZING OF THE MATHEMATICAL MODELS		
Processing systems	The mathematical model	The correlation coefficient
2D	$Y = -0.2\,x + 6.267$	$R^2 = 0.9611$
	$Y = 1.432\,x + 22.96$	$R^2 = 0.9792$
	$Y = 0.001\,x + 0.047$	$R^2 = 0.9455$
3D	$Z = a + b/x + c/y$	$R^2 = 0.9818$

It is very important to mention that the values for the parameters referred to in treatment conditions correspond to the values for the untreated materials considered as standard. The analysis of the histograms represented in the figures 5, 7 and 9 justify this fact.

CONCLUSIONS

Considering the main purpose of the research and namely, the optimization of treatment parameters so that the main indicators of the product can be maintained within normal limits in the sealing area in comparison with those of the material not undergoing this process, the specific values being considered as standard, the following conclusions can be drawn as a result of the theoretical and experimental results:

- The fact that at a treatment temperature of 250–300°C, the 0,00004 Pa pressure and the speed of 0,0132 m/s, the vaporization indicator, the thermal conductivity coefficient and the indicator for the passage of air are close to the standard, these values are considered to be optimal, respectively the thermal conductivity coefficient of 0,0669 W/m°C, the vaporization indicator of $2{,}19 \cdot 10^{-6}$ kg/m²s and the indicator for the passage of air of 0,0104 kg/m²s.

- Both the tables containing the experimental database and the histograms and verifiable mathematical models can be considered as optimization elements, also taking into account the limits of the values of correlation coefficients which both in the 2D and the 3D system have values above 0.95. This fact also results from table 5 which centralizes the mathematical models obtained after the processing's in the 2 systems.

- In order to justify the above-mentioned statements, we take into account the mathematical model obtained at the processing in 3D system having the form specified in the figure, namely:

$$z = a + b/x + c/y \qquad (1)$$

where:

z corresponds to the thermal conductivity coefficient;

x – the vaporization indicator;

y – the indicator for the passage of air.

For $a = 0{,}050$, $b = 0{,}105$ and $c = -0{,}445$, the identity of the mathematical model 1 is verified.

BIBLIOGRAPHY

[1] Loghin, C. *Sudarea materialelor textile.* Editura Performantica, Iaşi, 2003
[2] Mitu, S. *Confortul şi funcţiile produselor vestimentare.* Editura Gheorghe Asachi, Iaşi, 2000
[3] Loghin, C., Nicolaiov, P., Ionescu, I., Hoblea, Z. *Functional design of equipments for individual protection.* Management of technological chances, 2009, vol. 2, p. 693
[4] Badea N., Loghin, C., Mihai, A. *Intelligence – the basic concept of protection.* Management of technological chances, 2007, vol. 1, p. 27, IDS nr: BHF41
[5] Loghin, C., Ionescu, I., Hanganu, L. *Functional design of protective clothing with intelligent elements.* Annals of DAAAM for 2009 & Proceedings of the 20th International DAAAM Symposium, 2009, p. 435
[6] Loghin, C., Mureşan, R., Ursache, M., Mureşan, A. *Surface treatments applied to textile materials and implications on their behavior in wet conditions.* În: Industria Textilă, 2010, nr. 6, p. 284, ISSN 1222-5347
[7] Loghin, C., Ursache, M., Ionescu, I. *Experimental research on the sewability of ferromagnetic micro-wires.* In: Tekstil ve Konfeksiyon, October–December 2010, vol. 20, issue 4
[8] Matenciuc, C. C., Dulgheriu, I. *Model de evaluare a calităţii materialelor destinate realizării vestimentaţiei.* În: Industria Textilă, 2011, nr. 2, p. 99, ISSN 1222-5347

Authors:

Drd. ing. IONUŢ DULGHERIU
Drd. ing. CRISTIAN-CONSTANTIN MATENCIUC
Drd. ing. DORIN IONESI
Universitatea Tehnică Gheorghe Asachi
Facultatea de Textile, Pielărie şi Management Industrial
Bd. D. Mangeron nr. 53, 700050 Iaşi
e-mail: idulgheriu@tex.tuiasi.ro
cmatenciuc@tex.tuiasi.ro
dionesi@tex.tuiasi.ro

Dr. ing. JUDITH MORICZ
Colegiul Tehnic NAPOCA
e-mail: judith_moritz@yahoo.com

The effect of the usage of fiber protecting agent and dye class on the damage of Angora fibers occurred during dyeing process

RIZA ATAV

ABBAS YURDAKUL

REZUMAT – ABSTRACT – INHALTSANGABE

Efectul folosirii unui agent de protecţie a fibrei şi al clasei de coloranţi asupra deteriorării fibrelor Angora, în timpul procesului de vopsire

Proprietăţile fibrelor Angora sunt afectate serios, atunci când sunt supuse unui proces de vopsire prelungit, la diferite temperaturi de fierbere, iar una dintre alternative, pentru păstrarea luciului acestora, este folosirea unui agent de protecţie, în timpul vopsirii. Acest studiu se concentrează asupra efectului folosirii agentului de protecţie, în vederea prevenirii deteriorării fibrei Angora, în timpul tratamentelor desfăşurate la diferite temperaturi de fierbere. Totodată, a fost determinat şi efectul clasei de coloranţi asupra deteriorării fibrei. Potrivit rezultatelor experimentale, în timpul procesului de vopsire la temperatura de 100ºC, prin adăugarea unui agent de protecţie a fibrei în baia de vopsire, gradul de deteriorare scade, ajungând la unul similar nivelului de vopsire la 80ºC. Se poate concluziona că vopsirea reactivă bifuncţională este avantajoasă pentru protecţia fibrei, în timpul procesului de vopsire.

Cuvinte-cheie: Angora, agent de protecţie a fibrei, vopsire, colorant

The effect of the usage of fiber protecting agent and dye class on the damage of Angora fibers occurred during dyeing process

Angora fiber's properties are affected adversely when dyed for prolonged periods at the boiling temperature, and to preserve its luster, one of the alternatives is to use a fiber protecting agents in dyeing. This study has focused on the use of fiber protecting agent to preserve Angora fiber during dyeing treatments carried out at boiling point. Furthermore the effect of dye class on fiber damage during dyeing was also determined. According to the experimental results, in dyeing process at 100ºC by adding fiber protecting agent into the liquor degree of fiber damage decreases and reaches to damage value of fiber dyed at 80ºC. Furthermore, it can be concluded that bifunctional reactive dye usage is advantageous for the aim of fiber protecting during dyeing.

Key-words: Angora, fiber protective agent, dyeing, color

Effekt der Anwendung eines Faserprotektionsmittels und einer Farbstoffklasse auf die Beschädigung der Angorafaser, während der Färbungsprozesses

Die Eigenschaften der Angorafaser werden stark beeinflusst, wenn sie einem verlängertem Farbprozess bei unterschiedlichen Temperaturen ausgestezt werden und eine Möglichkeit für den Glanzschutz ist die Anwendung eines Protektionsmittels während der Färbung. Diese Untersuchung konzentriert sich auf die Auswirkungt der Anwendung von Protektionsmittel für die Beschädigungsvorbeugung der Angorafaser, während der Vehandlung bei unterschiedlichen Kochtemperaturen. Es wurde gleichzeitig auch der Effekt der Farbstoffklasse bei 100ºC auf die Faserbeschädigung bestimmt. Gemäss der experimentellen Ergebnissen, sinkt der Beschädigungsgrad durch Beifügung eines Protektionsmittels für Faser im Färbebad, bei einer Färbung mit der Temperatur von 100ºC gleich einer Färbung mit 80ºC. Man kann schlussfolgern, dass die reaktive bifunktionelle Färbung günstig für die Faserprotektion während dem Färbeprozess ist.

Stichwörter: Angora, Faserprotektionsmittel, Färbung, Farbstoff

The Angora rabbit is a very old breed of rabbit, believed to have originated in Turkey in the town of Angora. Angora production is truly an international industry. Until 1965 France was the leading producer, with the world market now being dominated by Chinese produced fiber. China now provides in excess of 90% of the trade Angora fiber. The other producers are France, Chile, Argentina, Hungary, Germany, Finland and India [1]. Partly because rabbit hair is produced on small-scale farms, actual production figures are difficult to establish, but it is estimated the world production is around 3 000 tons [2]. Angora fibers are used in the production of inner and outer garments (hats, sweaters, blankets etc.) either alone, as well as by blending with other fibers (particularly with fine wool), due to being quite light and having high heat retention capacity [3].

As generally known, wool fiber is easily damaged by aqueous treatments, particularly at high temperature or high pH level [4]. This fact is also valid for Angora fiber and its properties are affected adversely when dyed for prolonged periods at the boiling temperature, and to preserve its luster it is generally necessary to use short dyeing cycles or low dyeing temperatures [5]. Another alternative is to use a fiber protecting agents. These agents fall into three categories:

- products based on water-soluble proteins
- products based on fatty sulphonic acid esters or alkylsulphonic acids
- products based on formaldehyde or other chemicals capable of cross linking wool.

The first group of products was developed following the observation that wool is less damaged if dyed in previously used dye baths, since the dissolved protein residues in the standing dye bath reduce the rate of hydrolysis of the wool protein. The second group is claimed to be effective due to the bonding of large molecules at the surface of the wool, thus forming a thin hydrophobic coating which resists penetration by the liquor. Products in the last group act by cross linking the wool and thus replacing broken cystine disulphide cross links by $S–CH_2–S–$ groups, which are more stable [4].

This study has focused on the use of fiber protecting agent to preserve Angora fiber during dyeing treatments carried out at boiling point. Furthermore the effect of dye class on fiber damage during dyeing was also determined. In our previous study we have given the results for Mohair fiber [6, 7]. This study represents results for Angora fiber.

MATERIALS AND METHODS

Angora fiber of 16.82 l'm mean fiber diameter was used in all experiments. In literature it was stated that dye class used in dyeing also affects the degree of fiber damage. For this reason in this study milling acid dye
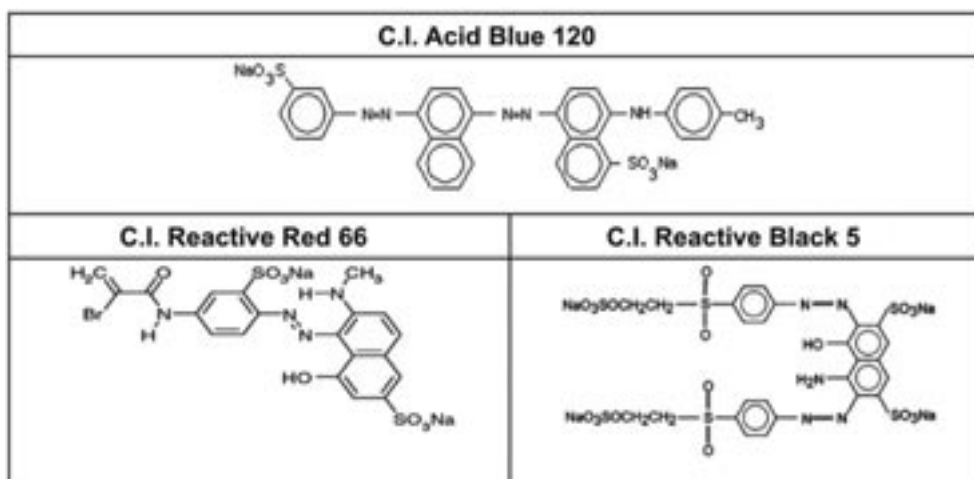
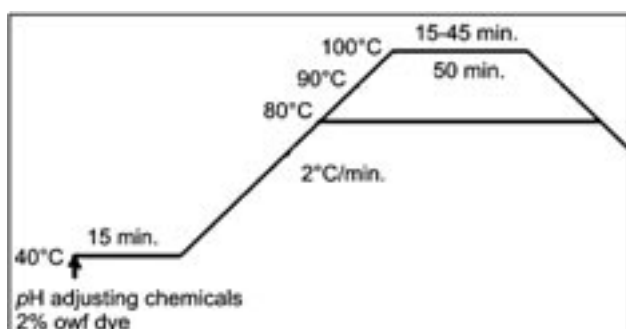Fig. 1. Chemical formulas of dyes used in experiments
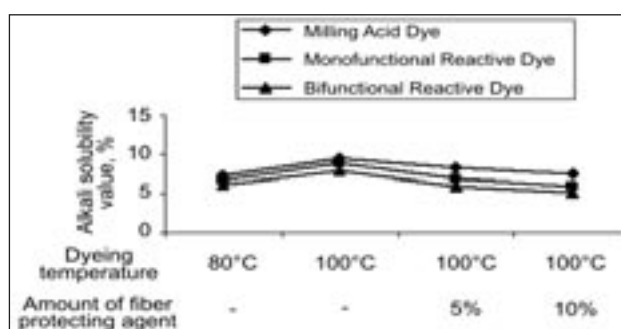

Fig. 2. The dyeing profile

Fig. 3. Alkali solubility values (%) of Angora fibers dyed with different dye classes

(C.I. Acid Blue 120), monofunctional reactive dye (C.I. Reactive Red 66) and bifunctional reactive dye (C.I. Reactive Black 5) were used. Chemical formulas of dyes used in experiments are given in figure 1.

Dyeing procedures were carried out at liquor to goods ratio of 30:1 and a dyeing depth of 2% owf in the absence and presence (5% and 10%) of fiber protecting agent at two different temperatures (100°C and 80°C), where the total dyeing time was constant (90 minute) (fig. 2). pH was adjusted to 5 by using acetic acid. After dyeing, the liquor was cooled down to 60°C with a rate of 2°C/minute and the fibers were taken out. Then dyed samples were rinsed with cold (5 minute) – warm (at 50°C 5 minute) – cold (5 minute) water respectively and dried at 80°C. All experiments were carried out by using soft mill water in Thermal HT type dyeing machine.

Color yield (K/S) and CIEL*a*b* color values of dyed samples were measured and washing fastness tests were carried out. Furthermore alkali solubility values of dyed samples were determined. Test method IWTO-4-60 was followed for alkali solubility test. It was calculated as a percentage of the original mass, according to equation given below:

$$Alkali\ solubility\ (\%) = M_1 – M_2/M_1 \times 100$$

where:

M_1 is the mass of the oven-dried sample before sodium hydroxide treatment;

M_2 – the mass of the oven-dried sample after sodium hydroxide treatment.

RESULTS AND DISCUSSIONS

Alkali solubility results of samples dyed with different dye classes at 80 and 100°C in the presence and absence of fiber protecting agent, can be seen from figure 3.

When figure 3 is examined, it can be said that fiber damage increases in the range of fiber dyed with milling acid dye > fiber dyed with monofunctional reactive dye > fiber dyed with bifunctional reactive dye. Zahn has suggested that the hydrolysis reaction responsible for the damage to the wool fibre when dyeing under slightly acid to neutral conditions is brought about by the action of the highly basic ε-amino group of lysine on amide groups in the wool peptides. Acylation of this group by reactive dyes may thus help to stabilize the wool proteins [4]. This situation explains why lower alkali solubility values obtained in samples dyed with reactive dyes. The reason of bifunctional reactive dyes to give lower alkali solubility values compared to monofunctional dyes is thought to be the formation of cross-linkings among fiber macromolecules during dyeing with bifunctional dyes. Because, if the reactive groups of bifunctional dyes form covalent bonds through two alternate macromolecules, fiber macromolecules will be cross-linked over reactive dye molecule.

Generally alkali solubility values are lower for dyeing carried out at 80°C compared to 100°C in the absence of fiber protecting agent, but by adding fiber protecting agent into the liquor degree of fiber damage decreases and reaches to damage value of fiber dyed at 80°C. Furthermore, according to color measurement and
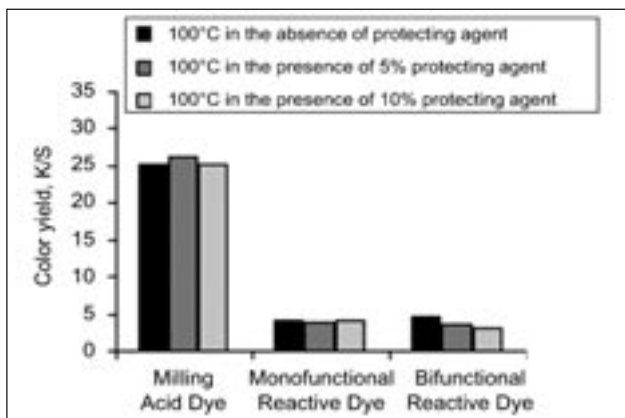
Fig. 4. Color yield results of Angora fibers dyed with different dye classes

CIEL *a*b* VALUES OF ANGORA FIBERS DYED WITH DIFFERENT DYE CLASSES				
Dye	Protecting agent	L*	a*	b*
Milling Acid Dye	–	16.685	2.729	−11.054
	5%	16.498	3.174	−12.090
	10%	17.236	3.104	−13.916
Monofunctional Reactive Dye	–	47.647	36.266	−12.548
	5%	48.818	38.927	−14.258
	10%	47.656	35.091	−13.909
Bifunctional Reactive Dye	–	44.139	−4.276	−14.386
	5%	45.185	−3.307	−13.353
	10%	46.756	−4.355	−13.025

EFFECT OF PROTECTING AGENT USAGE ON THE WASHING FASTNESS PROPERTIES OF DYED ANGORA SAMPLES (WO: Wool, PAC: Polyacrylonitrile, PES: Polyester, PA: Polyamide, CO: Cotton, CA: Cellulose Acetate)							
Dye	Protecting agent	Washing Fastness					
		WO	PAC	PES	PA	CO	CA
Milling Acid Dye	–	5	5	5	4–5	4–5	5
	5%	5	5	5	4–5	4–5	5
	10%	5	5	5	4	4–5	5
Monofunctional Reactive Dye	–	5	5	5	4–5	4–5	5
	5%	5	5	5	4–5	4–5	5
	10%	5	5	5	4–5	4–5	5
Bifunctional Reactive Dye	–	5	5	5	4–5	4–5	5
	5%	5	5	5	4–5	4–5	5
	10%	5	5	5	4–5	4–5	5

fastness test results it can be said that fiber protecting agent usage does not have important effect on color and washing fastness properties of dyed samples, as can be seen from figure 4, table 1 and 2.

CONCLUSIONS

As generally known luxury fibers such as Angora is damaged during dyeing carried out at boiling temperature, but decreasing the temperature reduces the dye-uptake of fibers [7]. For that reason in order to prevent the decrease in dye-uptake at lower temperatures, dyeability of Angora fibers should be improved for exemple by pretreating them with dendrimers [8]. Another solution for this problem could be dyeing these fibers at boiling temperature in the presence of fiber protective agents. Furthermore, in the light of experimental studies, it can be concluded that bifunctional reactive dye usage is advantageous for the aim of protecting the fiber during dyeing.

BIBLIOGRAPHY

[1] Schlink, A. C., Liu, S. M. *Angora Rabbits: A potential new industry for Australia*. RIRDC Publication no. 03/014, RIRDC Project No CSA-19A, April 2003
[2] Hunter, L., Hunter, E. L. *Silk, Mohair, Cashmere and other luxury fibres*. Edited by R. R. Franck, Boca Raton Boston New York Washington DC, U.S.A, 2000, p. 68
[3] Atav, R., Ozdogan, E. *Fibers gained from rabbit family – Angora*. In: Tekstil ve Konfeksiyon, April–June 2004, vol. 14, no. 2, p. 75
[4] Lewis, D. M. *Wool dyeing*. Society of Dyers and Colourists, England, 1992, pp. 104, 246
[5] Atav, R. PhD Thesis (Supervisor: A. Yurdakul). *Improvement of dyeing properties of some important protein fibers other than wool*. Ege University Textile Engineering Department, Izmir, Turkey, February 2009
[6] Atav, R., Yurdakul, A. *The usage of fiber protecting agent in dyeing of Mohair fibers*. 10th World Textile Conference AUTEX, Book of Abstracts, 123, Vilnius – Litvania, 21–23 June 2010
[7] Atav, R., Yurdakul, A. *The use of dendrimers to obtain low temperature dyeability on mohair and Angora fibers*. In: Industria Textilă, 2010, vol. 61, no. 2, p. 57
[8] Atav, R., Yurdakul, A. *Comparison of dyeing characteristics of luxury fibers (mohair and Angora) with wool*. In: Industria Textilă, 2009, vol. 60, no. 4, p. 187

Authors:
RIZA ATAV
Namık Kemal University
Department of Textile Engineering
Corlu, Tekirdag, Turkey
e-mail: ratav@nku.edu.tr

ABBAS YURDAKUL
Ege University
Department of Textile Engineering
Bornova, Izmir, Turkey

PROPOSTE 2011

Cea de-a XIX-a ediție a târgului **Proposte** s-a desfă-șurat la Villa Erba, Cernobio/Italia, în perioada 4–6 mai 2011.

Comparativ cu anul 2010, numărul total al parti-cipanților a scăzut cu 2,69%. Așa cum era de așteptat, a scăzut participarea Greciei cu 33% și a Japoniei cu 20%.

Trebuie semnalat faptul că a crescut numărul parti-cipanților din străinătate de la 59% la 61%. Numărul vizitatorilor din S.U.A. a crescut cu 21%, a celor din China aproape s-a dublat, iar al indienilor și rușilor a rămas constant.

Aceste cifre indică un interes tot mai mare, la nivel internațional, pentru mărcile *Made in Italy* și *Made in Europe*.

Așa cum afirma președintele Mauro Cavelli, producția de textile pentru amenajări interioare a crescut în medie cu 4% anual, însă va fi nevoie de aproximativ 8 ani pentru ca aceasta să revină la nivelul de dinainte de re-cesiune.

Europa continuă să fie una din cele mai importante piețe exportatoare pentru țesături și perdele. Producția a fost excelentă mai ales în țări ca: Franța, Marea Britanie, Olanda, Polonia, Portugalia și Elveția.

„Acest târg este unic în lume: peste 100 de expozanți lansează aici tendințele de top în domeniul decora-țiunilor interioare, acestea fiind transmise apoi în peste 70 de țări din întreaga lume, prin clienții companiilor. Proposte atinge un nivel de excelență datorită vizitatorilor selecți, expozanților, cercetătorilor, dar și eforturilor depuse pentru a crea colecții care combină competent stilurile clasic, eclectic, romantic și tehnic" – afirma Mauro Cavelli.

În data de 6 mai a avut loc o ceremonie de acordare a premiilor *Image 2012,* pentru trei finaliști: Alessandro Cocchia din Napoli – locul I, cu 39% din voturi, Davide Incorvaia – locul al doilea, cu 37% și Eliseu De Castro Leao – locul al treilea, cu 24%.

În standul fiecăruia dintre expozanți au fost prezente două elemente: producția – un element conceptual con-ținând un patrimoniu alcătuit din decorațiuni textile în toate stilurile imaginabile, construit de-a lungul unor decenii sau chiar secole de activitate și un element fizic și tangibil, cuprinzând colecțiile de produse inovatoare expuse.

Pe parcursul celor trei zile ale Proposte, au fost pre-zentate ultimele tendințe ale modei în lumea decora-țiunilor interioare.

Prima tendință o constituie folosirea materiilor prime din fibrele naturale: in, lână, mătase și bumbac. Inul a fost alegerea dominantă în aproape toate domeniile, dar și amestecurile de in cu fibrele sintetice, pentru a conferi o mai mare strălucire. Atunci când sunt folosite pentru perdele sau tapiserii, țesăturile din in sunt supuse unor tratamente de finisare speciale, pentru a căpăta un tușeu moale și o oarecare plinătate, voluminozitate și netezime.

Tușeul moale este ce de-a doua caracteristică defi-nitorie a acestui an. Lâna și mătasea, atunci când sunt folosite pentru perdele sau draperii, conferă încăperii impresia de personalitate puternică și de cămin confortabil.

Companiile participante la târg au expus țesături speciale, cu diferite modele pseudogeometrice, optice și chiar tridimensionale.

Tendința folosirii unor materiale naturale s-a concretizat în anumite tipare și culori predominante: modele micro-florale tip graffiti, arabescuri mari, dungi foarte late sau foarte subțiri, onduleuri și forme geometrice de o eleganță clară.

Colecțiile bio și verde s-au aliniat tendinței spre natural, nepericlitând sănătatea omului sau mediul.

Deși au fost prezente toate culorile curcubeului, tonurile de galben – în nuanțe de la galben deschis la galben muștar – au lăsat o impresie puternică. De neuitat au fost și nuanțele de roșu – de la rubiniu la roz și purpuriu, precum și cele de albastru - de la regal la albastrul cerului. Pe lângă fucsia, care transmite căldură și bună dispoziție, paleta de verde s-a bucurat de ascensiune, datorită capacității sale de a reprezenta nenumăratele nuanțe ale lumii vegetale. Nu au lipsit nuanțele naturale de bej, ivoriu, maro, alb sau galben pal.

Standurile cu textile tehnice, mai ales cele pentru aplicații contract și outdoor, au cuprins produse igni-fuge, antibacteriene, antifungice, rezistente la agenți atmosferici, hidrofobe, impermeabile și rezistente la pete.

O altă tendință notabilă a fost aceea spre luxuriant, în forma sa cea mai radicală. Decorațiunile au fost mai bogate și mai ieșite din comun decât în colecțiile create pentru piața Europei de Est, unde decorurile spec-taculoase sunt foarte cerute.

Produsele expuse erau ornate cu lamele metalice stră-lucitoare și broderie sidefată.

Pentru a crea efecte de strălucire, însoțită de rigoare și expresivitate, dar și de schimbare rapidă a culorii, au fost concepute anumite tapițerii și perdele cu fir auriu în urzeală și bătătură.

Candelabrele și brocarturile, cu modele jacard atât de fine încât puteau fi considerate picturi în ulei, au fost create pentru a evoca plafoanele reședințelor aristo-cratice din secolul al XVIII-lea. Merită menționată o tehnică specială care folosește firul contractat termic, pentru a conferi un aspect tridimensional țesăturilor plane.

În concluzie, temele abordate în colecțiile expuse au ținut cont de gusturile cele mai sofisticate, fiecare expo-zant întrecându-se pe sine, pentru a oferi clientelei internaționale produse adaptate pieței, inclusiv piețelor emergente.

Comunicat de presă. Milano, mai 2011

NOI REALIZĂRI ÎN DOMENIUL CONSTRUCŢIILOR DE MAŞINI TEXTILE

Dezvoltarea rapidă a sectorului de textile tehnice a în-curajat tot mai mult constructorii de maşini textile să-şi canalizeze resursele spre dezvoltarea echipamentelor specifice acestui sector. Acest lucru s-a reflectat şi în creşterea prezenţei acestora la târguri şi expoziţii internaţionale, cum ar fi Texprocess, Techtextil etc.

Constructorii de maşini continuă să dezvolte acest sector, noile inovaţii urmând a fi prezentate la ITMA 2011, care va avea loc la Barcelona, în perioada 22– 29 septembrie.

Fig. 1

Pregătirea fibrelor şi firelor

Swiss TexWinterthur şi **SwissTexFrance** (fosta RITM), au participat împreună la Techtextil, pentru prima dată, după preluarea de către SwissTexWinterthur a activelor şi vadului comercial al companiei RITM, în aprilie 2010. Swiss TexWinterthur AG – producător mondial de utila-je textile pentru extruderea filamentelor continue, este specializat în filamente continue voluminoase şi fire teh-nice şi industriale. Activitatea SwissTex France se con-centrează pe operaţiile de răsucire, asamblare, cablare, acoperire şi înfăşurare a firelor obţinute din fibre sinte-tice, artificiale, naturale şi minerale. Compania proiec-tează şi fabrică utilaje pentru producerea firelor tehnice destinate covoarelor, cauciucului, sticlei şi altor domenii industriale. În figura 1 este prezentată o maşină Swiss Tex, pentru fabricarea gazonului artificial.

Ţeserea

Procesul integrat de producere a textilelor tehnice pe maşini de ţesut multiaxiale cu graifăr, precum şi cel de realizare a ţesăturilor pentru aplicaţii casnice, pe maşini de ţesut cu jet de aer au câştigat, la **Techtextil 2011**, *Premiile pentru Inovaţie.* Premiul la categoria *Noi Teh-nologii* a fost acordat companiei **Lindauer Dornier,** pentru tehnologia de ţesere cu spată profilată (fig. 2).

Neţesute

Cu toate că activitatea de bază a companiei **A. Celli Nonwovens**, cu sediul în Italia, este producţia maşinilor
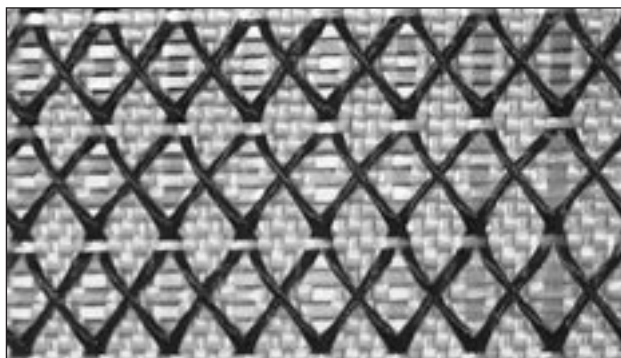

Fig. 2

de înfăşurare şi reînfăşurare secvenţială (fig. 3), desti-nate sectorului de neţesute, în ultimul timp aceasta şi-a concentrat atenţia pe dezvoltarea diferitelor tehnologii de imprimare, pentru a conferi materialelor neţesute o mai mare diversitate de desene şi modele. Managerii de proiect din sectorul tehnologiilor de uscare au brevetat o nouă tehnologie de formare a vălului cu jet de aer, cunoscută sub denumirea de Wingformer, a cărei dez-

Fig. 3

voltare s-a bazat pe experienţa companiei surori A. Celli Paper, producătoare de utilaje pentru fabricarea hârtiei. Pe lângă inovaţiile sale din domeniul fibrelor artificiale, compania **Trützschler Nonwovens** a realizat o nouă maşină de finisat ce poate fi utilizată ca unitate de ca-librare, calandrare, fulardare, stoarcere şi imprimare. În acest scop, s-au reproiectat calandrul, unitatea de fular-dare şi cea de calibrare, în vederea unificării unităţii cu doi cilindri într-o bază unică de construcţie. Maşina are o capacitate de producţie de până la 100 m/minut, o lăţime de lucru de până la 7 m şi o presiune a fluxului de 50 până la 600 N/cm. Reprezentanţii companiei sunt preocupaţi de dezvoltarea de noi pieţe pentru textilele interţesute, de exemplu pentru filtrele cu aer fierbinte, precum şi de îmbunătăţiri ale liniilor de interţesere şi de modul de economisire a energiei la utilajele de uscare şi de consolidare.

Sursa: www.technical-textiles.net

Nanotehnologii

O NOUĂ TEHNOLOGIE DE PRODUCERE A NANOFIBRELOR

În prezent, domeniile de aplicaţii ale nanofibrelor sunt încă destul de restrânse, iar produsele din nanofibre folosite la scară industrială sunt încă, în mare parte, legate de filtrare. Tehnologiile de producţie a nanofibrelor necesită costuri mari de investiţii, eforturi semnificative de service, iar productivitatea este scăzută.

Produsele de larg consum se limitează la gama de microfibre cu diametrul de peste 2–5 μm. Chiar dacă orice fibră cu diametrul sub 1 000 de nanometri poate fi numită nanofibră, definiţia cea mai larg acceptată impune un diametru sub 500 de nanometri.

În urma a peste cinci ani de muncă de dezvoltare, *Reiter OFT* împreună cu institutul german de cercetare *ITV Denkendorf* au dezvoltat o instalaţie de filare cu centrifugare a nanofibrelor, care poate produce fibre cu diametrul de 80 nm, folosind o configuraţie a maşinii simplă şi compactă, de mare productivitate.

Fig. 1

Maşina de filat centrifugă, cu doar trei capete, are un randament mai mare de 1 000 de ori decât cel al instalaţiei de electrofilare convenţionale, cu 25 de şiruri şi 1 250 de jeturi de filare, şi de 100 de ori mai mare decât cel al instalaţiei de electrofilare cu jet de aer.

Diennes Apparatebau oferă acum instalaţii de filare a nanofibrelor bazate pe tehnologia dezvoltată de *Reiter OFT*. Această tehnologie, care reprezintă o inovaţie în domeniu, este comercializată de Dienes Apparatebau GmbH. Tehnologia este disponibilă pentru instalaţii de laborator, dar şi pentru linii de producţie de mare capacitate, toate sistemele având aceleaşi avantaje tehnologice.

Pe aceste maşini poate fi prelucrată o largă gamă de polimeri: poliuretan, poliacrilonitril, acetat de celuloză, para-aramide, policaprolactamă, colagen, peptide etc. Materialele folosite pentru proiectarea componentelor pot fi adaptate la gradul de coroziune al fiecărui solvent specific. Deoarece polimerul este prelucrat sub formă de soluţie, trebuie ca masa moleculară să fie stabilă, pentru a evita degradarea. De obicei, vălurile de nanofibre nu sunt foarte stabile, majoritatea având o masă superficială de doar 0,3 g/m², iar substratul este acoperit.

Comparativ cu tehnologiile existente de electrofilare a nanofibrelor, care folosesc un câmp electric pentru obţinerea fibrelor şi formarea vălului, noua tehnologie de filare creează fibre printr-o combinaţie de forţe centrifuge şi forţe electrice, oferind un avantaj semnificativ, în sensul că pot fi acoperite şi substraturile grele, amortizarea câmpului electric de către substrat neinfluenţând producerea fibrelor. În plus, pompele de filare care alimentează centrifugele asigură o masă foarte omogenă a vălului pe fluxul de producţie şi un control precis al condiţiilor de filare. Capetele de filare foarte subţiri pot fi grupate uşor, astfel încât instalaţiile pentru mase relativ mari ale vălului pot fi integrate în liniile de producţie existente, fără a necesita mari cerinţe de spaţiu.

Ideală ar fi combinaţia dintre o unitate de producţie a nanofibrelor şi de interţesere într-o linie de neţesute multistratificate. Forţele slabe şi ajustabile ale jeturilor de apă sunt cea mai potrivită metodă pentru interţeserea vălului de nanofibre şi pentru îmbunătăţirea adeziunii între substratul purtător şi stratul de nanofibre. De asemenea, polimerilor termoplastici li se poate aplica calandrarea, atât timp cât compactarea produsului final este acceptabilă.

Datorită marii varietăţi de polimeri ce pot fi transformaţi în nanofibre prin această tehnologie, gama de aplicaţii poate fi semnificativ extinsă, introducându-se pe piaţă noi produse cu o valoare adăugată mare.

Pentru efectuarea testelor solicitate de clienţi şi dezvoltarea de produse, Dienes Apparatebau are un laborator şi o linie pilot cu lăţimea de lucru de un metru.

Smarttextiles and nanotechnology, iunie 2011, p. 3

Confecţii

ECHIPAMENTE DE PROTECŢIE BAZATE PE TEHNOLOGIA OUTLAST®

Survival-One Limited, lider mondial în proiectarea şi fabricarea echipamentelor de protecţie (fig. 1), a lansat recent un nou costum de supravieţuire ce încorporează tehnologia Outlast®, pentru pasagerii din elicoptere, care efectuează zboruri peste apă.

„Survival-One gestionează aproximativ 30 000 de costume de protecţie destinate pasagerilor elicopterelor, ce lucrează în industria de petrol şi gaze... Avem expe-

Fig. 1

rienţă în furnizarea de soluţii de supravieţuire, dar suntem mereu interesaţi în inovare. Vrem să oferim protecţie finală lucrătorilor, fără a compromite factorul uman. Cea mai recentă realizare a noastră este noul costum Seria 1000, care a intrat în prezent în uz, fiind purtat în timpul unui zbor peste Marea Nordului. Utilizăm materiale Outlast®, pentru a permite lucrătorilor maritimi să beneficieze de o izolare îmbunătăţită, care reglează microclimatul în interiorul costumului şi, prin urmare, îmbunătăţeşte confortul termic. Izolaţia termică ridicată, asigurată pentru a depăşi efectele scufundării în apă pe termen lung (de obicei, la mai puţin de 10°C), poate provoca stres termic purtătorului, iar utilizarea tehnologiei Outlast® este un mijloc de a atenua acest lucru... Nu te poţi lupta cu marea, dar bazându-ne pe cunoştinţele de proiectare, pe experinţa acumulată şi pe cele mai noi tehnologii, eficienţa echipamentului de protecţie poate fi sporită. Am realizat un adevărat progres cu această nouă generaţie de costume de supravieţuire, care oferă o protecţie maximă, fără a renunţa la confort" – afirmă Andy Wilson – manager de design şi dezvoltare la Survival-One Limited, din Marea Britanie.

Activitatea de bază a Survival-One este legată de furnizarea de costume de supravieţuire în interiorul elicopterelor, care să fie purtate de către echipaj şi de personalul maritim specializat în instalaţii în timpul transportului cu elicopterul la/de la instalaţiile de petrol şi gaze. Ele sunt concepute pentru a oferi protecţie împotriva imersiei în apă rece, în cazul în care elicopterul cade în mare. Aceste costume pot fi închiriate sau cumpărate de către cei ce lucrează în industria de petrol şi gaze.

În trecut, costumele de supravieţuire din sectorul Regatului Unit al Mării Nordului erau realizate conform Specificaţiei 19 CAA 19 din Marea Britanie. Noul costum nu numai că satisface cerinţele standardului european EASA, ci chiar depăşeşte cerinţele minime, asigurând capacităţi de performanţă şi supravieţuire excepţionale în apă. Oamenii care utilizează aceste costume, parcurgând drumul dinspre şi până la instalaţii trebuie să ştie că acestea sunt perfecte din punct de vedere tehnologic. Stratul exterior al costumului este impermeabil, respirabil şi ignifug. Căptuşeala termică foloseşte tehnologia Outlast® PCM, pentru o gestionare cât mai bună a căldurii.

Tehnologia Outlast® a fost dezvoltată iniţial pentru NASA, în scopul protejării astronauţilor de fluctuaţiile de temperatură din spaţiu. În cazul costumelor din Seria 1000, este controlat microclimatul din interiorul acestora, pentru a absorbi excesul de căldură din corpul utilizatorului. Căptuşeala Outlast® reţine excesul de căldură şi o eliberează treptat, pe măsură ce corpul purtătorului se răceşte. De asemenea, există un strat antimicrobian din 99,9% argint, care conferă materialului durabilitate, pentru mai mult timp şi un strat de 3 mm grosime, care captează aerul cald şi asigură o izolaţie mai bună.

Materialele Outlast® cu schimbare de fază absorb, stochează şi eliberează excesul de căldură din corpul utilizatorului. Sunt utilizate microcapsulele brevetate Outlast® Thermocules™, cca 3 milioane/cm², cu un înveliş stabil, ce nu poate fi distrus. În interiorul microcapsulelor sunt stocate substanţele similare parafinei, cu schimbare de fază.

Produsele Outlast® Adaptive Comfort® au o serie de avantaje: absorb excesul de căldură din corp, gestionează umiditatea, previn supraîncălzirea, reduc senzaţia de frig şi transpiraţia, se adaptează continuu la schimbările termice, asigurând un microclimat bine echilibrat şi o stare de confort optimă.

Sursa: www.outlast.com

CONFECŢII CU CONFORT SPORIT, PENTRU SPORT ŞI TIMP LIBER

Datorită succesului răsunător al utilizării textilelor funcţionale respirabile în confecţiile pentru sport şi timp liber, cercetătorii de la **Institutul Hohenstein** şi-au concentrat atenţia asupra caracteristicilor materialelor textile de control al căldurii şi umidităţii, în funcţie de diferitele părţi ale corpului.

Cu ajutorul aşa-numitei hărţi de confort al zonelor corpului, în viitor vor putea fi folosite materiale textile diferite într-un articol de îmbrăcăminte, care să corespundă acestei hărţi, pentru anumite părţi ale corpului.

Până recent, îmbrăcămintea sportivă a fost confecţionată integral dintr-un singur tip de material textil. Acest lucru s-a dovedit, de multe ori, nesatisfăcător din punct de vedere al confortului. Pentru a îndeplini anumite cerinţe privind eliminarea umezelii, izolarea termică şi protecţia împotriva intemperiilor, sportivii trebuie să poarte, deseori, câteva straturi de îmbrăcăminte.

În prezent, datorită structurilor textile inovative, acest lucru nu mai este necesar. În realizarea noilor materiale textile, se are în vedere faptul că acestea trebuie să asigure o reglare optimă a temperaturii şi umezelii, în funcţie de condiţiile de climă şi de tipul de activitate, şi, totodată, se iau în considerare aspectele senzoriale ale pielii, în vederea asigurării confortului în purtare.

Harta de confort ţine cont de distribuţia spaţială a căldurii şi umidităţii în anumite părţi ale corpului, pentru diferite tipuri de materiale textile purtate.

De exemplu, un anumit tip de material textil va proteja zona pieptului şi a spatelui împotriva vântului şi un altul mai respirabil va permite eliminarea transpiraţiei la subbraţ, oferind purtătorului senzaţia de uscat.

Principiul realizării acestei hărţi se bazează pe descoperirile legate de sistemul de termoreglare a corpului – un sistem complex, interconectat de receptori, care declanşează anumite reacţii fizice, atunci când primeşte mesaje de la creier. Aceste mecanisme de control sunt declanşate de stresul termic sau de stresul la frig. În condiţii de căldură extremă – de exemplu, vara, în timpul mersului pe bicicletă – sunt activate glandele sudoripare. Deoarece acestea nu sunt distribuite uniform pe tot corpul, cantitatea de transpiraţie eliberată variază în funcţie de anumite părţi ale corpului. În condiţii de stres la frig – de exemplu, la schi, mecanismele de control declanşează automat o funcţie de protecţie. Aceasta previne o pierdere semnificativă de căldură în părţile importante ale corpului şi în creier. În consecinţă, pielea şi extremităţile, în special mâinile şi picioarele, se răcesc. În piele se află receptori specifici senzaţiei de frig, responsabili de detectarea stresului la frig. Cu toate acestea, aceşti receptori nu sunt repartizaţi uniform pe

Fig. 1

suprafața pielii, ei fiind mai numeroși pe suprafața trunchiului și a capului și mai puțini la extremități.

Echipa de cerecetători condusă de Dr. Jan Beringer a dezvoltat un prototip de tricou, cu zone de confort bazate pe principiul hărții de confort al corpului, destinat celor care practică sporturi solicitante, cum ar fi ciclismul și alergarea (fig. 1).

Pe lângă criteriile termofiziologice, de control al temperaturii și umidității, în obținerea unui produs ideal, un rol important au avut și aspectele senzoriale ale pielii, cum ar fi tușeul moale și suplețea.

Într-o primă etapă, cercetătorii au identificat proprietățile pe care ar trebui să le aibă materialele textile, pentru a putea fi folosite în diferite zone ale corpului. În acest scop, au fost alcătuite profiluri ale proprietăților specifice pentru diferite materiale, combinând criteriile termofiziologice și senzoriale ale pielii. Aceste cerințe diferă în funcție de tipul de sport, de tipul de îmbrăcăminte, de partea corpului implicată și de condițiile climaterice. Compoziția materialelor este un factor deosebit de important în decizia de utilizare a fibrelor sintetice pentru anumite zone ale corpului și a fibrelor naturale higroscopice în alte zone.

Rezultatele indică obținerea unui beneficiu maxim prin utilizarea unor structuri textile inovative, acolo unde suprafața fibrei poate fi modificată în funcție de cerințe. Din punct de vedere științific, punctul central al acestui proiect îl constituie modul în care sunt combinate rezultatele studiilor investigațiilor termofiziologice – izolarea termică, respirabilitatea, controlul umidității și timpul de uscare – cu cele ale investigațiilor senzoriale ale pielii. Acestea au fost realizate în condițiile purtării îmbrăcămintei sport în contact cu pielea, oferind, pe lângă bune proprietăți termofiziologice, un excelent confort senzorial la nivelul pielii. Au fost necesare textile care să dea senzația de tușeu moale și suplețe și să nu producă iritații ale pielii – zgârieturi sau senzație de mâncărime. Îmbrăcămintea nu trebuie să se lipească de piele, chiar dacă aceasta este udă sau transpirată. Parametrii măsurați în timpul testelor au fost: indicele de aderență, indicele de umezire, indicele de suprafață, numărul punctelor de contact între materialul textil și piele, rigiditatea.

Etapa următoare în procesul alcăturii profilului condițiilor fiziologice ale articolelor de îmbrăcăminte a fost calculul precis al proprietăților specifice pe care trebuie să le îndeplinească un material, pentru a fi adecvat unui anumit tip de sport, anumitor condiții climatice etc.

Pentru a realiza acest lucru, cercetătorii și companiile partenere din industria textilă au elaborat un prototip de tricou cu mânecă scurtă, cu zone de confort pentru activități de jogging și ciclism.

Cu ajutorul unui manechin articulat termic, numit Charlie, care simulează sistemul de termoreglare uman, oamenii de știință au putut obține informația necesară pentru a proiecta acest tricou, prin efectuarea unor teste adecvate. În acest scop, manechinul articulat termic a fost divizat în 16 segmente. Fiecărui segment i-a fost atașat un sistem de încălzire controlat de calculator, ceea ce permitea reglarea căldurii în mod individual pentru fiecare secțiune. Testele au fost realizate pe manechin, atât în condiții de repaus, cât și în mișcare, folosind un dispozitiv care simulează mișcarea aerului sau turbulențele. Rezultatele acestor teste au fost completate de teste de purtabilitate, realizate pe subiecți voluntari, cărora le-au fost atașați senzori în poziții relevante pentru experiment și au fost testate diferite materiale în condiții climatice bine definite, folosind un dispozitiv de simulare a curenților de aer, în timpul mișcării pe o bandă de alergat sau pe o bicicletă medicală. Datele experimentale obținute au fost folosite apoi în proiectarea prototipului.

Smarttextiles and nanotechnology, iunie 2011, p. 10

Noi tehnologii

CONFECȚII BIOCOUTURE DIN CELULOZĂ REGENERATĂ

Confecțiile BioCouture (fig. 1), ultima realizare a designerului Suzanne Lee, au fost prezentate în cadrul expozițiilor *Trash Fashion: designing out waste,* de la London Science Museum – Marea Britanie, și *The Future that Never Was: Alter Nature,* de la ModeMuseum Hasselt – Belgia.

Proiectul BioCouture, pe care Lee îl derulează la Central Saint Martins College of Art and Design, investighează utilizarea microbilor pentru producerea de biomaterial textil.

În urma experimentelor, s-a constatat că anumite bacterii produc microfibrile din celuloză pură în timpul fermentării, ceea ce duce la formarea unui strat dens, care poate fi recoltat și uscat. Astfel, o cultură mixtă de celuloză bacteriană, drojdii și alte microorganisme a fost imersată într-o soluție zaharoasă de ceai verde, pentru a produce un văl flexibil de celuloză. S-a observat că bacteriile, care se hrănesc cu zahăr, produc fire subțiri de celuloză. Pe măsură ce acestea se lipesc

Fig. 1

unele de altele, ele formează un strat la suprafața lichidului. După două sau trei săptămâni, când grosimea stratului este de aproximativ 1,5 cm, stratul de celuloză este scos din baia de dezvoltare și turnat fie în stare umedă – într-o formă tridimensională, fie în stare uscată – într-o formă plană, pentru a putea fi folosit la confecționarea îmbrăcămintei. Materialul obținut poate fi vopsit și imprimat și este extrem de avantajos din punct de vedere ecologic, datorită faptului că necesită o cantitate mult mai mică de coloranți, decât în cazul altor fibre.

„O problemă ce trebuie rezolvată este legată de modul în care putem controla bacteriile, astfel ca acestea să producă celuloză în forma dorită, să se mențină flexibilitatea, să poată fi controlată biodegradarea și să se confere proprietăți hidrofobe... BioCouture promovează o nouă alternativă durabilă și prietenoasă mediului de producere pe scară largă a celulozei microbiene din fluxurile de deșeuri ce provin din industria alimentară și a băuturilor... Ceea ce a pornit ca proiect de modă a evoluat acum într-un proiect de dezvoltare a biomaterialor și abia acum începem să ne imaginăm posibile moduri de utilizare a acestui material. În acest moment, articolele de îmbrăcăminte create sunt prototipuri experimentale, nefiind disponibile comercial, și deoarece materialul se află încă în faza de dezvoltare, nu putem oferi mostre" – a explicat designerul Suzanne Lee.

Lee a condus seminare în colaborare cu departamentele de inginerie chimică și biologie sintetică de la Imperial College din Londra. Cercetările sunt în curs și membrii echipei ar fi deosebit de bucuroși să aibă vești de la alți oameni de știință care lucrează în acest domeniu sau în domenii conexe.

Smarttextiles and nanotechnology, iunie 2011, p. 8

IMPLANTURI TRIDIMENSIONALE PENTRU CHIRURGIA RECONSTRUCTIVĂ A ȚESUTURILOR MOI

În mod paradoxal, cu toate că țesutul adipos nu este dorit de nimeni, este deosebit de prețios. Oamenii de știință de la **Institutul Hohenstein** izolează și celule stem adulte din diverse surse, cum ar fi celulele de grăsime. De-a lungul mai multor ani, liposucția a fost considerată o procedură standard în chirurgia cosmetică, dar chirurgii sunt, în continuare, în căutarea unor susbtitute de țesut adipos, pentru a oferi un tratament mai bun pacienților cu defecte mari ale țesuturilor moi.

În acest context, oamenii de știință de la Institutul de Igienă și Biotehnologie din Boennigheim, Germania, au reușit să creeze, pentru prima dată, un implant de gră-
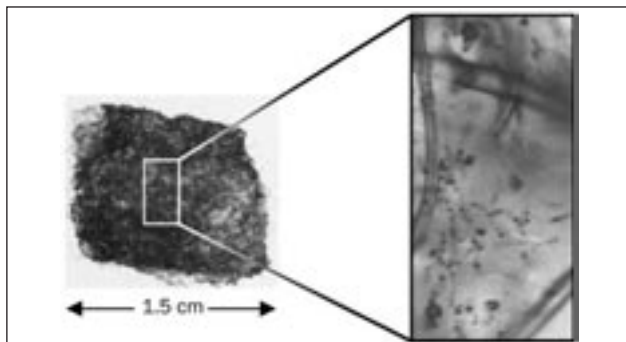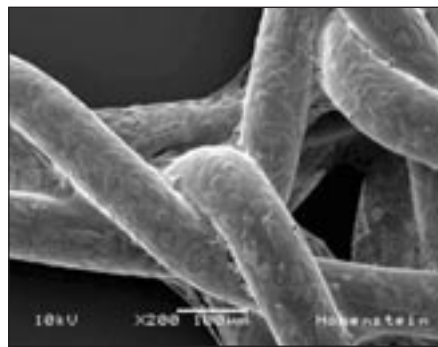

Fig. 1

Fig. 2

sime de dimensiuni rezonabile, în condiții de laborator. Mai întâi, ei au izolat cu succes celulele stem adulte în celule de grăsime, iar apoi acestea au fost cultivate și dezvoltate pe fibre biodegradabile. Ulterior, utilizând aceeași metodă, ei au avut posibilitatea de a cultiva celule umane stem adulte pe implanturi tridimensionale, pe care le-au diferențiat în celule de grăsime, pentru a realiza implanturi 3D, folosite în reconstrucția țesuturilor moi. În figura 1 este prezentat un implant tridimensional, cu o mare concentrație de celule de grăsime. Imagini detaliate, obținute cu ajutorul unui microscop electronic de scanare, ale celulelor stem umane adulte, dezvoltate pe un implant textil, sunt prezentate în figura 2.

În chirurgia reconstructivă, înlocuirea țesutului moale, pentru a trata rănile cu defecte mari de țesut, reprezintă o mare provocare. Așa se întâmplă, de exemplu, în cazul ulcerelor varicoase sau a cicatricelor mari. Până în prezent, chirurgii plasticieni foloseau lambourile musculo-cutanate și grefele de piele pentru reconstrucția țesutului moale – o procedură care solicita puternic țesutul sănătos din jur și, prin urmare, întregul corp al pacientului. În plus, s-a putut demonstra că celulele stem aplicate pe fibre eliberează factori de creștere, care promovează dezvoltarea de noi vase de sânge în zona implanturilor textile modificate biologic, formând o rețea capilară funcțională.

Cercetătorii de la Institutul Hohenstein au continuat experimentele, obiectivul lor fiind acela de a crea un substitut al țesuturilor moi pe bază de fibre polimerice cu biocompatibilitate sporită, adecvat pentru tratamentul diferitelor afecțiuni ale acestora. Există patru provocări majore în desfășurarea acestui proiect: cultivarea celulelor stem ale pacientului pe implanturi biodegradabile textile; formarea rapidă a noi vase de sânge în substitutul țesutului adipos, pentru a grăbi vindecarea rănii și pentru a asigura furnizarea de substanțe nutritive necesare în țesutul transplantat; diferențierea celulelor stem proprii pacientului în celule de grăsime, de preferat direct în corpul pacientului; adaptarea individuală a implantului la fiecare pacient, prin conturarea formei și aspectului tridimensional.

Oamenii de știință de la Institutul Hohenstein au reușit să obțină rezultate pozitive în cultivarea de celule stem ale pacienților pe implanturi tridimensionale, realizate din biopolimeri. Aceste celule stem adulte au putut fi diferențiate în celule adipoase, în scopul construirii unui substitut al țesuturilor moi, fără a provoca reacții inflamatorii sau respingerea transplantului.

Sursa: www.hohenstein.de/sites/de/uk/press.asp

NOI INOVAȚII ALE COMPANIEI SCHOELLER TEXTIL AG

Sănătatea generală devine un factor-cheie pentru multe ramuri economice și companii. **Schoeller Textil AG** a prezentat la *Techtextil 2011* noua tehnologie *iLoad®,* care abordează probleme precum starea de bine, prevenția sau terapia, generate de folosirea materialelor textile.

Folosind noua tehnologie, în materialele textile pot fi încorporate diferite substanțe benefice pentru organism sau substanțe cu efect terapeutic, care se eliberează treptat, pe parcursul purtării îmbrăcaminei, oferind purtătorului o stare de bine. Aceste materiale posedă stabilitate, capacitate de spălare permanentă și de încorporare/reîncorporare de medicamente sau alte substanțe active.
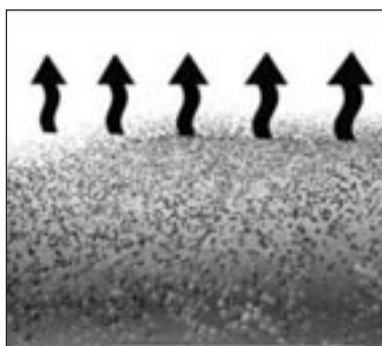
Fig. 1

Sistemul iLoad® constă în aplicarea unui strat special, donor de substanțe active, pe o țesătură de fond (fig. 1). În procesul de încărcare ulterior, acest strat donor, care acoperă fiecare fibră din țesătură, este combinat cu o emulsie specifică, care conține substanțe active, de exemplu produse terapeutice homeopate. Stratul donor, încărcat negativ, atrage ca un magnet emulsia încărcată pozitiv și o stochează ca un burete (fig. 2). Procesul de încărcare durează doar câteva minute și poate fi efectuat utilizând programele de spălare ale mașinilor de spălat industriale sau casnice. Datorită căldurii, vibrațiilor, umidității și transpirației, se declanșează un proces transdermic de descărcare constantă și de eliberare a substanței în stratul donor din piele (fig. 3). Timpul de desorbție, adică durata de timp necesară eliberării agentului activ, poate
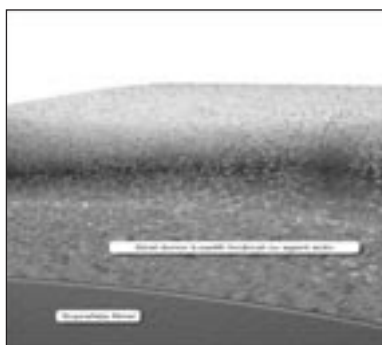
Fig. 2
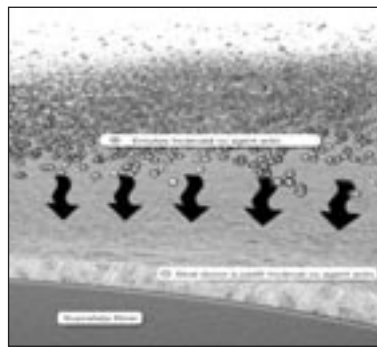
Fig. 3

fi adaptat în funcție de anumite scopuri specifice. La următoarea spălare, substanțele reziduale prezente sunt complet eliberate, iar iLoad® poate fi reîncărcat cu o nouă subtanță activă.

Compania Schoeller și-a continuat cercetările și a obținut un nou progres în domeniul textilelor – un model hibrid iLoad® cu capacitate de regenerare, care posedă atât proprietăți hidrofile, stocând agentul dorit și eliberandu-l în piele, cât și hifrofobe, acționând ca o zonă fără substanță. Exemple binecunoscute ale acestui principiu de funcționare sunt plasturii cu nicotină sau hormoni. Schoeller aplică acest hibrid pe suprafețele textile.

Această inovație este destinată, în special, echipamentelor de lucru și îmbrăcaminei sport, pentru asigurarea confortului și a stării de bine a purtătorului. Domeniul de aplicație medical includ include tulburările de somn, neurodermatitele, răcelile, escarele de decubit, îngrijirea pielii – revitalizarea și conferirea unei prospețimi de lungă durată etc. Sectorul de sănătate constituie o piață semnificativă de vânzări, de aceea, în viitor, furnizarea medicației pe bază de prescripție medicală și în colaborare cu personalul medical va reprezenta unul dintre principalele scopuri ale acestui proiect ambițios.

Timp de mai mulți ani, Schoeller a lucrat la această inovație, reușind în final să obțină parametri foarte buni de funcționare și de siguranță. Printr-o ajustare sistematică a stratului donor, a fost dezvoltat un material transportor foarte eficient și sofisticat, care s-a dovedit a fi stabil la temperaturi de până la 60°C și la peste 100 de cicluri de spălare. iLoad® a trecut cu ușurință și testul de citotoxicitate. Toate componentele sistemului au fost supuse celor mai riguroase testări existente în domeniul textilelor, acestea fiind în conformitate cu standardul Bluesign®. În următoarea etapă, variantele eficiente de agenți activi vor fi dozate și testate în colaborare cu parteneri specializați.

Sursa: www.schoeller-textiles.com

◌ **Textile nețesute**

NEȚESUTE DIN POLIPROPILENĂ CU CARACTERISTICI ÎMBUNĂTĂȚITE

Fibrele scurte de polipropilenă cu secțiune transversală trilobată, care pot fi consolidate termic, sunt puse, în prezent, la dispoziția producătorilor de materiale textile, pentru aplicații în domeniul sanitar.

La târgul internațional **Index 2011,** organizat la Geneva, în perioada 12–15 aprilie 2011, au fost prezentate

fibrele *HY-Light/T-194*, produse de compania **Fiber-Visions.** Aceste fibre pot fi utilizate la fabricarea de materiale nețesute, cu un grad ridicat de acoperire și cu un grad de uniformitate îmbunătățit. Ele își păstrează caracteristicile de rezistență și de tușeu moale, chiar și în cazul folosirii lor pentru realizarea de țesături ușoare. Compania din Varde, Danemarca, produce astfel de fibre, folosind o nouă tehnologie, care permite optimizarea proprietăților acestora, în vederea utilizării lor în procesele de fixare uscată a nețesutelor, în special pentru transformarea în țesături cardate consolidate termic. Nețesutele fabricate din aceste fibre au următoarele avantaje:

- o mare rezistență la tracțiune – fibrele trilobate furnizează materialului proprietăți echivalente cu cele ale fibrelor PP Fiber Vision, de cea mai bună calitate, pentru nețesute consolidate termic;
- o mai bună opacitate – nețesutele au o opacitate de până la 33% – în cazul fibrelor trilobate standard, și de 41% – în varianta cu opacitate maximă, comparativ cu opacitatea fibrelor PP clasice, cu secțiune rotundă, de 19%, masa specifică fiind aceeași în ambele cazuri;
- caracteristici de confort și tușeu moale îmbunătățite – fibrele oferă confort și drapaj mai bun și nu se încarcă electrostatic.

Fibrele HY-Light/T-194 au o masă specifică de 0,91 g/cm^3 – cu 50% mai mică decât a cea a poliesterului și cu 25% mai mică decât a poliamidei. Ele oferă o bună rezistență la alcalii, acizi și la majoritatea substanțelor organice și au proprietăți reduse de absorbție a umidității. Lungimea de tăiere a fibrei, gradul de ondulare și de lubrifiere a acesteia pot fi ajustate în funcție de necesități.

FibreVisions a dezvoltat, de asemenea, o fibră scurtă fină din polipropilenă, cu costuri reduse, destinată producerii nețesutelor cardate. Fibrele mai fine permit producătorilor de nețesute să obțină materiale ușoare, cu o mai mare uniformitate și un tușeu mai moale decât cele realizate anterior, menținând, în același timp, caracteristicile de rezistență și de acoperire.

Fiind concepute pentru procesele de fixare uscată, fixare umedă și fixare cu aer, fibrele au o masă specifică de aproximativ 0,9 g/cm^3 și o densitate de lungime de 1,0–1,7 dtex. De exemplu, un material cu masa de 13 g/m^2 și densitate de lungime a fibrei de 1,0 dtex oferă aceeași acoperire și uniformitate ca și unul cu masa de 15 g/m^2 și o densitate de lungime a fibrei de 1,2 dtex sau cu masa de 20 g/m^2 și densitatea de lungime a fibrei de 2,2 dtex. Astfel, producătorii pot fabrica materiale mai subțiri și mai ușoare.

Pe lângă testele de laborator, FiberVisions a realizat teste la scară industrială, pe linii pilot, pentru a confirma rezistența ridicată a materialelor nețesute cardate, consolidate termic, atât pe direcția mașinii, cât și perpendicular pe aceasta. Aria de suprafață mai mare a fibrelor mai fine poate fi exploatată, pentru a realiza produse de filtrare cu o mai mare eficiență decât cea a produselor existente pe piață.

Sursa: www.fibervisions.com